Bacterial chromosome replication:

Does precatenation occur *in vivo*?

Anna O. Tolmatcheva

Submitted in fulfilment of the requirements for the Degree of

Doctor of Philosophy

Institute of Molecular, Cell and Systems Biology

College of Medical, Veterinary and Life Sciences

University of Glasgow

Abstract

Each cell must replicate and segregate its DNA for the process of cell division. During the replication of the circular chromosome present in *Escherichia coli* the unwinding of the two parental strands leads to the formation of positive supercoils ahead of the replication fork. If the replication fork is free to rotate this might turn into precatenanes, intertwining of the two newly replicated chromosomes, behind the fork. If not resolved, supercoiling ahead of the fork can stall replication, while precatenation will turn into catenation at the end of replication, and will prevent chromosome segregation. Bacteria have mechanisms for the resolution of these undesired topologies which are performed by type II topoisomerases: Topoisomerase IV (Topo IV) and DNA gyrase. Topo IV is known to resolve precatenanes and catenanes, and gyrase can remove positive supercoiling. Both enzymes act by transporting one double stranded DNA helix through a gap made in a second double stranded segment of DNA.

Interestingly, there is no direct evidence for precatenane formation on chromosomal DNA in living cells. Therefore, the aim of this work was to develop a method to detect precatenation in the bacterial chromosome. We tried to answer the following questions: Does precatenation occur on the bacterial chromosome *in vivo*? Is it Topo IV or DNA gyrase that decatenates *in vivo*? Are there mechanisms other than Topo IV or DNA gyrase responsible for precatenane and catenane unlinking in *E. coli*?

The method consisted of using site-specific recombination between two recombination sites recognized by ΦC31 integrase. Once the integrase binds to the sites and recombines, the segment between the two sites is excised as a circle. After DNA replication, two circles will be produced, one from each sister chromosome. If the sisters were precatenated, the two circles might be catenated. Therefore, detection of catenanes after recombination occurred would indicate the presence of precatenation on the chromosome.

Catenanes were detected as products of site-specific recombination on plasmid DNA *in vivo* when both type II topoisomerases were inhibited, suggesting that both Topo IV and DNA gyrase can decatenate DNA *in vivo*. Site-specific recombination was then used to detect precatenation on a plasmid replication intermediate model and on the chromosome. Interestingly, the products of recombination on the replication intermediate model and on the bacterial chromosome were the monomer of the 2.5 kb circle and its dimer. Formation

of the dimer suggested that the two sister chromosomes co-localize after replication fork has passed and that might be due to precatenation. However, precatenation was not directly detected. Optimization of the method is required to obtain direct evidence of precatenation.

In additional work, the level of supercoiling ($Lk-Lk_0$) of a 398 bp circle produced by Xer recombination between closely spaced *psi* sites was determined to be -1. This together with previous results allowed the total linkage change of Xer recombination at *psi* to be determined as +4. Thus, the Xer reaction is driven by loss of four negative supercoils. This result is fully consistent with the Holliday junction model for strand exchange by the Xer recombinases and all other tyrosine recombinases.

Table of contents

List of tables

List of figures

Acknowledgements

Firstly, I would like to express my gratitude to my supervisor Sean Colloms for giving me this opportunity, for the motivation and support during the PhD. His knowledge and our long-lasting meetings made everything clearer and easier. His informative comments helped me in the writing of this thesis.

I would like to thank my secondary supervisor Marshall Stark for helping me finding the answers when Sean was not available.

I am grateful to the Leverhulme Trust foundation for sponsoring me in this life changing journey.

My sincere thanks also go to James Provan, Emanuele Conte, Steven Kane, Gillian Lappin and other lab members that I have met during the PhD. With their help this journey was very exciting. A special thank you goes to Femi Olorunniji for giving suggestions when I felt stranded.

With a special mention to my assessment panel Darren Monckton and Eirini Kaiserli for their insightful comments on my reports.

Finally, I would like to thank my family, especially my mother. She always supported me in all the possible ways and never doubted of my life choices. A big thank you also goes to my partner for the emotional support throughout the PhD and the writing of this thesis.

Author's declaration

"I declare that, except where explicit reference is made to the contribution of others, that this dissertation is the result of my own work and has not been submitted for any other degree at the University of Glasgow or any other institution."

Anna Tolmatcheva

10th January 2019

Abbreviations

Amp^R, ampicillin resistance gene

ATP, adenosine triphosphate

bp, base pairs

BSA, bovine serum albumin

Cm^R, chloramphenicol resistance gene

DNA, deoxyribonucleic acid

E. coli, *Escherichia coli*

EtBr, ethidium bromide

Int, ΦC31 integrase

IPTG, isopropyl β-D-1-thiogalactopyranoside

Km^R, kanamycin resistance gene

KO, knock out

LB, lysogeny broth

Lk, linking number

Lk_0, linking number of a relaxed molecule

Mbp, million base pairs

OD, optical density

oriC, origin of replication on the *E. coli* chromosome

PCR, polymerase chain reaction

RI, replication intermediate

RNA, ribonucleic acid

SDS-PAGE, sodium dodecyl sulphate - polyacrylamide gel electrophoresis

SSB, single-strand binding protein

SSG, ssDNA gap

ter sites, replication termination sites

Tet^R, tetracycline resistance gene

Tw, twist

Wr, writhe

X-gal, indolyl-β-D-galactopyranoside

1. Introduction

1.1 DNA topology

Deoxyribonucleic acid (DNA) contains the information necessary for formation and survival of all organisms. The correct replication and segregation of DNA to daughter cells is of the highest importance (Watson and Crick, 1953a; Watson and Crick, 1953b; Buck, 2009; Toro and Shapiro, 2010).

The field of DNA topology involves the study of aspects of DNA structure that can only be changed by breaking the DNA backbone. DNA topology can be described in terms of supercoiling, catenation and knotting (Mirkin, 2001; Lindsley, 2005; Deweese *et al*, 2008).

In DNA topology it is important to understand what topological domains are. Topological domains are segments of DNA in which the ends cannot rotate freely, circular molecules such as plasmids being the perfect example. These covalently closed circles do not have ends that would allow the topology to be dissipated. However, in the case of eukaryotes, the linear DNA can be attached to the nuclear membrane, or to protein complexes, leaving its ends unavailable for rotation with the same effect (Worcel and Burgi, 1972; Sinden and Pettijohn, 1981; Mirkin, 2001; Dixon *et al*, 2012).

When studying DNA topology two features must be considered. First, linking number (Lk) is the total number of crossings between two strands in a helix and between the double strand itself. The difference between the Lk and Lk_0 (Lk of the molecule in its relaxed state) defines the level of supercoiling in a DNA molecule. Supercoiling can either be plectonemic-wrapping of one DNA segment around another, or solenoidal in which one segment is coiled like the path of a spring. The second feature is knotting and catenation, which are properties of the path followed by the DNA axis in 3-dimensional space and are entanglement of the same molecule (knotting) or interlinking between two DNA molecules (catenation) (Cozzarelli *et al*, 1990; Dröge and Cozzarelli, 1992).

1.1.1 DNA supercoiling

DNA supercoiling plays its role in organizing and compacting the bacterial chromosome, so it can fit into the cell (Figure 1.1A). The *E. coli* chromosome is 4.6 Mbp and if stretched, it would occupy more than 1 mm in length. Moreover, the length of a typical bacterium is approximately 3 µm, and the region within the cell occupied by the genetic

material is less than 1 µm in diameter (Postow *et al*, 2004; Reshes *et al*, 2008; Wang *et al*, 2013). Supercoiling is an important driver within the cell for DNA compaction, leading to the formation of many separate plectonemically supercoiled domains in bacteria, which can be seen by electron microscopy (Boles *et al*, 1990). The supercoiling of the bacterial chromosome is plectonemic, unless the DNA is wrapped around the histone-like proteins producing solenoidal supercoiling (Figure 1.1B) (Zakharova *et al*, 2002; Pettijohn, 1988). In eukaryotic cells, the DNA is wrapped around the nucleosome, forming solenoidal supercoils (Figure 1.1B) (Finch and Klug, 1976). As well as leading to compaction of DNA, supercoiling can be used to store energy which can be used to drive a variety of processes such as DNA replication and transcription initiation, which require DNA unwinding.

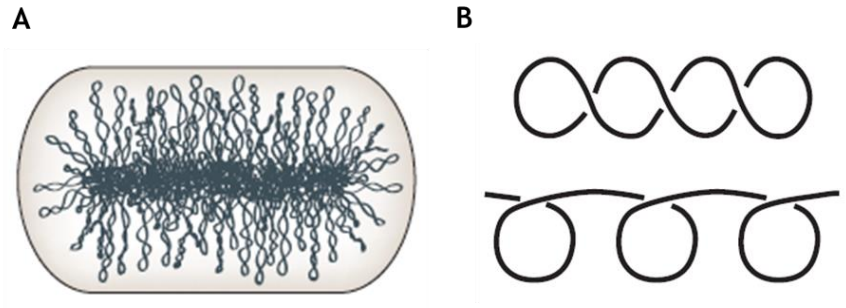

Figure 1.1 – Bacterial chromosome supercoiling. A) The bacterial chromosome is thought to be organized into a series of plectonemic loops. In electron microscopy there appears to be a nucleoid core from which the plectonemic loops emanate. From Wang *et al* (2013) with permission. Order number 4505940967134. **B)** The configuration of supercoils can be plectonemic (upper) or solenoidal (lower).

Lk is the sum of Twist (Tw) and Writhe (Wr) of a double stranded circular molecule. Tw is the intertwinings of the two strands of the double helix along the path of the DNA axis (Figure 1.2A). If the axis of a molecule coils in 3D space, then the DNA axis can cross itself in a different region, which forms the Wr (Figure 1.2B). One Tw in the double helix consists of two crossings of the individual DNA strands, whereas one Wr is one crossing of the double helix over another double helical section. Tw and Wr are not an integer, while Lk is an integer, and a fixed number that cannot be changed without transient introduction of a nick or a double-stranded break. On the other hand, Tw and Wr in a circular molecule can interconvert. For example, if the two strands are continually pulled apart, the Tw from that region are transferred to the rest of the molecule. At some point, due to increased tension caused by accumulation of Tw the duplex starts converting Tw to Wr (Mirkin, 2001).

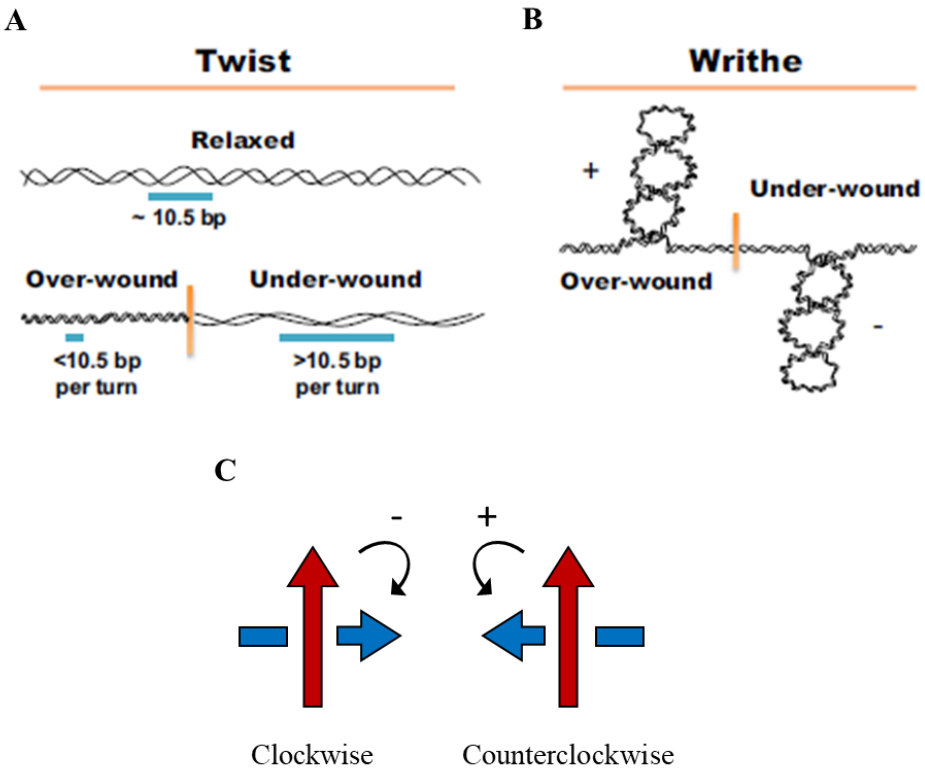

Figure 1.2 – Twist, writhe and supercoiling sign. A) Tw is the intertwinings between the two strands of the helix. The blue bar shows the region occupied by a helix turn in relaxed, over- and under-wound DNA. **B)** Wr is formed when the molecule coils around itself. If the molecule is over-wound the Wr is positive, and negative if it is under-wound. The orange bar represents the barrier which forms the topological domains. A) and B) adapted from Corless and Gilbert (2016) with permission. **C)** The convention used to determine if a crossing is positive or negative. The orientation of the arrows is followed along the whole molecule and not random. The strands must be denoted as parallel in the DNA.

Wr can be negative or positive, and the convention by which a crossing is said to be negative or positive is shown on Figure 1.2C. Both arrows represent the single or double strands, where one is overlying (red arrow) and the other is underlying (blue arrow). A negative node or crossing is formed when the overlying strand/arrow must be rotated clockwise to align with the second one. A positive node is present if the rotation is counterclockwise (Schvartzman and Stasiak, 2004).

In a relaxed molecule one helical turn of DNA consists of, approximately, 10.5 bp. The Lk of a relaxed circular molecule is therefore the total number of base pairs divided by 10.5 and it is termed Lk_0. Lk_0 is not an integer.

$$Lk_0 = \frac{Total\ number\ of\ base\ pairs}{10.5}$$

For a supercoiled molecule the Lk differs from that of a relaxed molecule. When a molecule is over-wound (positively supercoiled), there are fewer than 10.5 bp per helical turn and Lk is higher than the Lk_0 (Figure 1.2A). On the other hand, if it is under-wound (negatively supercoiled), there are more than 10.5 bp per helical turn and the Lk is lower than the Lk_0 (Figure 1.2A). ΔLk, the difference between Lk and Lk_0, indicates how supercoiled the molecule is and if it is over- or under-wound.

$$\Delta Lk = Lk - Lk_0$$

For example, a plasmid of 3150 bp in a relaxed state will have 10.5 bp per turn, so its Lk_0 is 300.

$$Lk_0 = \frac{3150}{10.5} = 300$$

If ethidium bromide (which intercalates between the bases of the molecule) is added to this plasmid, it now can have a relaxed helical repeat of 11 bp per turn. This changes Lk_0 of the molecule to 286 but does not change Lk.

$$Lk_{0\,EtBr} = \frac{3150}{11} = 286$$

Therefore, the ΔLk is +14, which indicates that the molecule is 14 turns over-wound compared to its relaxed state.

$$\Delta Lk = 300 - 286 = +14$$

If the DNA were now nicked and re-ligated, or relaxed with a topoisomerase, Lk would change to 286. Lk – Lk_0 would be 0 and the DNA would be relaxed in these conditions (in presence of intercalator). If the ethidium were then removed, Lk would remain unchanged at 286, but Lk_0 would return to 300, so that the DNA would now be 14 turns underwound (negatively supercoiled).

As explained above, supercoiling is the change of the molecule from the relaxed to an over- or under-wound state (Mirkin, 2001). Normally, in mesophilic bacteria the DNA is under-wound (negatively supercoiled). This favours strand separation and initiation of different processes such as replication and transcription (von Freiesleben and Rasmussen,

1992; Ljungman and Hanawalt, 1995). Therefore, maintaining negative supercoiling is of high importance to the cell. Although transcription initiation is facilitated by under-wound DNA, transcription is responsible for formation of positive supercoils ahead, and negative supercoils behind the RNA polymerase. This is known as the twin transcriptional-loop model and was proved by a set of experiments on plasmid in bacteria (Liu and Wang, 1987). The positive supercoiling produced ahead of RNA polymerase was shown to interfere with mRNA synthesis in yeast (Gartenberg and Wang, 1992). It was also shown to participate in removal of proteins associated to DNA ahead of the polymerase, making the DNA more accessible for the RNA polymerase complex (Sheinin *et al*, 2013).

In contrast, in hyperthermophile organisms, DNA is over-wound (positively supercoiled) helping to stabilize it against heat-induced melting (Ogawa *et al*, 2014).

1.1.2 DNA knotting and catenation

A double stranded DNA knot is a self-entangled molecule (Figure 1.3A) which can only be resolved by breaking the sugar-phosphate backbone of both strands of the helix (Lindsley, 2005; Witz and Stasiak, 2009). Whereas a knot is a single entangled DNA circle, a catenane is two or more interlinked DNA molecules (Figure 1.3A). Unlinking of catenanes also requires introduction of a double-strand break in one circle of the catenane (Witz and Stasiak, 2009).

Knots and catenanes can be classified according to their minimal crossing number: the number of crossings or nodes in their simplest representation in two dimensions. The higher the number of nodes, the more knotted or catenated the molecule is. This number is useful because knots and catenanes migrate approximately according to the minimal crossing number on agarose gels (Figure 1.3B). The more nodes they have, the faster they migrate on the gel (Dröge and Cozzarelli, 1992). Different type of knots and catenanes are possible with the same node number. For example, there are two knots with 5-nodes and three with 6-nodes. However, different knots with the same number of nodes can sometimes be distinguished by electrophoresis or electron microscopy for knots with increased number of crossings.

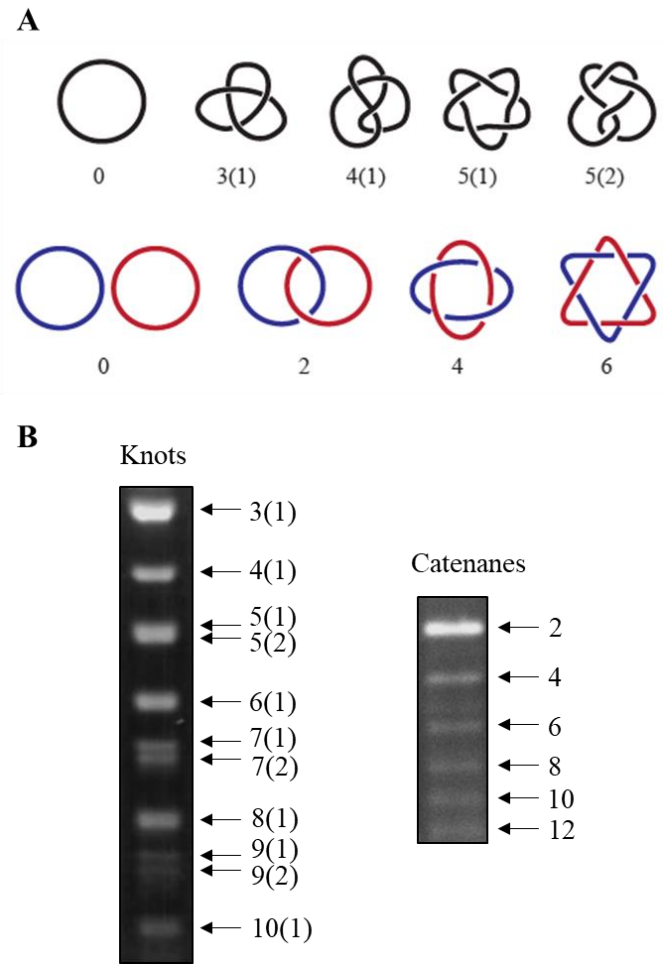

Figure 1.3 – Knots and catenanes. A) The trefoil knot is the simplest knot with three nodes. There is one knot with 4 crossings, and two knots with 5 crossings. A catenane with two crossings is the simplest catenane. The number of nodes increases in number of 2. **B)** Pictures representing electrophoretic mobility of knots and catenanes on agarose gel. The ladder of knots was taken from Vologodskii *et al* (1998) with permission. Order number 4505950206101. The ladder of catenanes was obtained by site-specific recombination on a plasmid *in vitro*.

Knots and catenanes are products formed during different processes such as replication and recombination (Pollock and Nash, 1983; Dröge and Cozzarelli, 1992; Lindsley, 2005). Understanding them not only gives us insight into how these topologies are formed, but also into DNA structure (Wasserman and Cozzarelli, 1985; Wasserman *et al*, 1985; Spengler *et al*, 1985).

Knotting and especially catenation interfere with biological processes such as segregation of sister chromosomes and plasmids. Therefore, removal of catenation and knotting is essential for cell proliferation. This is the role of enzymes in the cell known as topoisomerases.

1.2 Bacterial topoisomerases

In bacteria, topoisomerases are the enzymes used to control the level of supercoiling of the DNA, and to resolve undesired topologies such as positive supercoiling, precatenanes, catenanes and knots (Wigley, 1995; Deibler, 2001). Precatenanes are the intertwinings between the sister chromosomes behind the replication fork. If the intertwinings are formed prior to replication termination, they are named precatenanes. However, if the intertwinings persist after the replication finished, they are named catenanes. Topoisomerases are divided in two groups: type I and type II. Type I topoisomerases act by introducing a nick into one strand of the duplex, while type II topoisomerases introduce a double-strand break. In *E. coli* Topo I and Topo III are the type I topoisomerases, while DNA gyrase (also known as Topo II) and Topo IV are type II topoisomerases (Wigley, 1995). The two groups are described in detail in the following sections.

1.2.1 Type I topoisomerases

Topo I and Topo III, structurally, are proteins formed by four domains surrounding a cavity. An active-site tyrosine is present in domain III and the domains I and IV create a groove for DNA binding (Berger, 1998; Lima *et al*, 1994; Mondragón and DiGate, 1999). These topoisomerases alter DNA topology by introducing a single-strand nick into one strand of double-stranded DNA and passing the intact strand through the gap (Figure 1.4) (Brown and Cozzarelli, 1981).

Type I topoisomerases use divalent metal ions, such as Mg^{2+}, as cofactors (Zhu *et al*, 1997). These cofactors do not directly participate in DNA ligation and cleavage, but they bind specific residues of topoisomerase. Upon cofactor binding, the conformation of protein is altered, and this now can bind the DNA (Figure 1.4 (a)) (Zhu and Tse-Dinh, 2000). After DNA binding and cleavage (Figure 1.4 (b)), the nucleophilic tyrosine residue in domain III is covalently bound to the 5´ end of the strand (Lynn and Wang, 1989). The domain III lifts away from domain I so the intact single-strand can be passed through the gap (Figure 1.4 (c)). Then, the nicked strand is re-ligated (Figure 1.4 (d)) and the protein opens again to release the moved strand (Figure 1.4 (e)). The double strand is released, or another cycle of nicking and strand passage can take place (Figure 1.4 (f)).

The function of *E. coli* Topo I is to remove negative supercoils from the DNA to prevent the build-up of excessive negative supercoils (Wang, 1971; Perez-Cheeks *et al*, 2012). The removal of negative supercoiling by Topo I is balanced in the cell by the addition of negative supercoils by DNA gyrase.

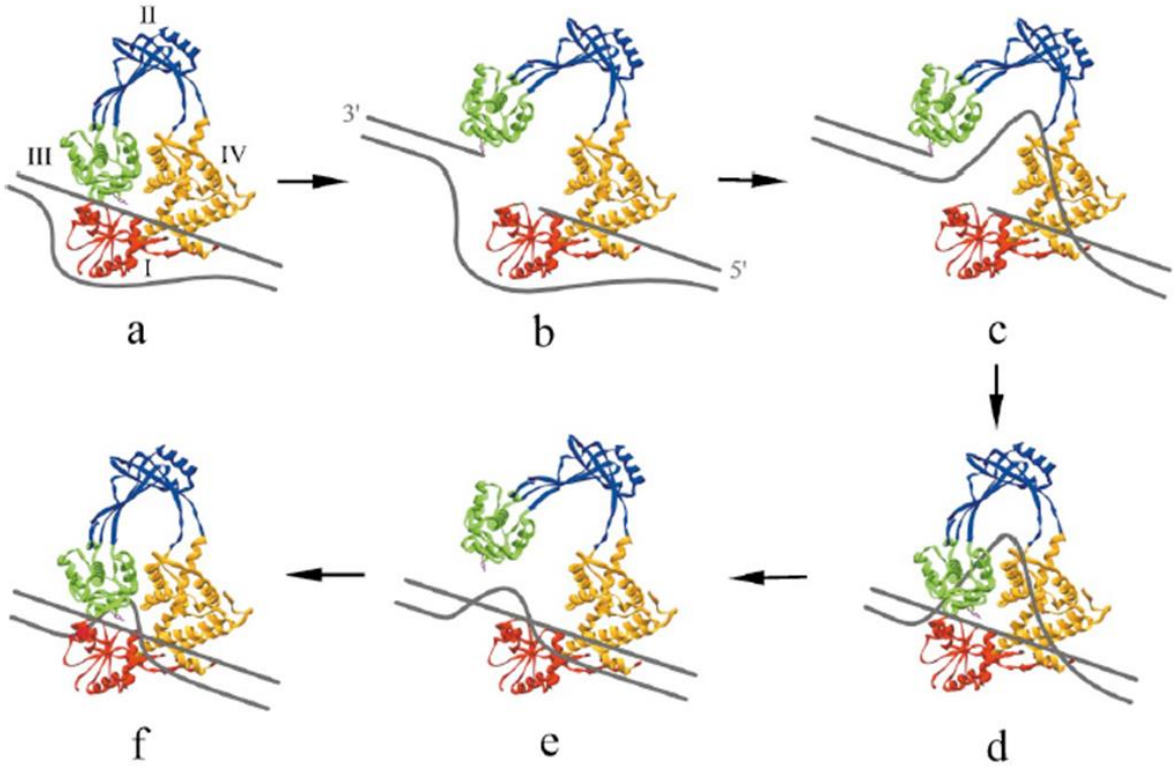

Figure 1.4 – Simplified mechanism used by Topo I. The four domains of the enzyme are coloured in red (I), blue (II) green (III) and yellow (IV). The double-stranded DNA is represented in grey. After the protein binds the DNA (a) it introduces a single-strand nick (b) through which the intact single-strand is passed (c). Then the protein re-ligates the strand (d) and releases it (e). The double-strand can be released by the protein or another cycle of nicking and strand passage can take place (f). From Champoux (2001) with permission. Order number 4510160846016.

Topo III is thought to be involved in passing a double-strand segment of DNA through a break in single-stranded DNA. One major role of Topo III might be to decatenate newly replicated DNA by passing the double-strand leading sister through a gap in the single-strand DNA of the lagging sister (Figure 1.5). Topo III is thought to be involved in precatenane and catenane resolution in plasmid DNA (DiGate and Marians, 1988; Hiasa *et al*, 1994) and in chromosome segregation (Perez-Cheeks *et al*, 2012).

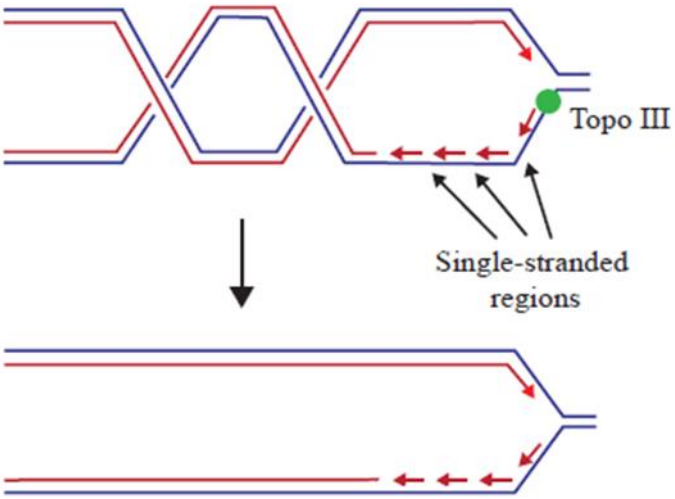

Figure 1.5 – Possible precatenane resolution by Topo III. During replication, in the lagging strand, single-stranded regions are formed between the Okazaki fragments and before the start of the first Okazaki fragment. Topo III binds to these regions and performs decatenation by passing the double-strand DNA through a gap in the single-strand DNA.

1.2.2 Type II topoisomerases

Type II topoisomerases are multimeric proteins which alter DNA topology by introducing a double-strand break in one DNA segment and transporting an intact double-strand segment of DNA through the gap. They participate in events such as DNA relaxation, supercoiling, catenation and decatenation (Wigley, 1995; Deweese *et al*, 2008).

The mechanism initiates by the binding of enzyme to a double-strand DNA fragment (G segment) (Figure 1.6 (a,b)). In presence of magnesium ions, the enzyme introduces a double-strand break in the DNA, with the 5´ end of each strand being covalently bound to the active-site tyrosine in each subunit of enzyme. Following ATP binding, the enzyme changes its conformation and a second segment of DNA is trapped and this segment is known as the T segment (Figure 1.6 (c,d)). The T segment is passed through the gap in the G segment (Figure 1.6 (e)). Then the G segment is re-ligated, and the T segment released (Figure 1.6 (f)). At the end of the cycle, the G-segment can be released upon ATP hydrolysis and protein conformation is altered to the one observed in the beginning, or another catalytic cycle can initiate (Wang, 1998; Nitiss, 2009). At the end of one cycle, the

DNA gyrase has introduced two negative supercoils into the DNA, while Topo IV has removed two intertwinings in a catenane (Brown and Cozzarelli, 1979).

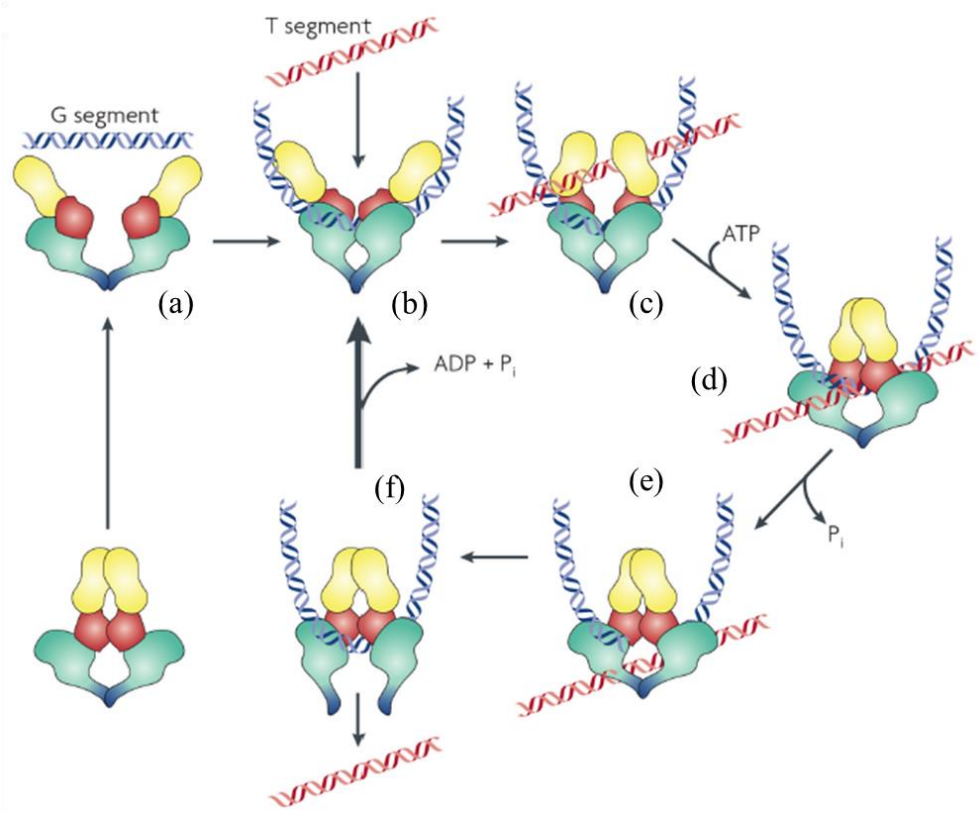

Figure 1.6 – Type II topoisomerase mechanism. In the represented mechanism, enzyme transports a double-strand fragment (T segment in red) through the gap made in the same or different molecule (G segment in blue). ATP binding and hydrolysis alter the conformation of the protein, necessary for T segment entrapment and G segment release, respectively. Adapted from Nitiss (2009) with permission. Order number 4505960198629.

DNA gyrase is a type II topoisomerase which introduces negative supercoiling into DNA in prokaryotes (Gellert *et al*, 1976). DNA gyrase starts by wrapping approximately 140 bp of DNA around itself in a right-handed manner, forming a positive supercoil (Couturier *et al*, 1998). At the end of the cycle, the positive supercoil is converted to a negative supercoil. It is the balanced action of gyrase and Topo I that regulates the supercoiling of DNA *in vivo* (DiNardo *et al*, 1982; Zechiedrich *et al*, 2000).

Topo IV is the major decatenase in bacteria. Adams and co-workers observed accumulation of interlinked plasmids upon Topo IV inhibition *in vivo* (Adams *et al*, 1992). By comparing the rate of catenane unlinking by Topo IV and DNA gyrase, Zechedrich and colleagues concluded that Topo IV was 100-fold more efficient in decatenating *in vivo*

(Zechiedrich and Cozzarelli, 1995; Zechiedrich *et al*, 1997). Topo IV has also been shown to be the topoisomerase that unknots knots *in vitro* (Ullsperger and Cozzarelli, 1996).

The roles of these enzymes are essential for cell survival. The steady level of supercoiling must be maintained so the DNA can be transcribed and replicated. After DNA replication termination, the sister chromosomes must be segregated into the daughter cells.

Quinolones are antibacterial agents that targets the type II topoisomerases in *E. coli* (Khodursky *et al*, 1995; Levine *et al*, 1998; Drlica, 1999). Norfloxacin is one of the first quinolone agents to be used clinically to treat numerous infections by inhibiting type II topoisomerases. This drug acts by forming an irreversible complex with the topoisomerase covalently attached to the DNA (Shen and Pernet, 1985; Shen *et al*, 1989). The trapped complex inhibits the replication fork from progressing resulting in fork breakage, decreased DNA synthesis and cell death (Hiasa *et al*, 1996; Khodursky and Cozzarelli, 1998; Fournier *et al*, 2000; Sharma *et al*, 2008).

1.3 *E. coli* chromosome replication and segregation

Replication of circular chromosome of *E coli.* initiates at the origin (*oriC*), which localizes in the middle of the cell, with the left (L) and right (R) arms of chromosome located to each half of the cell (Wang *et al*, 2013; Nielsen *et al*, 2006). The region where the two arms meet is the terminus region and it is located opposite to *oriC*. Upon replication initiation, each *oriC* migrates to one cell half and with it, the newly replicated chromosomes. At the end of replication, the two chromosomes are segregated to the two daughter cells with the original organization in L-R (Wang *et al*, 2013; Toro and Shapiro, 2010).

Due to high level of supercoiling of the DNA in the cell (Figure 1.1A), the replication machinery encounters different obstacles such as accumulated positive supercoiling or proteins bound to the DNA. Therefore, during replication, all the obstacles must be removed so the replication can proceed and terminate (Worcel and Burgi, 1972; Wang *et al*, 2013).

1.3.1 Positive supercoiling and precatenation during DNA replication

DNA replication initiates with replication machinery assembly at the origin of replication. The DNA double-strand is separated by the helicase in the replication machinery (Lee and Yang, 2006). This denaturation promotes local unwinding which in turn causes over-winding ahead of the replication fork. As the fork progresses the positive supercoiling accumulates ahead of the fork (Figure 1.7A) (Peter *et al*, 1998). Due to the presence of topological barriers the positive supercoiling cannot be resolved by free DNA rotation. Accumulation of positive supercoils ahead of the fork stalls the replication, therefore, the supercoils must be removed. DNA gyrase is the topoisomerase that acts ahead of the replication fork to assist in replication progression. Gyrase introduces negative supercoils ahead of the fork that cancel the positive supercoils generated by fork progression (Gellert *et al*, 1976). The rate at which gyrase introduces negative supercoils might be slower than the rate of helicase unwinding (Peter *et al*, 1998; Olavarrieta *et al*, 2002). This can still lead to accumulation of positive supercoils ahead of the fork. The more positive supercoils accumulate the higher the torsional tension in the unreplicated region. Potentially, this tension could make the replication machinery swivel around itself, resulting in right-handed interlinks between the replicated chromosomes, forming precatenanes (Figure

1.7B) (Champoux and Been, 1980; Hiasa *et al*, 1994; Peter *et al*, 1998; Cebrián *et al*, 2015). Failure to resolve precatenated sisters will lead to catenated sister chromosomes at the end of replication (Wang *et al*, 2008; Postow *et al*, 2001). Topo IV is the topoisomerase suggested to resolve precatenanes behind the replication fork.

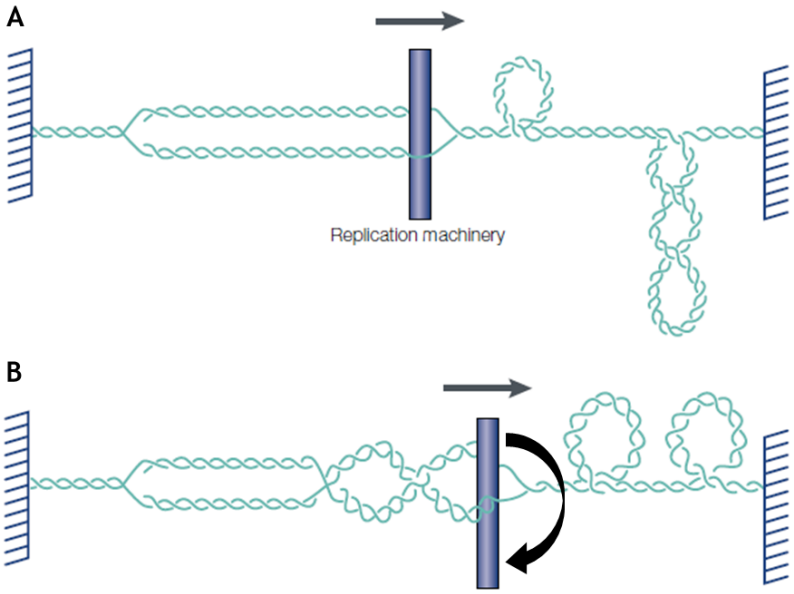

Figure 1.7 – Positive supercoiling and precatenation during replication. A) The replication machinery progression unwinds the DNA, so it gets over-wound ahead of the fork, leading to accumulation of positive supercoils. **B)** Rotation of the polymerase and the replication fork (curved arrow) releases the tension created by the over-winding and interlinks the replicated chromosomes behind the fork. Linear black arrows represent the movement of the replication machinery. Blue comb-like structures represent topological barriers. Adapted from Wang (2002) with permission. Order number 4505960445854.

At the end of replication of a covalently closed circle, the two forks approach each other (bacterial chromosomes or plasmids), or one fork approaches the origin (plasmid) and the unreplicated region gets too small for type II topoisomerases to act (Figure 1.8A) (Sundin and Varshavsky, 1981). For this reason, it is thought that the last intertwinings of the unreplicated region are converted into right-handed precatenanes behind the fork (Figure 1.8B). Therefore, when replication terminates, the two sister chromosomes are catenated, and require the action of type II topoisomerases for their segregation (Figure 1.8C) (Wang, 2002; Wang *et al* 2008; Branzei and Foiani, 2010), unless decatenated by Topo III (Perez-Cheeks *et al*, 2012).

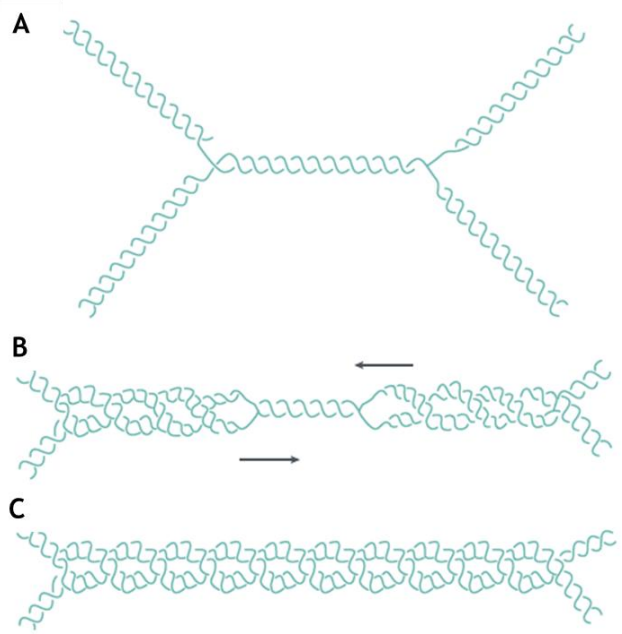

Figure 1.8 – Replication termination in a covalently closed circle. A) When the forks converge, positive supercoils are not removed by type II topoisomerases due to lack in space. **B)** The last stretch of DNA is replicated through replication machinery rotation and sister chromosomes precatenation. **C)** At the end of replication, the chromosomes are catenated. Black arrows represent the movement of the replication machinery. From Wang (2002) with permission. Order number 4505960445854.

1.3.2 Replication termination – terminus region of chromosome

The terminus region of the bacterial chromosome is located opposite to *oriC* (~180°) and the first studies in 1977 (Kuempel *et al*, 1977) showed that replication termination would occur in this region. Just over a decade later, two specific sites were shown to be the locations where each replication fork, coming from each direction, would stall until fused together (Hill *et al*, 1988). These sites were named replication termination sites, *ter* sites. Shortly after this discovery, several other *ter* sites were found in the terminus region (Hidaka *et al*, 1988; François *et al*, 1989; Hidaka *et al*, 1991; Sharma and Hill, 1992; Lewis, 2001). These sites are specifically oriented on the chromosome. The *terC*, *terB*, t*erF*, *terG* and *terJ* halt the clockwise replication fork, while *terA*, *terD*, *terE*, *terI* and *terH* block the counterclockwise fork (Figure 1.9) (Duggin *et al*, 2008). A replication fork halted at a *ter* site will wait there until the replication fork in the other direction meets up with it. Therefore, the *ter* system might be most important when one replication fork is

delayed or stalled by breaks in the DNA, for example, and has to restart. The *ter* sites positioned further from the inner ones (all but *terC* and *terA*) are thought to work as a backup system. For example, if the clockwise fork is not stalled upon reaching *terC* then it can be stalled by *terB* or further sites. The *ter* sites do not stall replication forks on their own. A specific protein, *Tus*, binds to the *ter* sites and inhibits DNA unwinding by helicase in the replication machinery (Hidaka *et al*, 1989; Hidaka *et al*, 1992).

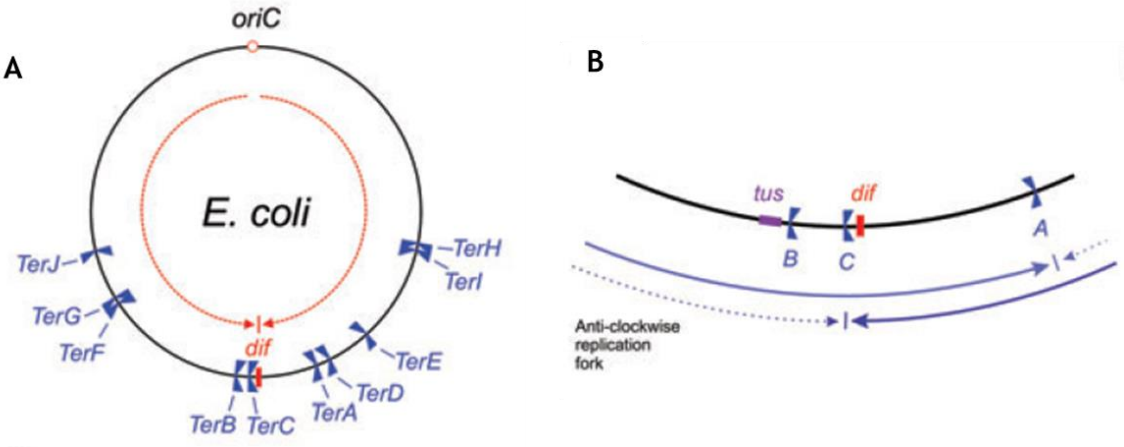

Figure 1.9 – Replication termination sites in the *E. coli* chromosome. A) The *E. coli* chromosome is represented by the black circle. Opposite to *oriC* is the terminus region with the *ter* sites. The red arrows represent the direction of the two replication forks. The *dif* sequence is in red, near *terC*. **B)** The *terC* is the first site that can trap the clockwise fork and *terA* is the first site to halt the anticlockwise fork. Located to the left of *terB*, *tus* gene codes for the protein that binds the *ter* sites and it is the DNA-protein complex that stalls the replication forks. Adapted from Duggin *et al* (2008) with permission. Order number 4505960902113.

A more recent work, based on bioinformatics, suggested the *dif* site as the replication termination site instead of the *ter* sites (Hendrickson and Lawrence, 2007). Localized at the terminus region of the chromosome, *dif* is a 28 bp site specific for binding of XerCD recombinases (Kuempel *et al*, 1991). XerCD recombinases act on *dif* to convert chromosome dimers into monomers (Blakely *et al*, 1993). In their bioinformatics approach, it is suggested that *dif* halts the replication forks produced from *oriC*. To test this theory, another group studied the termination position of the *oriC* produced replication. Their work supported that *ter* sites are the replication termination points and not *dif* (Duggin and Bell, 2009).

The discovery of *ter* sites not only allowed studying the termination of replication, but also provided a tool which helped studying topology of DNA by, for example, introducing a *ter*

site into the plasmid DNA and producing replication intermediates (RI) (Olavarrieta *et al*, 2002; Cebrián *et al*, 2015).

When a *ter* site is introduced in the correct orientation into a plasmid with a unidirectional origin of replication, the product of replication is a replication intermediate (Figure 1.10). Once the replication fork is stalled by a Tus-*ter* complex the positive supercoiling in the unreplicated region produced by fork movement can be converted to negative supercoiling by DNA gyrase. Moreover, the negatively supercoiled unreplicated region, with right-handed crossings, can promote fork rotation resulting in interlinking of replicated duplexes, with left-handed crossings (Figure 1.10) (Cebrián *et al*, 2015). Negative supercoiling ahead of the fork results in left-handed precatenanes (RI), while positive supercoils in right-handed precatenanes (final stages of replication of chromosome (Figure 1.8)).

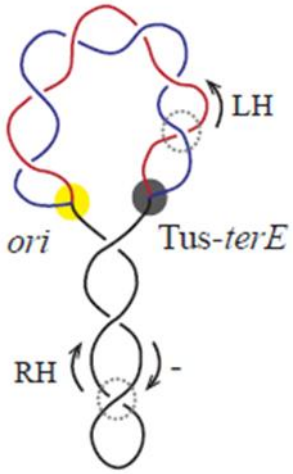

Figure 1.10 – Replication intermediate, structure of a θ. Replication initiates at the origin (yellow circle) and terminates at Tus-*ter* complex (grey circle). The unreplicated region is negatively supercoiled with right-handed (RH) crossings, while replicated regions are precatenated with left-handed (LH) crossings. o*ri*, origin of replication.

1.4 Homologous recombination

Homologous recombination is the process of DNA segment exchange between two molecules. It is used by bacteria for genetic diversification, and it is one of the main DNA repair mechanisms (Rocha *et al*, 2005). Homologous recombination takes place when the genome integrity is compromised by formation of ssDNA gaps (SSG), dsDNA breaks (DSB) and stalled replication forks (Bianco *et al*, 1998; Kowalczykowski, 2000). The SSGs and DSBs can be caused by anticancer drugs or ionizing radiation (Povirk *et al*, 1989; Weinfeld and Soderlind, 1991), while stalled replication forks are formed when the replication machinery collides with the transcription machinery or proteins bound to the DNA (French, 1992; Hill *et al*, 1989).

When a DSB is introduced into the DNA, the RecBCD complex binds to the broken end (Figure 1.11 (a)) and works as a helicase-nuclease by unwinding the DNA and degrading the 3´- terminal strand at the point of entry (Figure 1.11 (b,c)). The 5´- terminal strand is covered by single-strand binding (SSB) protein to prevent it from being degraded. As RecBCD unwinds the DNA it produces a loop-like structure of single-stranded DNA which extends from the RecBCD complex. Once the RecBCD complex finds a Chi site (χ), the degradation of the 3´- terminal strand is downregulated and a weaker degradation of the 5´- terminal strand is upregulated. This biochemical change promotes formation of a single-strand DNA with the χ site at the 3´ end and loading of RecA onto the strand (Figure 1.11 (d)). The RecA-DNA complex invades a homologous dsDNA and produces a recombination intermediate in form of a Holliday junction (Figure 1.11 (e)). Then, the Holliday junction is resolved and the DSB can be repaired by initiation of replication (Figure 1.11 (f)).

Stalled replication forks can be rescued by homologous recombination between the two sister chromosomes, which means that replication is dependent on homologous recombination (Asai *et al*, 1994; Kreuzer *et al*, 1995). When a replication fork encounters a lesion in the DNA, it can collapse (Figure 1.12). The produced DSB can be repaired by the RecBCD complex, since this is probably the major cellular function of RecA and RecBCD.

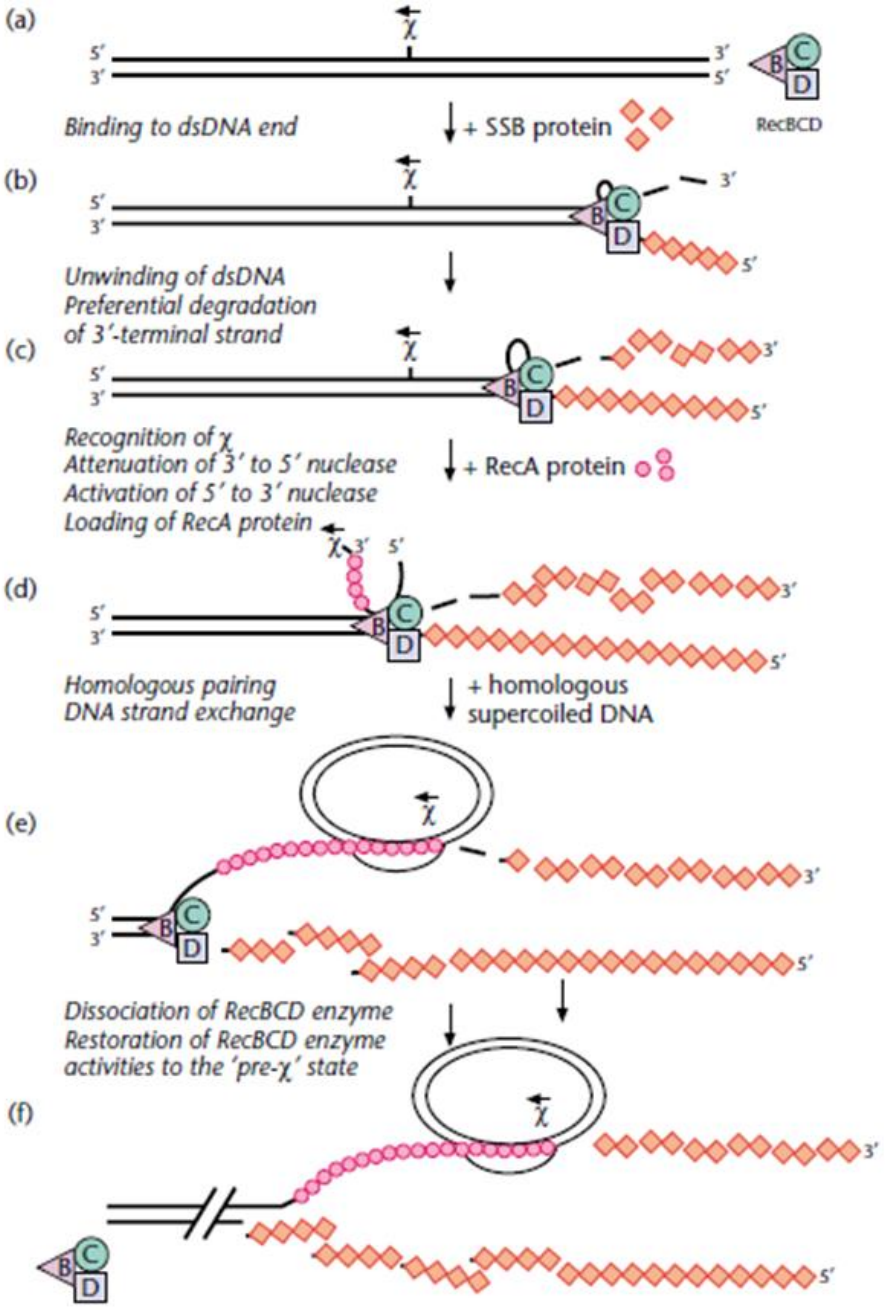

Figure 1.11 – Homologous recombination in DSB repair in *E. coli*. RecBCD complex works as a helicase-nuclease and it screens the DNA for the χ site. Once found, the site is covered by RecA protein which mediates strand invasion of a homologous dsDNA and repair of the DSB. From Arnold and Kowalczykowski (2001) with permission. Order number 4505961170640.

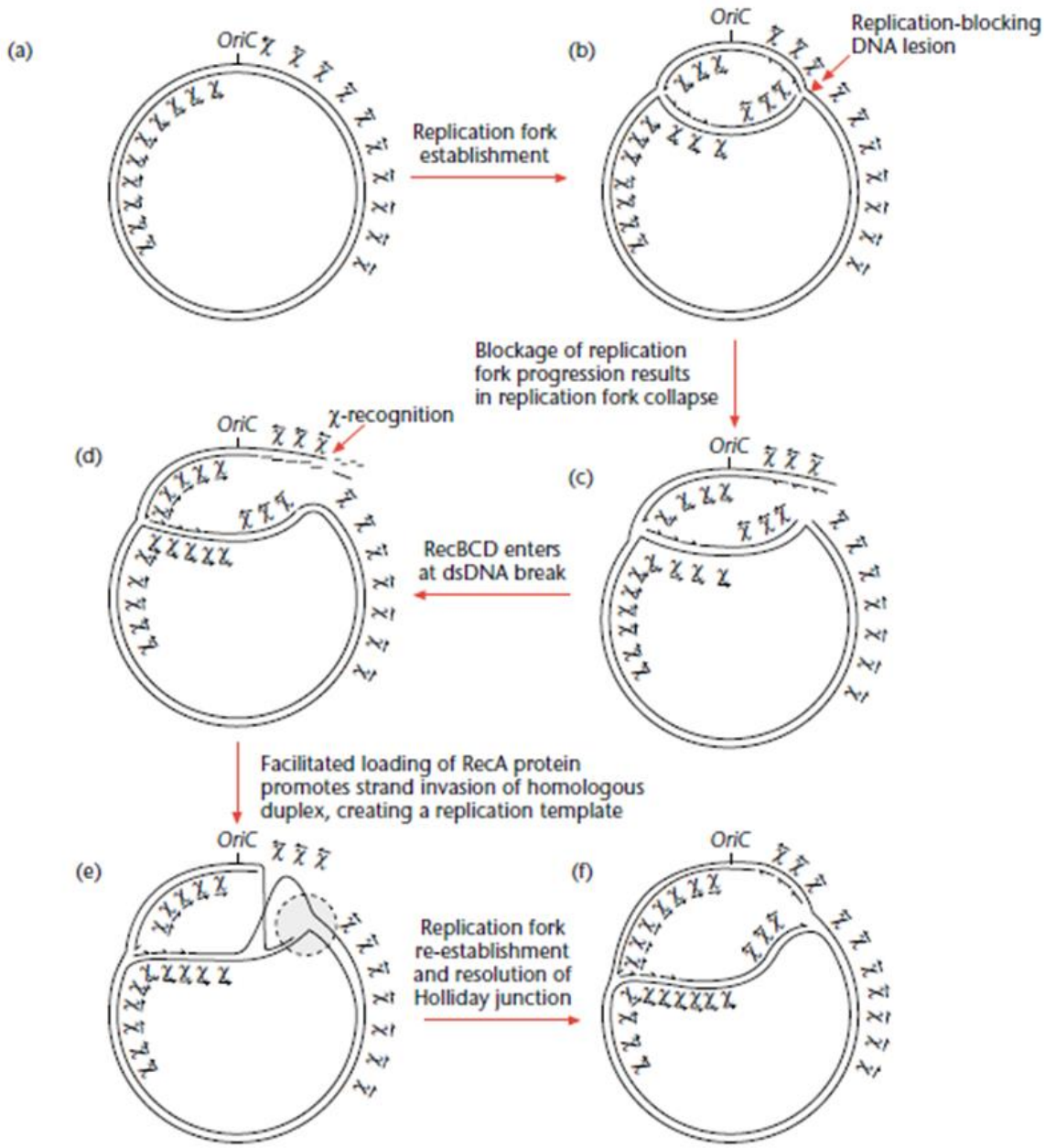

Figure 1.12 – Replication fork collapse and repair by homologous recombination in *E. coli*. (a) In *E. coli*, many χ sites were discovered distributed along the chromosome, and most of them are oriented towards the *oriC*. (b) After replication initiation at *oriC*, a replication fork can encounter a replication-blocking DNA lesion, such as a single-strand gap. (c) The replication is blocked, and the fork can collapse. (d) The RecBCD complex binds to the double-strand break and screens for the nearest χ site. (e) Once RecA is loaded on the χ site, it mediates strand invasion of the homologous strand creating a replication template (dotted circle). (f) The DSB is repaired and the replication fork re-established. From Arnold and Kowalczykowski (2001) with permission. Order number 4505961170640.

1.4.1 Use of homologous recombination for genome manipulation

Homologous recombination started to be used as a tool in gene replacement (Murphy, 1998; Zhang *et al*, 1998; Muyrers *et al*, 1999; Datsenko and Wanner, 2000). Most used original technology was a two-step process (Blomfield *et al*, 1991; Link *et al*, 1997). The double crossover for gene replacement consisted first of the integration of a full plasmid into the target region. This plasmid contained the gene (for example kanamycin resistance gene) to be inserted in the place of the gene to be deleted, and selective markers such as chloramphenicol resistance gene and *sacB* gene. After the second crossover, the selective markers together with the target gene were deleted by excision of a circle, and the kanamycin resistance gene remained inserted.

Some years later, the combination of the lambda red recombination system used by the λ bacteriophage and the arabinose inducible promoter, P_{BAD}, created an efficient one-step tool used quite widely in *E. coli* and other organism such as fungi (Chaveroche *et al*, 2000). The variant of the system developed by Chaveroche consists of a plasmid, pKOBEG, where KO stands for knock out, B for *bet* gene coding for a SSB, E for *exo* gene coding a 5´ exonuclease and G for *gam* gene coding for an inhibitor of the host RecBCD nuclease (Murphy, 1998). These genes are under the P_{BAD} promoter, so the recombination can be induced when required (Guzman *et al*, 1995; Chaveroche *et al*, 2000). Expression of the λ red system allows the use of linear DNA for homologous recombination in gene replacement.

Inside the cell, the double-stranded DNA that it is to be used in gene KO, is being converted into single-stranded by the Exo 5´ nuclease. The produced single-strand is bound by Bet proteins, which stimulate strand invasion and exchange by RecA. The Gam protein inhibits RecBCD nuclease, so it cannot destroy the double-stranded DNA before the recombination occurs. The linear DNA that is used for target gene KO can contain an antibiotic resistance gene surrounded by 50 bp tails homologous to the target region of the chromosome (Figure 1.13). In this way, the bacteria in which recombination occurs can be selected by growth on plates with the appropriate antibiotic.

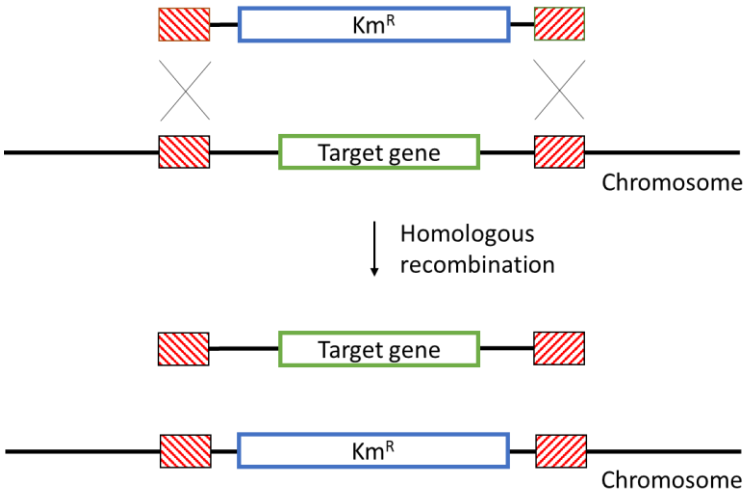

Figure 1.13 – Gene knock out by homologous recombination. To perform a KO of a target gene in the bacterial chromosome, the strain is transformed with a linear double-stranded DNA which has a selective marker, such as kanamycin resistance gene (Km^R). On each side of the kanamycin resistance gene there is a 50 bp tail (squares with red lines) homologous to the target region of the chromosome. The lambda red system catalyses the recombination between the homologous sites, which replaces the target gene in the chromosome by the insertion of the kanamycin resistance gene, resulting in the KO.

1.5 Site-specific recombination

Site-specific recombination differs from homologous recombination in that it requires specific sites in the DNA instead of homologous segments. It also requires specific recombinases to perform the recombination. These enzymes bind to the specific recognition sites, introduce breaks at these sites and re-ligate them (Figure 1.14) (Stark, 2014). Recombinases require two sites, which might be on the same DNA molecule or on separate molecules. If they are on separate circular DNA molecules, recombination results in integration (Figure 1.15). If they are on the same molecule there can be two outcomes: excision, if the sites are in direct repeat (head-to-tail), or inversion, if they are in inverted repeat (head-to-head) (Figure 1.15) (Grindley *et al*, 2006). Site-specific recombination is used by bacteriophage to integrate and excise their DNA from the bacterial chromosome (Barreiro and Haggard-Ljungquist, 1992); it is used by bacteria to assure the monomeric state of the plasmids (Colloms *et al*, 1996); and it also can be used by bacteria to switch gene expression on and off by inverting the promoter region relative to the gene (Abraham *et al*, 1985). There are two types of site-specific recombinases: serine and tyrosine recombinases, and they differ in the mechanism used during recombination and their amino acid sequences.

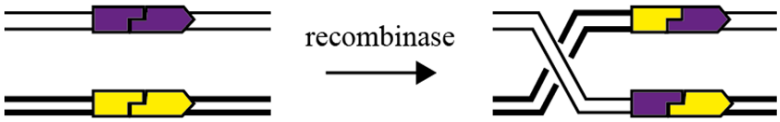

Figure 1.14 – Site-specific recombination. The two recognition sites (purple and yellow) are brought together by recombinase, cleaved, ends exchanged and re-joined.

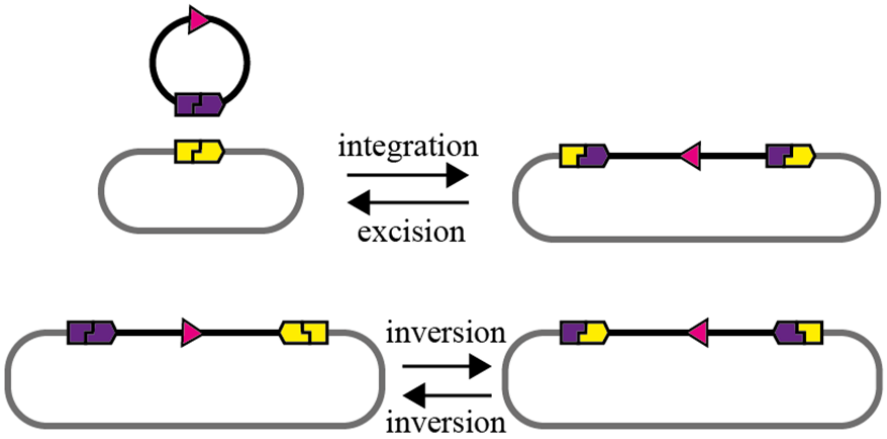

Figure 1.15 – Site-specific recombination products. Depending if the sites are on the same or different molecules, and on the directionality of the recognition sites (colourful boxes), the products of site-specific recombination can be integration, excision or inversion.

1.5.1 Serine recombinases – ΦC31 integrase

The serine recombinases family consists of the resolvases, invertases and integrases, and all use the same mechanism to perform strand exchange (Stark, 2014). The resolvases and invertases are known as small serine recombinases, while integrases as large serine recombinases. The recognition sites start from 25 bp in length, and longer sites usually contain multiple binding sites for different dimers. A dimer binds to a site which is an imperfect palindrome with an asymmetric core region of two nucleotides where the crossover and strand exchange takes place (Figure 1.16A). However, some recombinases require accessory DNA sequences, to which they or accessory proteins binds and help catalyse the reaction (Figure 1.16B) (Stark, 2014; Grindley *et al*, 2006).

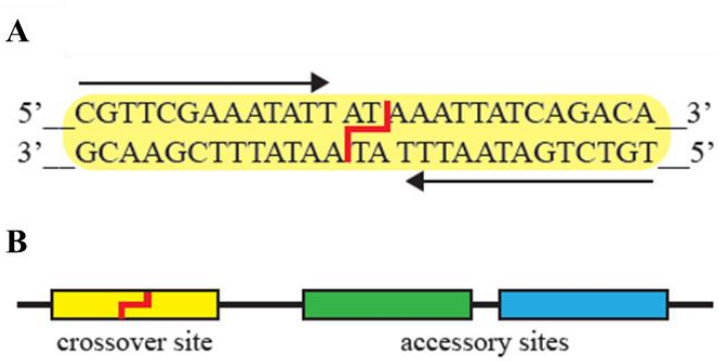

Figure 1.16 – Serine recombinase recognition site. A) The represented site is recognized by Tn3 resolvase. Black arrows represent the recombinase binding sites and the red line is the crossover-site, where the cleavage and strand exchange take place. After the cleavage, each 3´ end will have a 2-nucleotide overhang. **B)** Larger recognition sites contain accessory sequences downstream or upstream of the crossover site (A). For instance, the Tn3 resolvase site contains two additional accessory sites (II and III), each of which binds a dimer of resolvase.

First, the recombinase finds its two double-stranded recognition sites and brings them together by forming a tetramer (Figure 1.17). The serine residue in each recombinase monomer attacks the phosphodiester bond of DNA, with each monomer introducing a single-strand break in the site. The serine remains covalently bound to the 5´ phosphorous of each strand, forming four phosphoserine bonds. The half-sites are exchanged by 180° rotation of the subunit and re-ligated (Figure 1.17) (Stark, 2014).

ΦC31 integrase (Int) is an example of a large serine integrase isolated from *Streptomyces coelicolor* (Lomovskaya *et al*, 1972). This integrase is used by the phage to integrate its

circular DNA into the host's chromosome, by the mechanism just described. Int recognizes a site known as the 'phage' attachment site (*attP*) in the phage genome. A second *att* site is present in the bacterial chromosome (*attB*) (Figure 1.18). Both sites are around 40-50 bp and they are not identical. Once recombined they form two new sites, *attL* and *attR*, non-identical as well (Rausch and Lehmann, 1991). Recombination between *attP* and *attB* integrates the phage DNA into chromosome to produce integrated prophage flanked by *attL* and *attR*. This reaction is unidirectional, unless a recombination directionality factor (RDF) is expressed, which promotes *attL* x *attR* and inhibits *attP* x *attB* recombination (Thorpe and Smith, 1998) (Figure 1.18).

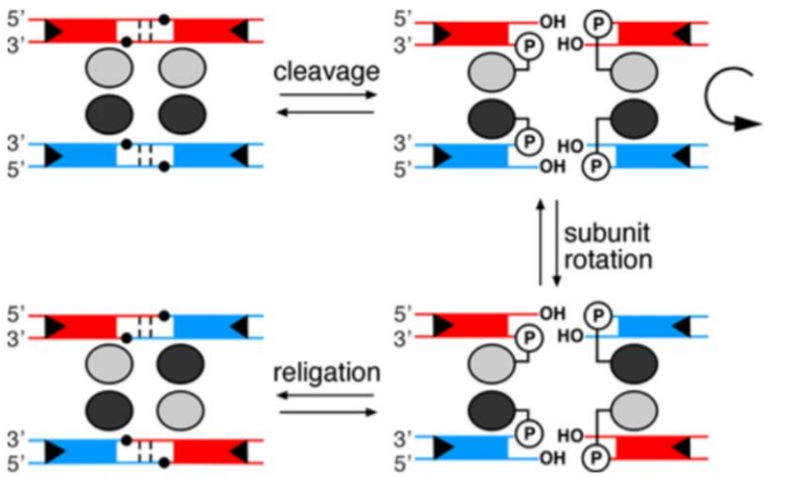

Figure 1.17 – Serine recombinase mechanism. The recombinase tetramer is represented by two grey and two black circles. The recognition sites are in red and blue. The central region of the sites, where the cleavage occurs is in white. The small black dots represent the phosphodiester groups attacked by serine residues and P represent the phosphoserine links. From Olorunniji *et al* (2015) with permission.

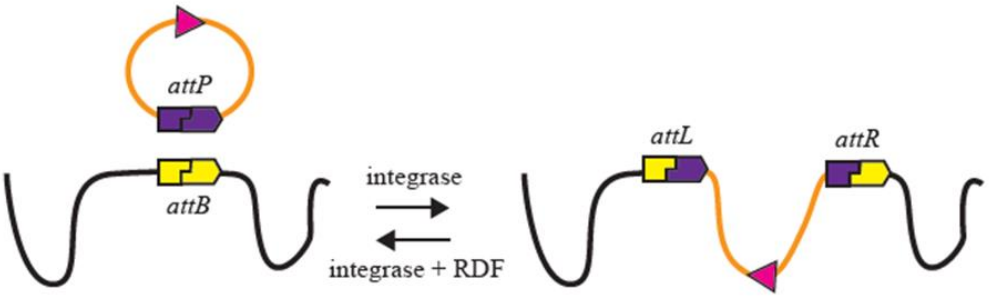

Figure 1.18 – ΦC31 integrase mediated recombination. Integrase recognizes the *attP* site (phage) and the *attB* site (host chromosome) and performs phage integration. Once integrated, the phage can only be excised by recombination between *attL* and *attR*, if the RDF is expressed with integrase.

Although the biological role of Int is integration of phage DNA by *attP* x *attB* recombination, and excision of prophage by *attL* x *attR* recombination, Int can perform fusion, deletion and inversion between *attP* x *attB* and *attL* x *attR* sites (Zieg *et al*, 1977; Colloms *et al*, 2014). Also, the *att* sites do not have to be supercoiled since Int can recognize and recombine linear sites (Colloms *et al*, 2014).

1.5.2 Tyrosine recombinases – XerC and XerD

Tyrosine recombinases differ from serine recombinases in the way they perform strand exchange, and in the recognition sites. The recognition site is also an imperfect palindrome but the spacer between the enzyme binding regions vary from 6 to 8 bp, unlike the fixed 2 bp for serine recombinases (Figure 1.16A) (Grindley *et al*, 2006). Examples of tyrosine recombinases are Cre and FLP recombinases, which participate in plasmid dimer resolution and increase in the plasmid copy-number, respectively (Austin *et al*, 1981; Volkert and Broach, 1986). Other tyrosine recombinases are the XerCD, which participate in chromosome dimer resolution (Sherratt *et al*, 1995).

The recombinase binds to its recognition sites and brings them together by formation of a tetramer (Figure 1.19A). Tyrosine recombinases do two sequential single-strand cleavages instead of two double-strand breaks at once. Two active monomers introduce a single-strand break in each crossover-site. These breaks are made by a nucleophilic attack by the hydroxyl group of the tyrosine, which establishes a phosphotyrosine bond with the 3´ end of each strand (Figure 1.19B). Then, the free 5´ ends attack the 3´ phosphotyrosine links of the opposite molecule, which creates a Holliday junction (structure with the two double-strands connected to each other) (Figure 1.19C). The intermediate is resolved by repetition of the previous steps by the other two recombinase monomers (Figure 1.19D-F) (Olorunniji *et al*, 2016; Jayaram *et al*, 2014).

Bacteria use XerCD recombination to resolve plasmid and chromosome dimers, produced by homologous recombination (Sherratt *et al*, 1995; Colloms *et al*, 1996; Barre *et al*, 2000; Grindley *et al*, 2006). This ensures faithful segregation of genetic material to the daughter cells. XerCD recognize the *dif* site, present in the chromosome terminus. The site consists of 11-bp recognized by XerC and another 11-bp by XerD, and they are separated by a 6-bp spacer region (Figure 1.20) (Colloms *et al*, 1996). Plasmids have many natural sites recognized by XerCD, examples of which are *cer* (plasmid ColEI) and *psi* (plasmid

pSC101) (Figure 1.20). Recombination on *cer* requires ArgR and PepA, while on *psi* ArcA and PepA (Stirling *et al*, 1988; Colloms *et al*, 1996; Colloms *et al*, 1997). The presence of accessory proteins in recombination on plasmid is thought to ensure intramolecular recombination to prevent multimerization (Summers and Sherratt, 1984).

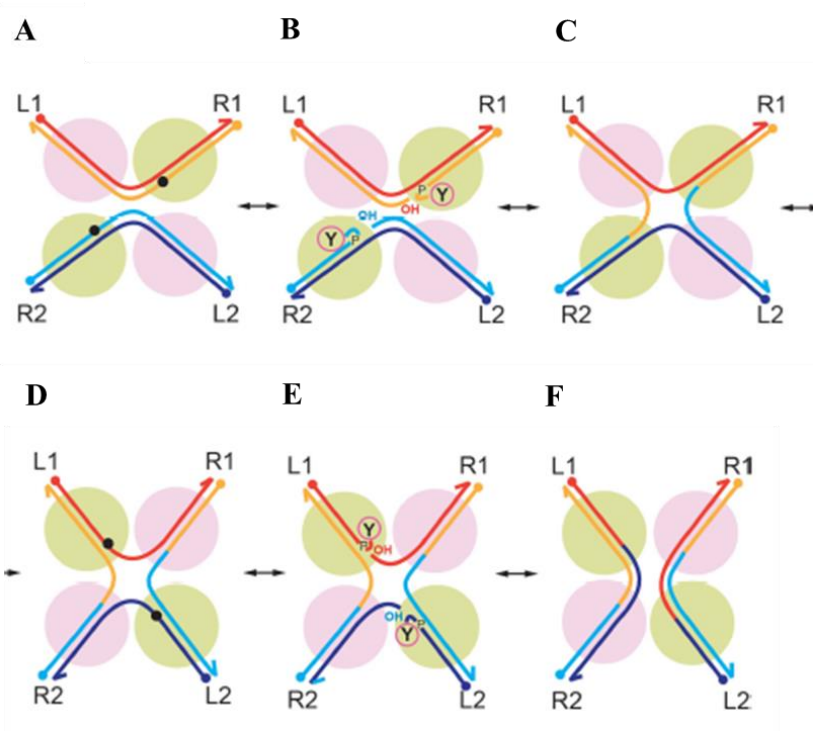

Figure 1.19 – Tyrosine recombinase mechanism. L1, L2, R1 and R2 are left and right sides of the recognition site bind by the recombinase, respectively. The four enzyme subunits are represented by the circles, being the active monomers coloured in yellow, and inactive in pink. The small black dots represent the phosphodiester groups attacked by tyrosine residues. The circled Y represents the phosphotyrosine links. From Jayaram *et al* © 2014 American Society for Microbiology. Used with permission. No further reproduction or distribution is permitted without the prior written permission of American Society for Microbiology.

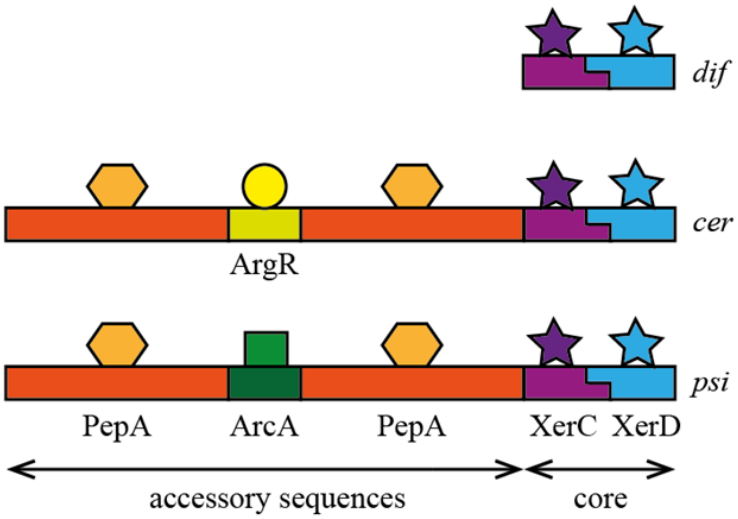

Figure 1.20 – Recombination sites recognized by XerCD recombinases. The core site contains the XerC and XerD binding sites separated by 6 (*dif* and *psi*) or 8 (*cer*) bp. The accessory sequences and proteins required for recombination on plasmid site *cer* are ArgR and PepA, and on *psi* are ArcA and PepA.

Chromosome dimer resolution by XerCD *in vivo* is assisted by FtsK, a DNA translocase. The FtsK N-terminal domain has transmembrane properties, which anchors the protein to the membrane of closing septum of the dividing bacteria (Figure 1.21) (Wang and Lutkenhaus, 1998). On the other hand, the C-terminal domain participates in chromosome dimer resolution, so each chromosome ends up in each daughter cell (Steiner *et al*, 1999). If a dimer is present, recombination at *dif* is required and FtsK is involved in activating Xer recombination.

Dimer resolution initiates by FtsK binding to the DNA and recognizing the FtsK-orienting polar sequences (KOPS), which are 8-bp sequences that point from *ori* to *dif* and promote translocation of the DNA towards the *dif* site by FtsK (Bigot *et al*, 2005; Sivanathan *et al*, 2006). This translocation allows each chromosome to migrate to the respective daughter cell and stops when FtsK reaches the XerC and XerD bound to the *dif* sites, with the two *dif* sites aligned in the bacterial septum (Figure 1.21). The site-specific recombination is initiated by direct contact between FtsK and XerD, which initiates the first strand exchange (1.19A-C) (Yates *et al*, 2006). The HJ formed by XerD is resolved by XerC (Figure 1.19D-F) (Aussel *et al*, 2002; Grainge *et al*, 2011). The chromosome dimer resolution by XerCD-*dif*-FtsK allows faithful DNA segregation and cell division.

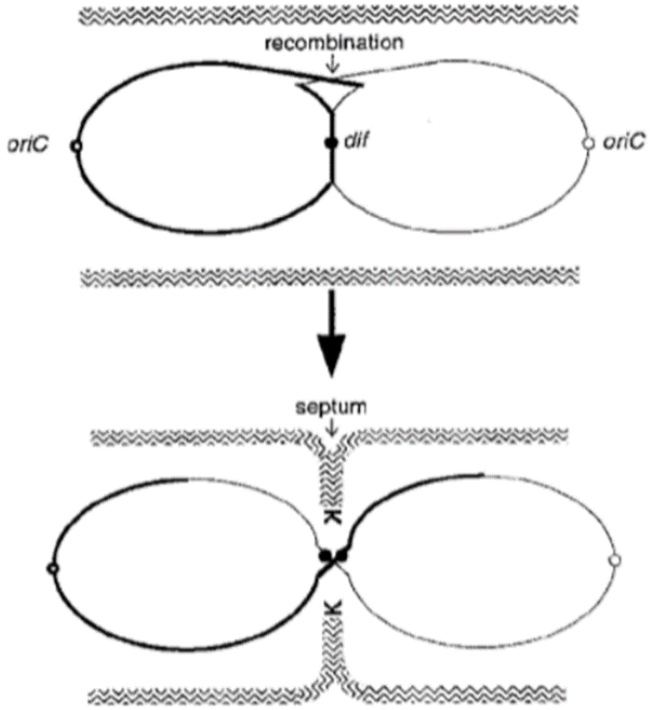

Figure 1.21 – FtsK-dependent chromosome dimer resolution. Homologous recombination prior to replication termination produces chromosome dimers. After replication termination, FtsK (K) promotes dimer resolution at the septum by activating XerCD recombination. *oriC*, origin of replication; hatched lines represent cell envelope. From Steiner *et al* (1999) with permission. Order number 4505971238905.

1.6 XerCD-*dif*-FtsK mediated recombination in decatenation

As described previously, bacteria use XerCD-*dif*-FtsK mechanism to resolve chromosome dimers, which are formed by homologous recombination during replication. Although catenanes are two intertwined circles, could XerCD-*dif*-FtsK promote decatenation by successive rounds of recombination between the *dif* site on each molecule? For instance, if the two chromosomes were intertwined six times, one round of recombination would produce a dimer with five nodes (Figure 1.22A), and another round of recombination would give a catenane with four crossings. So, the stepwise resolution of crossings between the two molecules would end in the two decatenated chromosomes (Figure 1.22B).

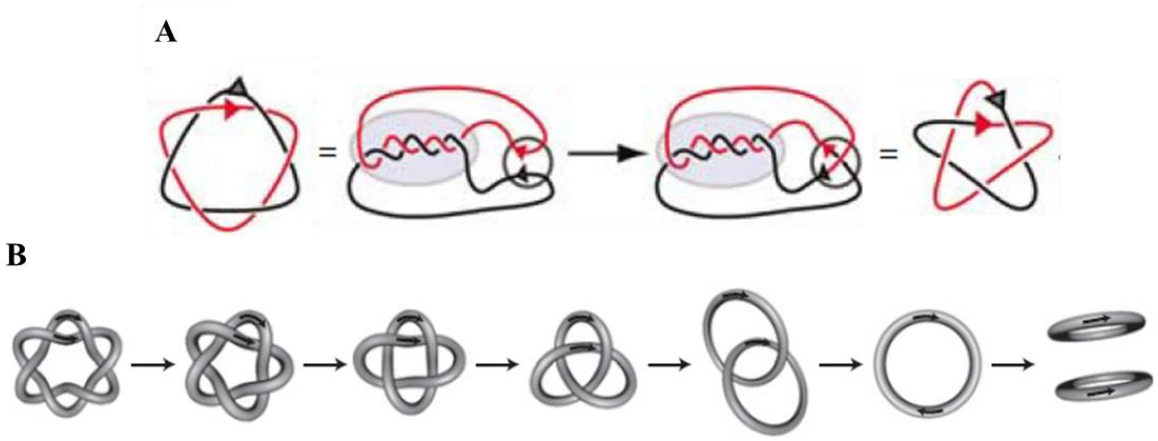

Figure 1.22 – Decatenation by XerCD-*dif*-FtsK recombination. A) Example showing the first step of recombination. Recombination between *dif* sites (black and red arrow heads) on the two chromosomes interlinked six times produces a dimer with five crossings. Adapted from Grainge *et al* (2007) with permission. Order number 4505980059683. **B)** Stepwise recombination between the *dif* sites (black arrows) on each chromosome leads to interconversion from catenane to knot, ending with the two unlinked circles. From Shimokawa *et al* (2013) with permission.

Catenated plasmids, formed through site-specific recombination, have been shown to be unlinked by XerCD-*dif*-FtsK *in vitro* (Ip *et al*, 2003). This mechanism also unlinked *in vitro*, catenated plasmids formed from replication *in vivo* (Grainge *et al*, 2007). However, there is no direct evidence of decatenation by XerCD-*dif*-FtsK recombination of the catenated chromosomes *in vivo*.

1.7 Aim of the study and thesis outline

Formation of precatenanes has been widely assumed to occur on chromosome and on plasmid DNA. Cohesion of sister chromosomes after replication fork passage is assumed to reflect precatenation that must be removed prior to segregation. There is evidence for precatenation of plasmids in *E. coli* (Cebrián *et al*, 2015); however, no direct evidence has been provided of precatenation of the bacterial chromosome.

In this work we tried to address the following question: does precatenation occur *in vivo*? Can a method be developed that would allow us to study formation of precatenation on the bacterial chromosome?

To obtain an answer, site-specific recombination was used as the main approach. Two recombination sites recognized by ΦC31 integrase (*attP* and *attB* sites) were introduced into the chromosome. After the replication fork has passed those sites, it produced two sister chromosomes, each with a pair of *att* sites. If the two chromosomes were not precatenated, the recombination products would be the deleted segments between the two sites on each chromosome (Figure 1.23A). Alternatively, if precatenation was present, the recombination would yield catenanes by entrapping the intertwines between the sister chromosomes (Figure 1.23B). The advantage of using phage ΦC31 integrase is that once formed, *attL* and *attR* sites will not recombine further. Thus, preserving the initial topology of the recombination products.

First, it was important to determine the condition necessary for catenane formation and develop a method for their detection (Chapter 3). To do so, site-specific recombination was performed on plasmid *in vivo* and Southern hybridization was used to detect the products. Second, we wanted to create a plasmid model that would mimic formation of precatenanes on the chromosome (Chapter 4). The *terE* site was inserted into a plasmid to create a replication intermediate and induced site-specific recombination to trap precatenation in the replicated region. This model could give us information about the efficiency of this method in studying precatenation on chromosome. Third, precatenation on the bacterial chromosome was studied by the method developed in Chapter 3 (Chapter 5). We studied precatenation in two regions of chromosome, both associated with replication termination.

An additional work was made to study the level of supercoiling in a small circle (398 bp) resultant from Xer site-specific recombination at closely spaced *psi* sites on a plasmid (Chapter 6). For example, would supercoiling present in that region be trapped and preserved in the 398 bp circle or would it be eliminated. These experiments gave insight on the linkage change of the site-specific recombination reaction by tyrosine recombinases.

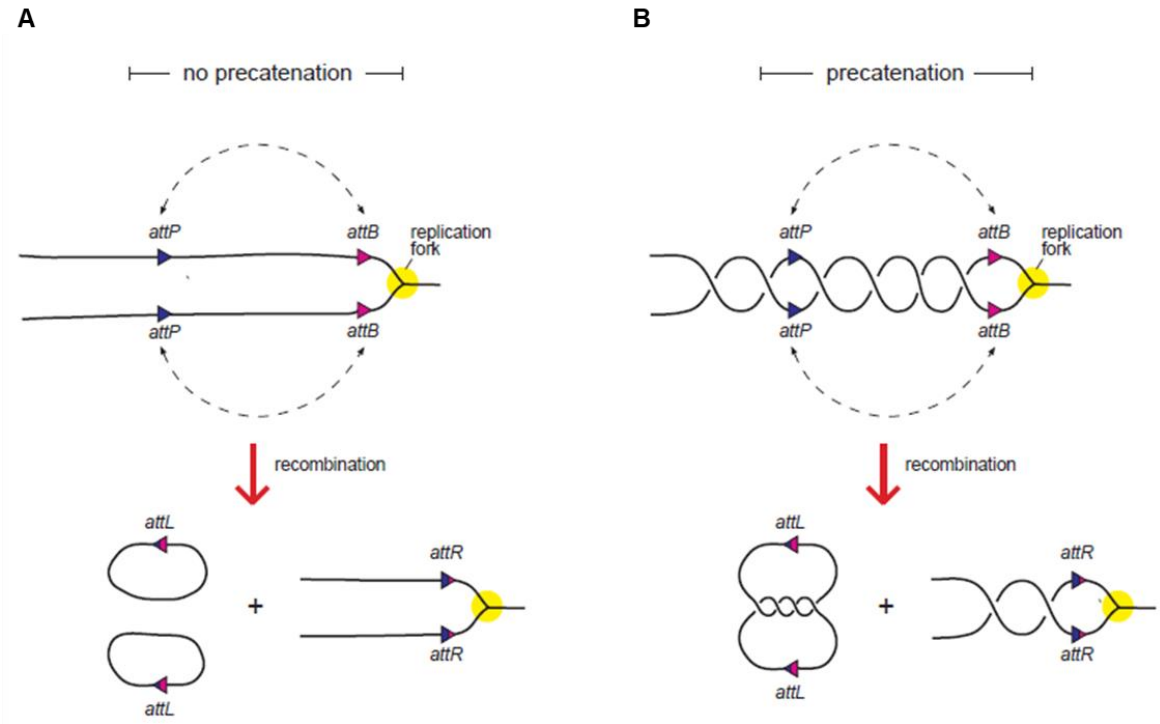

Figure 1.23 – Precatenane entrapment by site-specific recombination. A) If the replicated sister chromosomes are not intertwined, then recombination between the *att* sites results in unlinked circles and the rest of the chromosome. **B)** If the sister chromosomes are precatenated, then the recombination yields catenated circles.

2. Materials and Methods

2.1 Bacterial Strains

The derivation of bacterial strains used in this work are listed in Table 1.

Table 1 – **Bacterial strains**

Strain	Genotype	Reference
AB1157	F$^-$ *thr-1 araC14 leuB6*(Am) *Δ(gpt-proA)62 lacY1 tsx-33 qsr'-0 glnX44*(AS) *galK2*(Oc) *λ$^-$ Rac-0 hisG4*(Oc) *rfbC1 mgl-51 rpoS396*(Am) *rpsL31*(Str^R) *kdgK51 xylA5 mtl-1 argE3*(Oc) *thiE1*	DeWitt and Adelberg, 1962
C600	*thr-1 leuB6*(Am) *fhuA21 cyn-101 lacY1 glnX44*(AS) *λ$^-$ e14- rfbC1 glpR200(glp^c) thiE1*	Appleyard, 1954
C600S	C600 *recA* Str^R	Kratz *et al*, 1983
C600SN	C600S *gyrA^{L83}*	Heisig *et al*, 1991 Obtained from D. Sherratt
W1485	F$^+$ *glnV42(AS) λ$^-$ rpoS396(Am) rph-1*	Lederberg and Lederberg, 1953
CB0129	F$^-$ W1485 *thyA leu deoB or C supE*	Berg and Curtiss III, 1967
LN2666	CB0129 *rpsL2666* (Str^R)	Cornet *et al*, 1994
CP100	LN2666 *ΔlacI*	Nolivos *et al*, 2010 Obtained from F. Cornet
DH5	F$^-$ *Δ(lacZYA-argF) U169 recA1 endA1 hsdR17 (r_k-, m_k+) phoA supE44 λ- thi-1 gyrA96 relA1*	Hanahan, 1985
DH5α	DH5 *Φ80 lacZ*ΔM15	Hanahan, 1985
DS941	AB1157 *recF lacI^q lacZ*ΔM15	Summers and Sherratt, 1988
DS9008	DS941 *xerD2::Tn10-9* Km^R	Blakely *et al*, 1993
DS984	DS941 *xerC::Y17* (::mini Mu Cm^R)	Colloms *et al*, 1990
Am – amber mutation, UAG mutation at leucine 6; AS – amber suppressor, tRNA inserts glutamine instead of stop codon; Oc – ochre mutation, GAA to TAA at residue 134.		

2.2 Plasmids

The plasmids used in this work and their descriptions are listed in Table 2.

Table 2 – **Plasmids**

Plasmid	Antibiotic	Description	Reference
pBH400	Amp^R	XerC expression vector	B. Hallet
pBR322	Amp^R Tet^R	Cloning vector with pMB1 origin of replication; low copy number plasmid	Bolivar *et al*, 1977
pKOBEGC	Cm^R	Recombination vector which contains λ phage Red operon system; $pSC101^{ts}$ origin of replication	Chaveroche *et al*, 2000
pMS183	Km^R	Cloning vector; pSC101 origin of replication	M. Stark
pMS183Δ	Km^R	Derivative of pMS183 with a 16 bp deletion (NdeI-NdeI); used as a cloning vector	Olorunniji *et al*, 2017
pMTL23	Amp^R	Cloning vector with ColEI origin of replication; high copy number plasmid	Chambers *et al*, 1988
pRM132	Amp^R	XerD expression vector	Blakely *et al*, 1993
pSDC153	Amp^R	Plasmid containing two *psi* sites in direct repeat	Colloms *et al*, 1997
pTRC99a	Amp^R	Expression plasmid, source of $lacI^q$ fragment	Amann *et al*, 1988
pUC4K	Amp^R Km^R	Source of Km^R fragment	Vieira *et al*, 1982
pZJ7	Cm^R	pBAD33-based expression vector for ΦC31 integrase under arabinose inducible promoter; p15a origin of replication; *int* gene with the starting codon ATG	Zhao, 2015

pZJ7m	Cm^R	pZJ7-based plasmid with the *int* gene starting codon changed to GTG	Zhao, 2015
pAOT1	Amp^R Km^R	pMTL23-based plasmid containing Km^R fragment from pUC4K	Chapter 3
pAOT2	Amp^R Km^R	pAOT1-based plasmid containing directly repeated *attP* and *attB* sites surrounding Km^R gene	Chapter 3
pAOT3	Amp^R Km^R	pAOT2-based plasmid containing $lacI^q$ fragment from pTRC99a, inserted between Km^R gene and *attB* site	Chapter 3
pAOT5	Km^R	pMS183Δ-based plasmid containing the NgoMIV-NcoI fragment from pAOT3 with *attP* and *attB* sites, Km^R and $lacI^q$	Chapter 3
pAOT10	Amp^R Km^R	pBR322-based plasmid containing *terE*, and the BamHI-NcoI fragment from pAOT3 with *attP* and *attB* sites, Km^R and $lacI^q$	Chapter 4
pAOT12	Amp^R Km^R	pAOT3-based plasmid containing *terE*	Chapter 4

2.3 Antibiotics

The antibiotics used in this work are listed in Table 3.

Table 3 – **Antibiotics used**

Antibiotic	**Stock concentration**	**Selective concentration**
Ampicillin (Amp)	100 mg/ml in H_2O	100 µg/ml
Chloramphenicol (Cm)	25 mg/ml in ethanol	25 µg/ml
Kanamycin (Km)	25 mg/ml in H_2O	25 µg/ml
Norfloxacin (Nor)	10 mg/ml in H_2O (10 µl of acetic acid glacial added per 1ml)	10 µg/ml
Streptomycin (Str)	50 mg/ml in H_2O	50 µg/ml

2.4 Chemicals and buffer solutions

The chemicals used in this work are listed in Table 4.

Table 4 - **Chemicals**

Chemicals	**Source**
General chemicals, biochemicals, organic solvents	Sigma/Aldrich, VWR chemicals, Fisher Scientific
Agarose, acrylamide	Invitrogen, VWR chemicals
Restriction enzyme, ligase and PCR buffers	New England Biolabs

The buffers used in this work are listed in table 5.

Table 5 – **Buffer solutions**

Buffer solutions	**Composition**
Agarose gel loading dye	30% glycerol, 0.5% SDS, 0.25% bromophenol blue in TE buffer
Agarose gel loading dye + protease K	30% glycerol, 0.5% SDS, 0.25% bromophenol blue, 0.2 mg/ml protease K in TE buffer
Loading dye for SDS-PAGE of proteins	250 mM Tris-HCl (pH 6.8), 30% glycerol, 10% SDS, 0.05% bromophenol blue, 0.1 M DTT
TE	10 mM Tris-HCl (pH 8.0), 1 mM EDTA (pH 8.0)
TE0.1	10 mM Tris-HCl (pH 8.0), 0.1 mM EDTA (pH 8.0)
TAE 1x	40 mM Tris base, 20 mM acetic acid, 1 mM EDTA (pH 8.0)
E buffer 1x	40 mM Tris base, 25 mM acetic acid, 1 mM EDTA (pH 8.0), 20 mM sodium acetate
Tris Glycine running buffer (5x)	0.12 M Tris base, 1.25 M glycine, 0.5% SDS
TA-$CaCl_2$ 1x	40 mM Tris base, 20 mM acetic acid, 10 mM $CaCl_2$
20x SSC	0.3 M Tri-sodium citrate, 4.4 M NaCl
100x Denhardt's solution	2% (w/v) BSA, 2% (w/v) Ficoll 400, 2% (w/v) polyvinylpyrrolidone
ΦC31 integrase dilution buffer (IDB)	25 mM Tris-HCl (pH 7.5), 1 mM DTT, 1 M NaCl, 50% glycerol
ΦC31 integrase reaction buffer (4x IRB)	200 mM Tris-HCl (pH 7.5), 0.4 mM EDTA, 20 mM spermidine [3HCl], 0.4 mg/ml BSA
Topo I dilution buffer (calf thymus)	30 mM K-phosphate buffer (pH 7.0), 5 mM DTT, 0.1 mM EDTA, 0.2 mg/ml BSA, 50% glycerol, 0.1% (w/v) Triton X-100
XerC dilution buffer	50 mM Tris-HCl (pH 8.0), 1 M NaCl, 1 mM EDTA, 50% glycerol

XerD dilution buffer	50 mM Tris-HCl (pH 8.0), 0.9 M NaCl, 1 mM EDTA, 1 mM DTT, 50% glycerol
PepA dilution buffer	20 mM Tris-HCl (pH 7.5), 400 mM NaCl, 50% glycerol
XerC/D PepA reaction buffer (4x *psi* buffer)	200 mM Tris-HCl (pH 8.0), 100 mM KCl, 5 mM EDTA, 20 mM spermidine [3HCl]
NEB CutSmart (10x)	0.5 M potassium acetate, 0.2 M Tris-acetate, 0.1 M magnesium acetate, 1 mg/ml BSA, pH 7.9 at 25°C

2.5 Oligonucleotides

All oligonucleotides were synthesised commercially by Integrated DNA Technologies (Eurofins MWG Operon). These were dissolved in $TE_{0.1}$ buffer to a concentration of 100 pmol/µl and stored at -20°C. Detailed information of the oligonucleotides is listed in Table 6.

Table 6 – **Oligonucleotides**

Oligo name	Length	Sequence (5´ -> 3´)	Purpose
BsrGI-lacI-F	34 bp	AAAAAATGTACAGCATGCATTTACGTTGACACCA	Forward primer used to amplify *lacI* from pTRC99a
XbaI-lacI-R	36 bp	AAAAAATCTAGAGATCAATTCGCGCTAACTCACATT	Reverse primer used to amplify *lacI* from pTRC99a
attP-SB-top	59 bp	TCGACAGTAGTGCCCCAACTGGGGTAACCTTTGAGTTCTCTCAGTTGGGGGCGTAGGGG	Top oligo used to insert *attP* into pAOT1 digested with SalI and BamHI
attP-SB-bot	59 bp	GATCCCCCTACGCCCCCAACTGAGAGAACTCAAAGGTTACCCCAGTTGGGGCACTACTG	Bottom oligo used to insert *attP* into pAOT1 digested with SalI and BamHI
attB-SE-top	69 bp	CCCGCGGTGCGGGTGCCAGGGCGTGCCCTTGGGCTCCCCGGGCGCGTACTCCACCTACCGGTTGTACAG	Top oligo used to insert *attB* into pAOT1 digested with SacI and EcoRI
attB-SE-bot	77 bp	AATTCTGTACAACCGGTAGGTGGAGTACGCGCCCGGGGAGCCCAAGGGCACGCCCTGGCACCCGCACCGCGGGAGCT	Bottom oligo used to insert *attB* into pAOT1 digested with SacI and EcoRI
dif+::km-lac-F	68 bp	TGATGCGAAGTGCTTTTCTGGTAGTCGTTATTCGTTCAGGGTTCAAGAACATGCCATGGTACCCGGGA	Forward primer used to amplify *attB-lacI*-Km^R-*attP* from pAOT3 and insert it on the chromosome near *dif*
dif+::km-lac-R	70 bp	CCATTTCTGATACCGGAGTGGACTCATTCCCGCTTGATCCGTCCTTAAATCCAGTGAATTGCCGGCGATA	Reverse primer used to amplify *attB-lacI*-Km^R-*attP* from pAOT3 and insert it on the chromosome near *dif*
dif-flank-F	20 bp	GTTGCATGGACGGTTAAGCC	Forward primer used to verify *attB-lacI*-Km^R-*attP* insertion into chromosome

lac-mid-R	20 bp	CCGCTTCGTTCTACCATCGA	Reverse primer used to verify *attB-lacI*-Km^R-*attP* insertion into chromosome
kan-mid-F	20 bp	CGGTTTGGTTGATGCGAGTG	Forward primer used to verify *attB-lacI*-Km^R-*attP* insertion into chromosome
dif-flank-R	20 bp	GACTCTCCAAACATCCGCGA	Reverse primer used to verify *attB-lacI*-Km^R-*attP* insertion into chromosome
dif-out-F	21 bp	TGCATGGAGAAATAGCCTGGT	Forward primer used to verify *attB-lacI*-Km^R-*attP* insertion into chromosome
gyrAL83 fwd	21 bp	GCGGCTGTGTTATAATTTGCG	Forward primer used to verify gyrAL83 mutation on chromosome
gyrAL83 rev	20 bp	ACGACCGTTAATGATTGCCG	Reverse primer used to verify gyrAL83 mutation on chromosome
terE + NcoI site top	35 bp	AATTCGGCTTAGTTACAACATACTTTAACCATGGA	Top strand used to clone *terE* site into pBR322 digested with EcoRI and HindIII
terE + NcoI site bottom	35 bp	AGCTTCCATGGTTAAAGTATGTTGTAACTAAGCCG	Bottom strand used to clone *terE* site into pBR322 digested with EcoRI and HindIII
incassette_ lacI_fwd	20 bp	TAGCGGGCCCATTAAGTTCT	Forward primer used to verify *attB-lacI*-Km^R-*attP* insertion into chromosome

incassette_ kmR_rev	20 bp	TCGCGAGCCCATTTATACCC	Reverse primer used to verify *attB-lacI*-Km^R-*attP* insertion into chromosome
tam::cassette fwd	68 bp	TTTATCAATTTTATCTACAATTGGGGTAACGCGCTGACGGGAG TAAAAAAATGCCATGGTACCCGGGA	Forward primer used to amplify *attB-lacI*-Km^R-*attP* from pAOT3 and to replace *tam* for the cassette on chromosome
tam::cassette rev	70 bp	AATTCCAGCAAAAATTCTTCCCGATCGTCATTACCAGCTGACG TGATATTCCAGTGAATTGCCGGCGATA	Reverse primer used to amplify *attB-lacI*-Km^R-*attP* from pAOT3 and to replace *tam* for the cassette on chromosome
tam_fwd	20 bp	ACGTAATCCAGTGGCAGTCA	Forward primer used to verify *tam* presence/absence on the chromosome
tam_rev	20 bp	CACCGCCCTTCTACAACAAC	Reverse primer used to verify *tam* presence/absence on the chromosome
tam_flank_ rev	21 bp	GGAATCTTTAATGACCGGGCC	Reverse primer used to verify *attB-lacI*-Km^R-*attP* insertion into chromosome
terE + EcoRI site top	35 bp	CCGGCGGCTTAGTTACAACATACTTTAAGAATTCG	Top strand used to clone *terE* site into pAOT3 digested with NgoMIV and BamHI
terE + EcoRI site bottom	35 bp	GATCCGAATTCTTAAAGTATGTTGTAACTAAGCCG	Bottom strand used to clone *terE* site into pAOT3 digested with NgoMIV and BamHI

2.6 Bacterial growth conditions

Bacteria were grown in liquid LB (10 g/L peptone, 5 g/l yeast extract and 5 g/l sodium chloride) with appropriate antibiotic at 37°C and in a 225 rpm shaking incubator (New Brunswick Scientific, Excella E24 Incubator Shaker Series) overnight, unless a temperature sensitive plasmid was present. These strains were grown at 30°C instead. Solid media was made by adding 15 g agar per litre of liquid broth. All media was autoclaved at 121°C for 30 min. For bacteria grown on solid agar the plates were incubated at 37°C overnight. For blue/white screening, X-gal was used at 40 µg/ml and was directly added to the melted agar before pouring. For growth of CP100, thymidine was added at 70 µg/ml to the media.

2.7 Preparation of chemically competent cells

3 ml of LB was inoculated with the desired *E. coli* strain and grown overnight in the shaking incubator. The next day, 0.4 ml of this culture was diluted 50-fold into 20 ml of fresh LB and grown for 90 min with shaking. Cells were pelleted at 6,000 x *g*, 4°C for 3 min, then resuspended in 10 ml of ice-cold 50 mM $CaCl_2$ and left in ice for at least 1 h. Competent cells were pelleted as described above and resuspended in 1 ml of ice-cold $CaCl_2$, ready for transformation.

2.8 Transformation of chemically competent cells with plasmid DNA

Chemically competent cells were used for routine transformation with plasmid DNA. In each transformation, 100 µl of competent cells were used together with 1 µl of plasmid DNA, or 2 µl of ligation reaction. The mixture was incubated on ice for 20 min, then heat shocked at 42°C for 1 min and returned to ice for 2 min. 200 µl of LB was added to each tube and they were incubated at 30°C or 37°C for 60-90 min to allow expression of the antibiotic resistance genes. For the final step, 100-200 µl of culture with bacteria were spread on L-Agar plates containing the appropriate antibiotic. Plates were incubated at 30°C or 37°C overnight.

When using commercially competent cells (for example Library Efficiency DH5α (Invitrogen)) the transformations were made according to the manufacturer's instructions.

2.9 Preparation of electrocompetent cells

To perform a gene knockout in a strain, the strain was first made chemically competent and transformed with pKOBEGC (Chaveroche *et al*, 2000), which codes for the λ red machinery and has a temperature sensitive origin of replication. Transformants were therefore grown at 30°C. After the strain had been transformed with pKOBEGC, it had to be made electrocompetent as described below, prior to electroporation with linear DNA for gene knockout.

3 ml of LB was inoculated with the desired *E. coli* strain containing pKOBEGC and grown overnight in the presence of chloramphenicol at 30°C with shaking. The next day, this culture was diluted 20-fold into 25 ml of fresh LB and grown at 30°C until OD_{600} of 0.2 was reached. At this point, 0.2% arabinose was added to the culture to induce expression of the λ phage Red operon. Cells were grown further at 30°C until OD_{600} of 0.6 was reached (approx. 120 min). Cells were cooled on ice for 10 min and harvested at 6,000 x *g*, 4°C for 3 min. The cell pellet was washed in 26 ml of ice-cold 10% glycerol and bacteria harvested by centrifugation as described above. Cells were washed again in 26 ml of ice-cold 10% glycerol and harvested by centrifugation. The pellet was resuspended in 1 ml of ice-cold 10% glycerol and centrifuged at 15,700 x *g*, 4°C for 30 sec. The final cell pellet was resuspended in 200 µl of ice-cold 10% glycerol, ready for electroporation.

When electrocompetent cells were made without pKOBEGC, the incubation steps were made at 37°C instead of 30°C and no arabinose was added.

2.10 Electroporation of electrocompetent cells with linear DNA

Electrocompetent cells were used in electroporation with linear DNA. Linear DNA was amplified by PCR (see section 2.21 in this chapter), the sample was treated with *DpnI* for template degradation and linear DNA purified by QIAquick PCR purification kit (QIAGEN). To avoid UV exposure, which was found to reduce recombination efficiency severely, the DNA was not purified from a gel.

40 µl of electrocompetent cells were used per reaction together with 2-5 µl of PCR amplified, purified linear DNA. The mixture was put on ice and then transferred to an ice-cold electroporation cuvette. Electroporation was made with the Bio-Rad MicroPulser, which was pre-programmed at EC2 (one pulse at 2.5 kV in 0.2 cm cuvettes with time constant at approx. 6 ms) according to the cell type and cuvette size. After the electrical pulse was delivered, 1 ml of LB was added, the mixture was transferred to a 1.5 ml eppendorf and incubated at 30°C, 400 rpm (Eppendorf, Thermomixer compact) for 2-3 h. 200 µl of cells were spread on selective agar plates and incubated at 30°C and/or 37°C overnight. The homologous recombination between the linear DNA and the chromosome occurred during the expression step, leading to gene knockout.

2.11 Plasmid DNA preparation

Plasmid DNA was prepared using different techniques including alkaline lysis methodologies (Mini- and Midiprep) and non-denaturing ones for the isolation of replication intermediates.

2.11.1 Plasmid extraction by alkaline lysis

Plasmid DNA was extracted using QIAprep Spin Miniprep Kit (QIAGEN). For each plasmid, 4-5 ml of overnight culture was used, and the plasmid extracted using the manufacturer's instructions. The HiSpeed Plasmid Midi Kit (QIAGEN) was used for large scale plasmid DNA preparation, and the starting overnight culture was 150 ml.

2.11.2 Preparation of crude lysate by Triton lysis

When trying to isolate plasmid replication intermediates, denaturing methods such as Midi and Miniprep Kits (QIAGEN) are not suitable. During denaturation, the replicated double-strands of the intermediate are separated, and the single-strands with no covalently closed ends are lost. During renaturation, the two single-strands that were used as template by DNA polymerase hybridise together, producing the original plasmid without the replication intermediate topology. The method described below was modified from Heilig *et al*, 1998.

An overnight culture containing the desired plasmid was diluted 40-fold into 500 ml of fresh LB with the appropriate antibiotic. Cells were grown at 37°C with shaking until OD_{600} of 0.6, chilled on ice and centrifuged at 6,000 x *g*, 4°C for 5 min. The pellet was resuspended in 5 ml of 25% (w/v) sucrose, 50 mM Tris-HCl (pH 8.0) and 100 mM EDTA. To this suspension, the following solutions were added sequentially: 1.5 ml of 10 mg/ml lysozyme in 25 mM Tris-HCl (pH 8.0), 2 ml 0.5 M EDTA, 25 µl of 10 mg/ml RNase. The solution was mixed by gentle inversion at the end and was then incubated on ice for 15 min. To lyse the cells 2.5 ml Triton solution (3% (v/v) Triton X-100, 150 mM Tris-HCl (pH 8.0) and 200 mM EDTA) was added. The tube was inverted 3 times and incubated on ice for 20 min. Then the sample was centrifuged at 40,000 x *g*, 4°C for 60 min and the supernatant poured in a new tube. To this supernatant, 5 ml of prewarmed (37°C) proteinase K digestion buffer (1 M NaCl, 10 mM Tris-HCl (pH 9.0), 1 mM EDTA and 0.1% SDS) and 50 µl of 10 mg/ml of proteinase K were added. The solution was mixed and then incubated at 37°C for 30 min. Proteins were extracted twice with 16 ml of phenol:chloroform (1:1) and once with 16 ml of chloroform:isoamyl alcohol (24:1). 0.6 volumes of isopropanol were added to the final aqueous phase and this was left to stand at room temperature for 10 min. Then the DNA was pelleted at 15,000 x g for 10 min, washed with 2 ml of 70% ethanol and pelleted again. After drying at room temperature, the DNA was resuspended in 0.8-1 ml of H_2O.

2.12 DNA agarose gel electrophoresis

Agarose gel electrophoresis was used for routine DNA separation. Small (7cm x 8cm; 50 ml) and medium (9cm x 11cm; 80 ml) gels were 1% agarose made in 1x TAE and run at 80-90 V. These were used for separation of plasmid DNA, digestions, ligations and PCR products. Large gels (16cm x 23.5cm; 270 ml) were 0.7% or 1% agarose made in 1x E buffer and run overnight at 35 V. These were used for separation of topologies formed during recombination reactions and replication intermediates. Small and medium gels were stained with ethidium bromide and visualized in the Bio-Rad UV Transilluminator using Quantity One software. Large gels were stained with ethidium bromide or SYBR Gold (Thermo Fisher), and visualized in the Bio-Rad UV Transilluminator using Quantity One software, or using the Typhoon FLA 9500 (EtBr – LPG filter with excitation at 518 nm; SYBR Gold – LPB filter with excitation at 495 nm). The molecular marker used in all gels was 1 Kb Plus DNA Ladder (Invitrogen).

2.13 DNA PAGE

Small circle topology was studied by polyacrylamide gel electrophoresis. First, 40 ml of 5% polyacrylamide gel were made (5 ml Acrylogel 40% solution (37.5:1 acrylamide to bisacrylamide), 4 ml of 0.4 M Tris-acetate and 0.1 M $CaCl_2$, 30.5 ml H_2O, 0.5 ml of 10% APS and 20 µl of TEMED), poured between two glass plates spaced by 1.5 mm, comb inserted and allowed to polymerise at room temperature (size of gel 13cm x 17.5cm). Once solidified, the glass plates with the gel were inserted into the running tank, which was filled with 1x TA-$CaCl_2$ buffer. After the DNA samples were loaded into the wells the DNA was separated at 60V for 17 h. On the next day the gel was stained with SYBR Gold and the DNA detected with Typhoon FLA 9500 (LPB filter with excitation at 495 nm).

2.14 Protein SDS-PAGE

Proteins were separated by 10% sodium dodecyl sulphate-polyacrylamide gel electrophoresis. This gel is discontinuous, which means it is made of two different gels. First, the 10% acrylamide resolving gel was made (1.25 ml Acrylogel 40% solution (37.5:1 acrylamide to bisacrylamide), 1.25 ml 1.5 M Tris-HCl (pH 8.8), 50 µl 10% SDS, 2.42 ml H_2O, 50 µl 10% APS and 5 µl TEMED) and poured between two glass plates spaced by 0.75 mm. Some isopropanol was added to the top to prevent any bubbles from forming. The gel was let to polymerise at room temperature for 30 min. Then, isopropanol was washed away with water and the 4% acrylamide stacking gel was made (0.15 ml Acrylogel 40% solution (37.5:1 acrylamide to bisacrylamide), 0.375 ml 0.5 M Tris-HCl (pH 6.8), 15 µl 10% SDS, 15 µl 10% APS and 1.5 µl TEMED), poured up to the top of the glass plates and a comb inserted. After the gel had polymerised, it was inserted into the running tank and 500 ml of 1x Tris Glycine buffer added. Prior to gel loading, 100 µl of loading dye (5x) was added to 100 µl of protein samples, these were heated at 90°C for 5 min and 20 µl was loaded on the gel. Then proteins were separated at 90 V for 2 h and at the end gels were stained with Coomassie Blue for 1 h and destained in a solution containing 10% methanol and 10% acetic acid overnight.

2.15 DNA extraction from agarose gels

When a product of digestion was to be purified, all the DNA was first separated by agarose gel electrophoresis and stained with ethidium bromide. Upon visualization of the gel on the

UVP ultraviolet transilluminator (365 nm wavelength) the desired segment was cut from the gel and the DNA extracted using QIAquick Gel Extraction Kit (QIAGEN), according to the manufacturer's instructions. Gels for DNA extractions were prepared with SeaKem GTG agarose (BMA), certified for the recovery of nucleic acids.

2.16 Ethanol precipitation of DNA

To precipitate DNA, 1/10 volume of 3 M Na-Acetate (approx. pH 8.0) was added to the sample. Then 2.5 volumes of ice-cold 100% ethanol was added, the solution mixed and stored at -20°C for 1-4 h. The precipitated DNA was centrifuged at 15,700 x *g* for 60 min at 4°C and the pellet washed once with 70% ethanol. After drying at room temperature, DNA was resuspended in H_2O and stored at -20°C.

2.17 Phenol:chloroform and chloroform:isoamyl alcohol extractions of DNA

The DNA extractions with phenol:chloroform were made after DNA was used in reactions with ethidium bromide or other components such as proteins which had to be removed. Phenol and chloroform were added in equal parts (1:1), centrifuged for faster phases separations and stored at -20°C in a tube wrapped with foil. During the extraction, an equal volume of phenol:chloroform was added to the sample. The mixture was vortexed and centrifuged on a bench centrifuge at 15,700 x *g* for 3 min. The aqueous phase containing the extracted DNA was collected and analysed by gel electrophoresis or used in ethanol precipitation.

Chloroform:isoamyl alcohol were sometimes used to get rid of phenol from phenol:chloroform extracted DNA. The aqueous phase from a phenol:chloroform extracted sample was transferred to a new tube and an equal volume of chloroform:isoamyl alcohol (24:1) was added. Then the samples were centrifuged as above and the aqueous phase containing the extracted DNA was collected and analysed by gel electrophoresis or used in ethanol precipitation.

2.18 Restriction endonuclease digestion of DNA

Each reaction contained 2 µl of 10x reaction buffer (NEB), approx. 500 ng DNA, 10 U of enzyme (NEB) and water up to 20 µl. When the product of a recombination reaction was to be digested, instead of extracting and precipitating the DNA, the recombination reaction was directly used in digestion. This reaction contained 3 µl of 10x reaction buffer (CutSmart, 3.1 or 2.1 – NEB), 20 µl of DNA (recombination reaction), 10 U of enzyme and water up to 30 µl. DNA digestions were carried out at 37°C for 1 h and verified by agarose gel electrophoresis. When samples were digested with DpnI the reaction was carried out at 37°C overnight.

2.19 Ligation of DNA

Each ligation reaction contained 1 µl of 10x T4 DNA ligase reaction buffer (NEB), 4 µl of vector/fragment 1, 4-5 µl of insert fragment, 0.5 µl (200 U) of T4 DNA Ligase (NEB) and water up to 10 µl. The reaction was carried out at room temperature overnight.

2.20 DNA nicking

Some experiments involved DNA nicking with the purpose of removing the supercoiling in the molecules. This is required for the analysis of different topologies formed during recombination reactions. Two approaches were chosen to nick the DNA: using DNase I in the presence of ethidium bromide or using the nicking endonucleases.

2.20.1 DNase I

Each reaction contained 500 ng of DNA or 20 µl of digestion/recombination reaction, 3 µl of 10x DNase I reaction buffer (50% glycerol, 0.15 M NaCl, 10 mM Tris-HCl (pH 7.5), 0.1 M $MgCl_2$, 3 mg/ml EtBr, 10 µg/ml DNase I) and water up to 30 µl. The nicking reactions were carried out at 37°C for 1 h. Then 7.5 µl of loading dye were added and samples were incubated on ice for at least 15 min. Before loading the samples on the gel, ethidium bromide was removed by extraction with phenol:chloroform.

2.20.2 Nicking endonucleases

Each reaction contained 2 µl of 10x CutSmart (NEB), 500 ng DNA, 10 U of nicking endonucleases (NEB) and water up to 20 µl. When the product of a recombination or digestion reactions was to be nicked, instead of extracting and precipitating the DNA, the recombination or digestion reactions were directly used in digestion. These reactions contained 3 µl of 10x CutSmart (NEB), 20 ul of DNA (recombination or digestion reaction), 10 U of nicking endonuclease (NEB) and water up to 30 µl. Reactions were carried out at 37°C for 1 h and analysed by agarose gel electrophoresis.

2.21 Polymerase Chain Reaction (PCR)

PCR was used for amplification of the cassette, to be inserted into the chromosome, and for verification of the insertion. The primers used are listed in Table 6.

The cassette used for insertion near *dif* was amplified using Phusion High-Fidelity DNA Polymerase (NEB) and the reaction were carried out in 1x Phusion HF buffer with the following additions: 2.5 µl 2 mM dNTPs, 0.5 µl 50 mM $MgCl_2$, 0.75 µl 100% DMSO, 2.5 µl 5 µM dif+::km-lac-F, 2.5 µl 5 µM dif+::km-lac-R, 1 µl pAOT3 diluted 1000-fold in water, 0.5 µl (1 U) Phusion and water up to 25 µl. The program used started by 1 min denaturation at 98°C, followed by 30 cycles of denaturation at 98°C for 20 sec, annealing at 59°C for 30 sec and extension at 72°C for 2 min 30 sec, and a final extension at 72°C for 10 min.

The amplification of the cassette used for knockout of *tam* was made as described above but the following primers were used: tam::cassette fwd and tam::cassette rev.

Verification of cassette insertion was made using *Taq* 2x Master Mix (NEB). The enzyme was supplied in a buffer which already contained dNTPs and $MgCl_2$. For this reason, 25 µl reactions were carried out in half volume of *Taq* 2x Master Mix with the following additions: 1 µl 5 µM primer forward, 1 µl 5 µM primer reverse, 1 µl of plasmid diluted 1000-fold or 1 µl of a suspension of a colony in 10 µl of water. The program used started by 10 min denaturation at 95°C, followed by 25 cycles of denaturation at 95°C for 20 sec, annealing at 55°C for 30 sec and extension at 68°C for 1 min 30 sec, and a final extension at 68°C for 5 min.

2.22 PCR product purification

A QIAquick PCR Purification Kit (QIAGEN) was used when the PCR product was to be purified from the reaction mixture. The purification was made according to the manufacturer's instructions.

2.23 *In vitro* ΦC31 integrase mediated site-specific recombination

In vitro recombination with ΦC31 integrase were carried out on plasmid DNA or replication intermediates. The purified ΦC31 integrase was provided by co-workers. Each 20 µl reaction contained 0.5-1 µg of DNA, 5 µl of 4x IRB, 2 µl of 2-4 µM integrase and water up to 20 µl. After mixing, the reaction was carried out at 30°C for 30 min and the integrase inactivated at 80°C for 10 min. Control reactions were carried out with integrase dilution buffer (IDB) instead of ΦC31 integrase. When required, the sample was used in further procedures, such as nicking or digestion.

2.24 *In vivo* ΦC31 integrase mediated site-specific recombination

In vivo recombination mediated by ΦC31 integrase was carried on plasmid DNA or cassettes inserted into the bacterial chromosome. The aim of this experiment was to test the conditions required for catenane formation, as well as to entrap any formed precatenanes in growing bacteria.

2.24.1 Recombination on plasmids

E. coli strain DS941 was made chemically competent and transformed with the substrate plasmid (pAOT5) containing the *attP* and *attB* sites, and the integrase coding plasmid (pZJ7m). Transformants were selected on plates containing kanamycin, chloramphenicol and 0.2% glucose. An overnight culture grown in 0.2% glucose was diluted 40-fold into three flasks containing 30 ml LB with kanamycin and chloramphenicol. The cultures were grown at 37°C with shaking until OD_{600} of 0.6 was reached. 5 ml of each culture with bacteria were taken, plasmid DNA was extracted and used as timepoint 0. Afterwards, 0.2% arabinose, 10 µg/ml norfloxacin or both (norfloxacin was added 2 min after arabinose) were added to the different cultures. Samples of 5 ml were taken at 10, 20 and 30 min of incubation with arabinose, norfloxacin or both. Bacteria were pelleted at 11,000

x *g* for 3 min at 4°C and the pellets were stored at -20°C until all timepoints were collected. Then, plasmid DNA/catenanes were extracted using QIAprep Spin Miniprep Kit (QIAGEN) and verified by agarose gel electrophoresis.

2.24.2 Recombination on the chromosome

CP100, DS941 and C600SN containing a chromosomal *attP-lacI*-Km^R-*attB* cassette were used. Bacteria were made chemically competent and transformed with the integrase coding plasmid (pZJ7 or pZJ7m). Transformants were selected on plates containing kanamycin, chloramphenicol and 0.2% glucose. An overnight culture grown in 0.2% glucose and antibiotics was diluted 40-fold into 50 ml LB containing 0.2% glucose and chloramphenicol. The culture was grown at 37°C with shaking for 4 h until OD_{600} of 1. Then, 10 ml of culture were poured into four centrifuge tubes each and the cells were centrifuged at 6,000 x *g* for 3 min at 4°C. Each pellet was resuspended in 10 ml of LB containing chloramphenicol; chloramphenicol and 0.2% arabinose; chloramphenicol and 10 µg/ml norfloxacin; or chloramphenicol, 0.2% arabinose and 10 µg/ml norfloxacin (norfloxacin was added after 2 min of incubation with arabinose at 37°C). Bacteria were grown at 37°C with shaking for another 30 min and the DNA extracted from all cultures using QIAprep Spin Miniprep Kit (QIAGEN). The extracted DNA was used in further procedures as digestion or nicking.

2.25 Southern hybridization – neutral transfer

Southern hybridizations were made to detect topological species present in low levels in recombination reactions on agarose gels.

2.25.1 Agarose gel treatment

After the DNA was separated on a large 0.7% or 1% agarose gel overnight, the gel was incubated in 500 ml of depurination solution (0.125 M HCl) for 10 min. Next the DNA was denatured by incubating the gel in 500 ml of denaturation solution (1.5 M NaCl, 0.5 M NaOH) for 30 min, and neutralized by incubation in 500 ml of neutralization solution (1.5 M NaCl, 0.5 M Tris-HCl (pH 7.5)) for 30 min. All incubation steps were performed with shaking on a Luckham shaking platform (model R100 rotatest shaker).

2.25.2 Capillary blotting

After this treatment, the gel was subjected to capillary blotting. First, a tray was filled with transfer buffer (20x SSC), a platform was put in, and 3 sheets of 3mm paper (Whatman) saturated in transfer buffer were put on it. The gel was placed on the paper, followed by the nylon membrane (15 cm by 18 cm) (Amersham Hybond-N+, GE Healthcare). The membrane was covered with 3 sheets of 3 mm paper (Whatman) cut to size and saturated in buffer. The gel was surrounded by cling film to prevent direct absorption of the buffer by the paper towels. A stack of absorbent paper was stacked, on which a glass plate with a weight (approx. 500 g) was placed and the transfer made overnight. On the next day, DNA was fixed to the membrane by an UV exposure of 120 mJ/cm^2, using crosslinker CL-508 (Uvitec).

2.25.3 Biotin labelled probe synthesis and preparation for hybridization

Biotin labelled probes (random primed) were prepared using Biotin DecaLabel DNA Labeling Kit (Thermo Scientific), following the instructions of the manufacturer. The template for *lacI* gene probe synthesis was the BsrGI-DraIII 1240 bp fragment from pAOT3. The template for Km^R gene probe synthesis was the SalI-DraIII 1225 bp fragment from pAOT3.

A 20 µl sample containing 10-15 µl of probe and water was denatured in boiling water for 7-10 min and cooled on ice just prior to use.

2.25.4 Pre-hybridization and hybridization

The pre-hybridization solution (5x SSC, 5x Denhardt's solution, 0.5% SDS) was made and poured into the hybridization tube already containing the membrane. 500 µl of 0.1 mg/ml sonicated salmon sperm DNA was denatured by boiling it for 5 min and cooling on ice and then added to the pre-hybridization. The pre-hybridization step was made at 65°C for 1 h, after which 20 µl of probe was added directly to the hybridization tube. The hybridization step was carried out at 65°C overnight.

2.25.5 Stringency washes

Stringency washes are used to wash away the unbound and poorly bound probes. First, the membrane was washed in low stringency solution (2x SSC, 0.1% SDS) twice for 5 min at room temperature. Second, the membrane was washed in medium stringency solution (1x SSC, 0.1% SDS) twice for 10 min at 65°C. Finally, the membrane was washed in high stringency solution (0.1x SSC, 0.1% SDS) four times for 5 min at 65°C. The volume of solution in each wash was approximately 125 ml.

2.25.6 Chemiluminescent nucleic acid detection

Signal detection was carried out using Chemiluminescent Nucleic Acid Detection Module (Thermo Scientific). Detection was made according to manufacturer's instructions with the volumes of solution adjusted to the size of membrane. The membrane was blocked in 25 ml of blocking buffer. Then the membrane was incubated with fresh 25 ml of blocking buffer with 83 µl stabilized streptavidin-horseradish peroxidase. To wash the unbound streptavidin, the membrane was washed four times in 40 ml of 1x wash buffer (50 ml of 4x wash buffer were added to 150 ml of H_2O). After the washes, the membrane was incubated with 50 ml of substrate equilibration buffer. Finally, a mixture of 7.5 ml of luminol/enhancer solution and 7.5 ml of stable peroxide solution were added to the membrane. The detection was made by exposing the membrane to the CCD camera of Fusion FX or to an X-ray film.

2.26 XerC and XerD expression

XerC was expressed from pBH400 in DS9008 and XerD from pRM132 in DS984. Both were expressed using the same protocol, starting with an overnight culture grown at 37°C with shaking. The cultures were diluted 40-fold into 400 ml LB containing ampicillin and grown at 37°C with shaking until OD_{600} of 0.4. At this point the expression was induced by addition of IPTG to a concentration of 0.5 mM and the cultures grown further at 37°C with shaking for 4 h. The bacteria were pelleted at 6,000 x *g* for 10 min at 4°C, washed in 50 ml of 50 mM Tris-HCl (pH 8.0) and 50 mM NaCl, centrifuged as above and the pellets frozen at -70°C.

2.27 XerC purification

The bacteria were thawed on ice and resuspended in 6 ml of lysis buffer (50 mM NaCl, 50 mM Tris-HCl (pH 8.0), 1 mM EDTA and 0.1% Tween-20). Then, sonication was carried out by six pulses at 20% amplitude and 20 sec each, with 1 min break in between (Sonics & Materials Inc., VibraCell, button probe). The insoluble protein including XerC was pelleted at 12,000 x *g* for 10 min, washed in 6 ml of the same buffer and centrifuged again. The pellet was resuspended in 8 ml of lysis buffer with 8 M urea and left on ice for 20 min. Urea allowed XerC solubilization. The mixture was centrifuged as above, and the supernatant transferred to a dialysis bag. Dialysis was made against 8 ml of 1 M NaCl, 50 mM Tris-HCl (pH 8.0), 0.5 mM EDTA, 5 mM CHAPS (zwitterionic detergent) and 2.5 mM Sulfobetaine 3-12 (SB3-12, zwitterionic detergent), for 30 min on ice. Then, the dialysis buffer was changed to 16 ml of a fresh one and the dialysis continued for 30 min on ice. Once more, the buffer was changed to 20 ml of fresh one and the dialysis continued for 15 min on ice. The dialysed sample was transferred to a tube, made 50% glycerol and transferred to a new dialysis bag. Final dialysis was made against 400 ml of 1 M NaCl, 50 mM Tris-HCl (pH 8.0), 1 mM EDTA and 50% glycerol, at 4°C overnight. Next day, the sample was centrifuged at 40,000 x *g* for 20 min at 4°C and the supernatant with soluble XerC stored at -20°C. The purity of the protein was verified by SDS-PAGE. XerC was quantified using Bio-Rad Protein Assay according to manufacturer's instructions.

2.28 XerD purification

ÄKTA Protein Purification System (HPLC, GE Healthcare) was used for XerD purification. Bacteria were thawed on ice and resuspended in 5 ml of buffer 1 (50 mM Tris-HCl (pH 8.0), 0.3 M NaCl, 10% glycerol and 5 mM imidazole). Then, sonication was carried out by six pulses at 20% amplitude and 20 sec each, with 1 min break in between (Sonics & Materials Inc., VibraCell, button probe). The sample was centrifuged at 27,000 x *g* for 20 min at 4°C and the supernatant was loaded onto a HisTrap HP column (GE Healthcare), washed with 10 ml of buffer 2 (50 mM Tris-HCl (pH 8.0), 0.3 M NaCl, 10% glycerol and 400 mM imidazole) and equilibrated with buffer 1. Although XerD does not contain a His tag it naturally binds to a nickel column. The elution was made at 10 mM, 20 mM, 200 mM and 400 mM of imidazole. 20 µl were taken from the samples that showed protein presence (280 nm peak) and analysed by SDS-PAGE, while the rest were kept in ice overnight at 4°C. XerD was eluted at approx. 200 mM of imidazole. After confirming

XerD presence in the eluents, the samples were pooled together and dialysed against 1 L of buffer 3 (50 mM Tris-HCl (pH 8.0), 0.3 M NaCl, 1 mM EDTA, 1 mM DTT and 10% glycerol) over day and against 1 L of fresh buffer 3 overnight. In the second part of the purification, the sample containing XerD was centrifuged at 11,000 x *g* for 10 min at 4°C and the supernatant loaded onto a Heparin column (GE Healthcare), already washed with 10 ml of buffer 4 (50 mM Tris-HCl (pH 8.0), 1.5 M NaCl, 1 mM EDTA, 1 mM DTT and 10% glycerol) and equilibrated with buffer 3. XerD was eluted between 0.3 M and 1.5 M NaCl in 20 min. 20 µl were taken from the fractions that showed protein presence (280 nm peak) and analysed by SDS-PAGE. Glycerol was added to 50% to the remaining volume of the fractions containing XerD and these were stored at -20°C. XerD was quantified using Bio-Rad Protein Assay according to manufacturer's instructions.

2.29 *In vitro* XerC, XerD and PepA mediated recombination

XerC, XerD and PepA were used to recombine pSDC153 to form a 4-noded catenane with one circle of 398 bp and the other with 3039 bp. This in turn was used to study the supercoiling level of the smaller circle (398 bp). A 400 µl reaction contained 1x *psi* buffer, 10% glycerol, 3.5 µg pSDC153, 2.3 µg XerC, 2.2 µg XerD and 12.9-25.8 µg *E. coli* PepA (provided by James Provan). The reaction was carried out at 37°C for 1 h, then DNA was recovered by one phenol:chloroform extraction, one chloroform:isoamyl alcohol extraction and ethanol precipitation. The purified DNA was resuspended in 200 µl of H_2O. Recombination efficiency and sample purity were verified by agarose gel electrophoresis.

2.30 Topo IV mediated decatenation

ParC and ParE proteins were a gift from David Wigley. Topo IV was reconstituted by mixing equal volumes of stock ParE and 20-fold diluted ParC in Topo IV dilution buffer (50 mM Tris-HCl (pH 7.5), 150 mM NaCl, 1 mM EDTA, 5 mM DTT, 50% glycerol) on ice. Reconstituted Topo IV was diluted 10-fold in the same dilution buffer prior to use.

The decatenation reaction was in a total volume of 20 µl consisting of 5 µl 4x Topo IV reaction buffer (40 mM Tris-HCl (pH 7.5), 100 mM potassium glutamate, 6 mM $MgCl_2$, 50 µg/ml BSA), 0.15 µl 1 M DTT, 1.4 µl 0.4 mM ATP, 500 ng DNA and 1 µl of 10-fold diluted Topo IV (1.4 pmol). The reactions were carried out at 37°C for 45 min and stopped at 65°C for 15 min. Samples were nicked and analysed by agarose gel electrophoresis.

2.31 Linear DNA degradation by lambda exonuclease and RecJ^f

The large product linear DNA (3039 bp) had to be degraded when studying supercoiling of the small circle in Xer reactions as it migrated at a similar position as the nicked or relaxed small circle on polyacrylamide gels.

Lambda exonuclease (NEB) recognizes linear double-stranded DNA and catalyses the removal of one strand in the 5´ to 3´ direction. RecJ^f (NEB) recognizes single-stranded DNA and catalyses its removal in the 5´ to 3´ direction (Balagurumoorthy *et al*, 2008).

Prior to lambda exonuclease and RecJ^f treatment, a sample containing the 4-noded catenane (formed from recombination on pSDC153) was digested with EcoRI in a 15 µl reaction to linearize the bigger circle. To this 15 µl reaction was added: 2 µl 10x lambda exonuclease buffer (NEB), 1 µl 5 U/µl of lambda exonuclease and 2 µl 30 U/µl RecJ^f. The reaction was incubated at 37°C for 50 min and enzymes inactivated by heat at 75°C for 10 min.

RecJf has its own buffer (NEB buffer 2) but its activity in CutSmart is 100%, and the EcoRI digestion was performed in CutSmart.

2.32 Relaxation of circular DNA by calf thymus topoisomerase I in presence of ethidium bromide

Calf thymus topoisomerase I (Thermo Fisher) removes positive and negative supercoiling of a molecule. However, if increasing concentration of ethidium bromide is added to the reaction and then removed by extraction with phenol after relaxation with Topo I, the DNA becomes more negatively supercoiled.

The aim of relaxing a small DNA circle in presence of ethidium bromide was to create a ladder of small circles with different level of supercoils. The replication intermediates were also treated with Topo I in presence of ethidium bromide to verify their level of supercoiling.

30 µl reactions were set up by mixing: 3 µl 10x Topo I reaction buffer (500 mM Tris-HCl (pH 7.5), 500 mM KCl, 100 mM $MgCl_2$, 5 mM DTT, 1 mM EDTA, 300 µg/ml BSA); 20

µl of small circle treated with lambda exonuclease and RecJ^{f} or 500 ng DNA; 1-3 µl 1 U/µl Topo I; 0, 1, 3 or 6 µg/ml EtBr and water up to 30 µl. Reactions were incubated at 37°C for 45 min and the enzyme heat inactivated at 80°C for 10 min. DNA was extracted once with phenol:chloroform prior to separation on PAGE or agarose.

3. Formation and detection of catenanes produced by site-specific recombination *in vivo*

3.1 Introduction

Replication of the bacterial chromosome is associated with formation of different DNA topologies such as positive supercoiling and precatenation (Peter *et al*, 1998; Wang *et al*, 2008). However, no study has yet shown evidence for precatenane formation on the chromosome *in vivo*.

The main aim of this work was to study precatenation through formation of catenanes by site-specific recombination on the bacterial chromosome *in vivo*. Therefore, in this chapter a method to be used for catenane detection was developed.

The method was developed by detecting catenanes produced by site-specific recombination on plasmid DNA. This DNA is a good tool for studying topology, since plasmids are usually present in the cell in more than one copy, are easily extracted and can be relatively easy manipulated. An *in vitro* site-specific recombination reaction catalysed by ΦC31 integrase, between directly repeated *att* sites on a plasmid, produces two smaller circles. Integrase brings the sites together by random collision, such that random amounts of supercoiling of the substrate plasmid are entrapped between the two product circles, producing catenanes (Olorunniji *et al*, 2012). Different amount of supercoiling leads to different complexity catenanes, which can be extracted and analysed by agarose gel electrophoresis.

3.2 Construction of a plasmid containing *attP* and *attB* sites

A plasmid was constructed to obtain a substrate for site-specific recombination mediated by ΦC31 integrase. In this plasmid, the *attP* and *attB* sites were in direct repeat, so that recombination would lead to deletion. A kanamycin resistance gene and the *lacI* gene were inserted between the two *att* sites and were used as genetic markers for bacterial selection in later work.

First, pUC4K containing a kanamycin resistance gene was digested with PstI and the kanamycin resistance gene obtained was ligated to PstI digested pMTL23, leading to pAOT1 (Figure 3.1A). *attP* and *attB* (annealed oligonucleotides) were introduced into

pAOT1 to produce pAOT2 (Figure 3.1B). Finally, the *lacI* gene was amplified from pTRC99a and introduced into pAOT2 forming pAOT3 (Figure 3.1B). This plasmid contained kanamycin resistance and *lacI* genes and the ΦC31 integrase recombination sites *attP* and *att*B. To obtain a lower copy-number plasmid, pAOT3 was digested with NcoI and NgoMIV and the desired fragment was ligated to pMS183 (containing a pSC101 origin of replication and a Km^R gene) digested with the same enzymes, forming pAOT5 (Figure 3.1C).

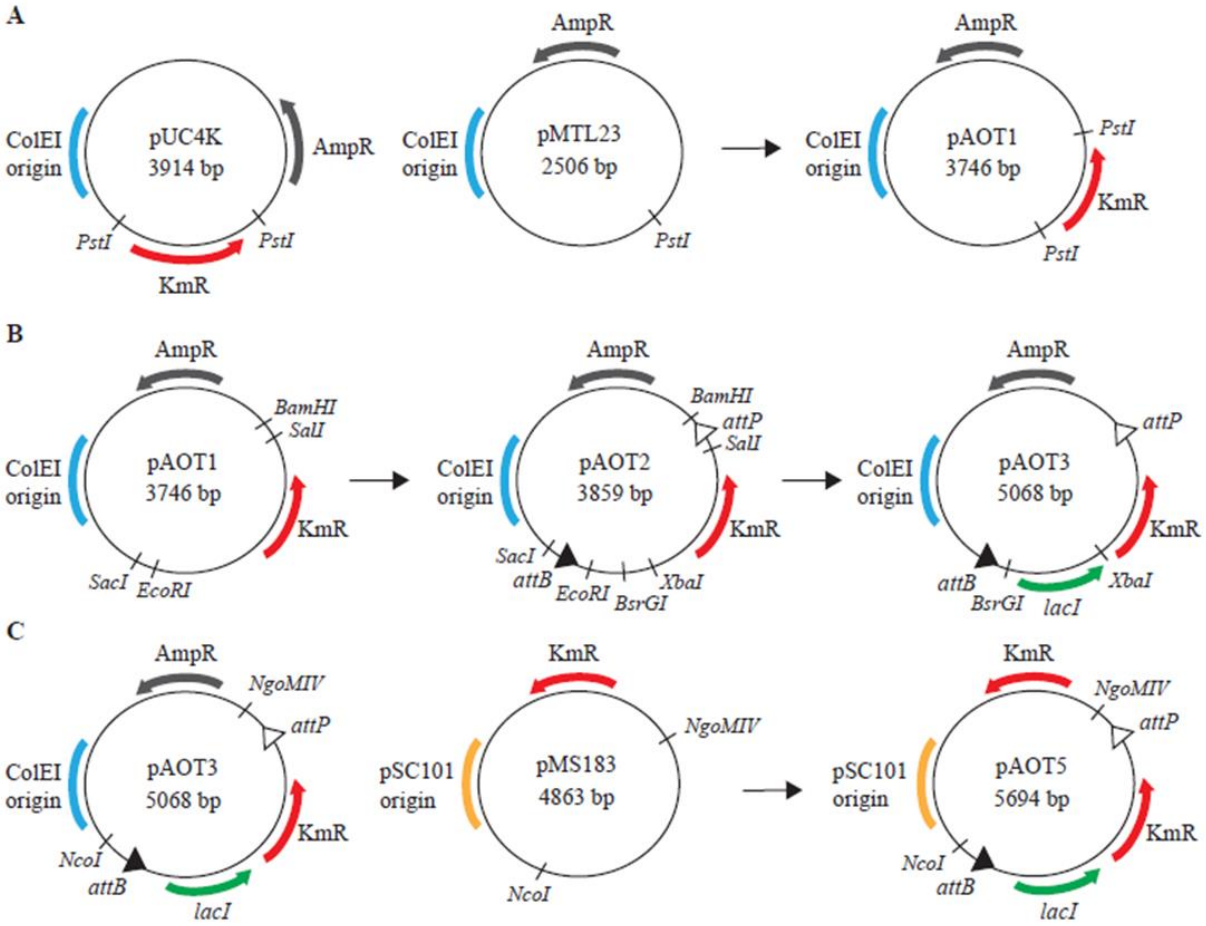

Figure 3.1 – Construction of plasmids for site-specific recombination. A) Construction of pAOT1 with kanamycin resistance gene inserted into PstI digested pMTL23. **B)** *attP* was inserted into pAOT1 digested with BamHI and SalI, and *attB* was inserted into pAOT1 digested with SacI and EcoRI, producing pAOT2. pAOT2 was digested with BsrGI and XbaI to insert the *lacI* gene amplified from pTRC99a, producing pAOT3. **C)** pAOT3 was digested with NgoMIV and NcoI and the fragment containing the cassette was inserted into NgoMIV and NcoI digested pMS183, forming pAOT5.

3.3 Recombination between *attP* and *attB* sites on pAOT5

After plasmid construction it was important to determine whether recombination would occur between the *att* sites on pAOT5. This plasmid has two EcoRV restriction sites, so cleaving pAOT5 with EcoRV yields fragments of 4046 bp and 1648 bp. The recombination products consist of two circles each with one EcoRV site, so digestion with EcoRV linearizes both, yielding fragments of 3149 bp and 2545 bp (Figure 3.2A).

Recombination on pAOT5 was tested *in vivo* with ΦC31 integrase. Int is encoded by the plasmid under the control of the arabinose inducible P_{BAD} promoter (Guzman *et al*, 1995; Zhao, 2015). This promoter allows Int expression in the presence of arabinose and is inhibited in presence of glucose. Due to possible leakage in Int expression, pZJ7m was used (see Chapter 2, section 2.2). In this plasmid, the starting codon of the *int* gene was mutated to GTG instead of ATG (pZJ7), which decreased the level of expression of Int and made it more controllable (Zhao, 2015). This way, the leakage in Int expression could be avoided.

Plasmids pAOT5 and pZJ7m were introduced into *E. coli* DS941 by co-transformation and colonies were selected for resistance to kanamycin and chloramphenicol on plates containing 0.2% glucose. A colony was picked and inoculated into LB containing the same antibiotics and 0.2% glucose and grown overnight. The culture was diluted into fresh LB without glucose and grown until OD of 0.6 was reached. Integrase expression was induced by addition of 0.2% arabinose and a fixed volume of cells was taken at different timepoints. Bacteria were pelleted by centrifugation and plasmid DNA was extracted as quickly as possible using QIAprep Spin Miniprep Kit. DNA was digested with EcoRV and separated by agarose gel electrophoresis.

At the timepoint 0a, taken just before arabinose induction no recombination products were detected, as expected (Figure 3.2B). Similarly, when plasmid DNA was extracted just after arabinose addition (timepoint 0b) no recombination was observed. However, recombination occurred efficiently after 30 minutes of induction with arabinose. At this point, the recombination seemed already to achieve completion, since only the products of 3149 bp and 2545 bp were observed. The 3149 bp circle inherits the origin of replication, which allows it to replicate throughout the time course. The 2545 bp product cannot replicate and the band on the gel corresponding to it maintained its intensity while the 3149

bp circle increased intensity over the same time. As a control, bacteria containing pAOT5 and pZJ7m were grown without arabinose for the same amount of time and as a result some recombination occurred, probably due to leakage in expression of Int.

In summary, these results show that recombination between the *att* sites on pAOT5 occurs efficiently, and the expression of ΦC31 integrase can be tightly controlled by presence of arabinose or glucose. However, some leakage does occur during growth in the absence of glucose and arabinose.

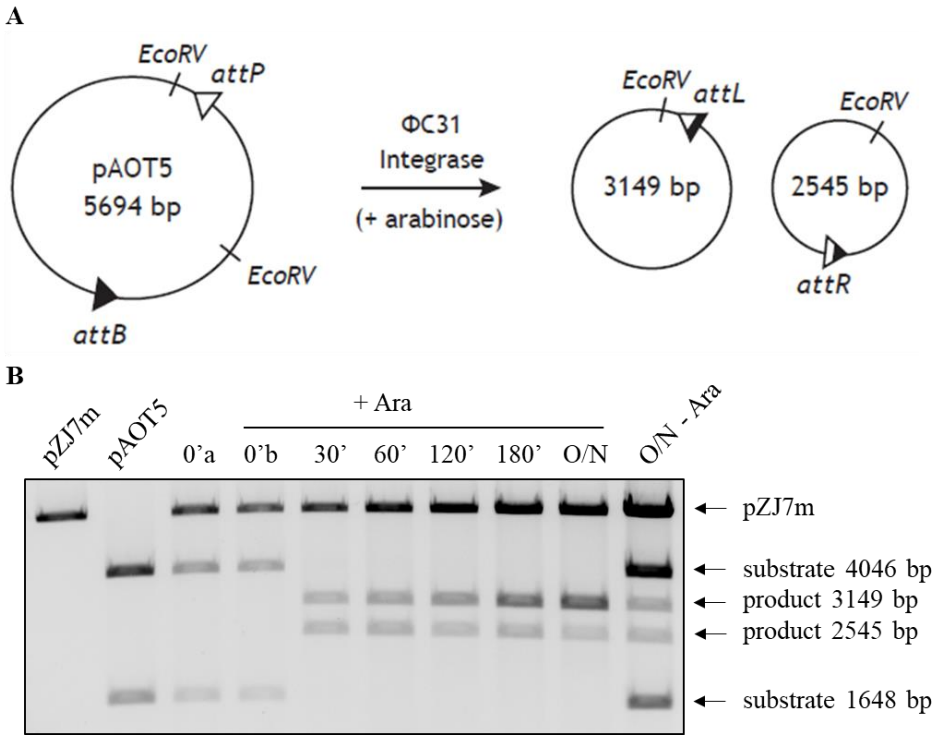

Figure 3.2 – Site-specific recombination on pAOT5. A) The principle for determination of recombination occurrence through digestion with EcoRV. **B)** 1% agarose gel run at 90V and stained with ethidium bromide showing recombination *in vivo*. DNA was extracted from 5 ml of culture for every time point. 0'a sample was taken before arabinose induction and 0'b just after arabinose addition. As controls, pZJ7m and pAOT5 were digested with EcoRV for markers of linear Int expression vector and substrates, respectively. O/N, overnight; O/N – Ara, cells grown overnight without arabinose.

3.4 Decatenation by Topo IV

Intramolecular site-specific recombination mediated by Int *in vitro* can produce different topological products such as catenanes and knots (Olorunniji *et al*, 2012). When analysing the recombination products by agarose gel, all the supercoiled catenanes and knots migrate close to each other just ahead of supercoiled circle and appear in form of a smear on the gel. For this reason, the products must be nicked for removal of supercoiling, so they can migrate according to number of crossings in each catenane and knot. The higher the number of crossing, the more compact the molecule is and the faster it migrates on an agarose gel. Like this, a ladder of catenanes and knots can be created (Figure 1.3).

What would be an easy way to confirm that a ladder observed on a gel is made of catenanes and knots? In *E. coli*, Topo IV is the topoisomerase that decatenates catenanes and unknots knots. Hence treating a sample containing catenanes and knots with Topo IV would yield two unlinked circles and an unknotted substrate. When analysing the untreated and Topo IV treated samples on an agarose gel, catenanes and knots produced by recombination should be absent after Topo IV treatment.

To produce catenanes, pAOT5 was incubated with ΦC31 integrase *in vitro* and the reaction carried out at 30°C for 30 minutes and the integrase inactivated at 80°C for 10 minutes. Then half of the sample was treated with Topo IV and the other half left untreated. Finally, both samples were nicked for elimination of supercoiling and separated by agarose gel electrophoresis. Topo IV was a gift from Dale Wigley's group in late 1990s and it was stored at -70°C since that time. For this reason, the enzyme needed to be tested for its activity and the required conditions.

After nicking, it could be seen that the recombination reaction was not complete, since unreacted substrate pAOT5 was still present (Figure 3.3 lane 2). The main products were the two separate circles of 3149 bp and 2545 bp. The bands migrating between pAOT5 and 3149 bp circle showed a ladder-like migration which is typical of nicked catenanes. When the sample from lane 2 was treated with Topo IV, all the bands thought to correspond to catenanes were no longer present (Figure 3.3 lane 3). After Topo IV treatment, two main bands were observed on the gel which corresponded to the unlinked recombination products of 3149 bp and 2545 bp. Curiously, other two bands remained present, migrating above and below pAOT5 (Figure 3.3 lane 3). These bands corresponded to the dimers of

the 3149 bp and 2545 bp circles which cannot be monomerized by Topo IV. Dimers are formed when recombination is intermolecular, that is, it takes place between an *attP* site on one plasmid and an *attB* site on the other plasmid (Figure 3.4). The resulting 11388 bp plasmid still has two unreacted *att* sites, which when recombined produce circles of 6298 bp and 5090 bp. The 2545 bp circle dimer (5090 bp) co-migrated on the gel with the 2-noded catenane.

Altogether, these results show that catenanes can be formed *in vitro* by site-specific recombination, mediated by ΦC31 integrase. These catenanes are efficiently decatenated by Topo IV in the conditions used.

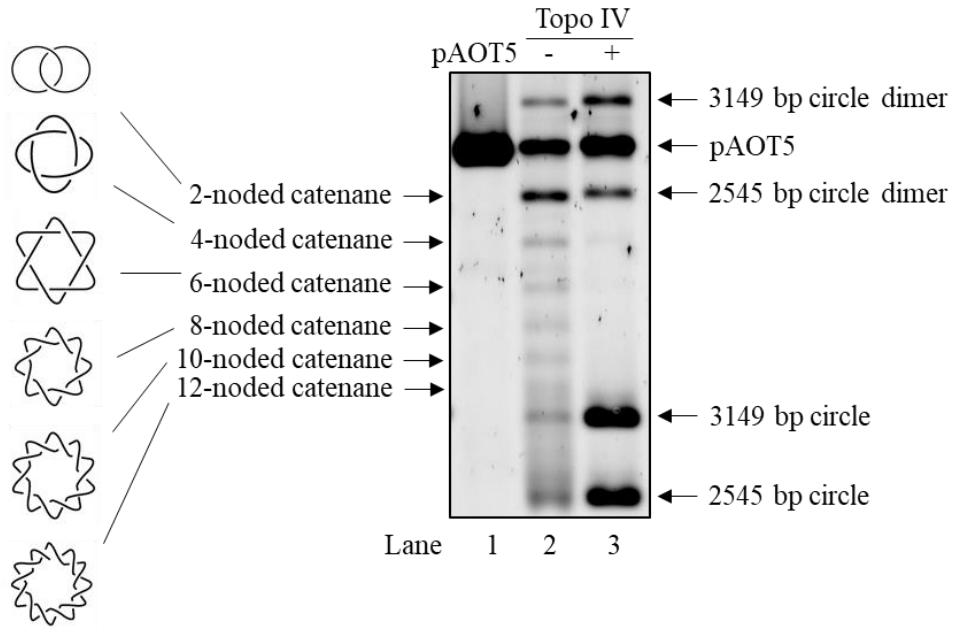

Figure 3.3 – Topo IV treatment of catenanes. 0.7% agarose gel run at 35V showing pAOT5 (lane 1), site-specific recombination products (lane 2) and Topo IV treated sample from lane 2 (lane 3). All the samples presented here were nicked with Nb.BbvCI for elimination of supercoiling. Nb.BbvCI nicks once in 3149 bp and once in 2545 bp circles.

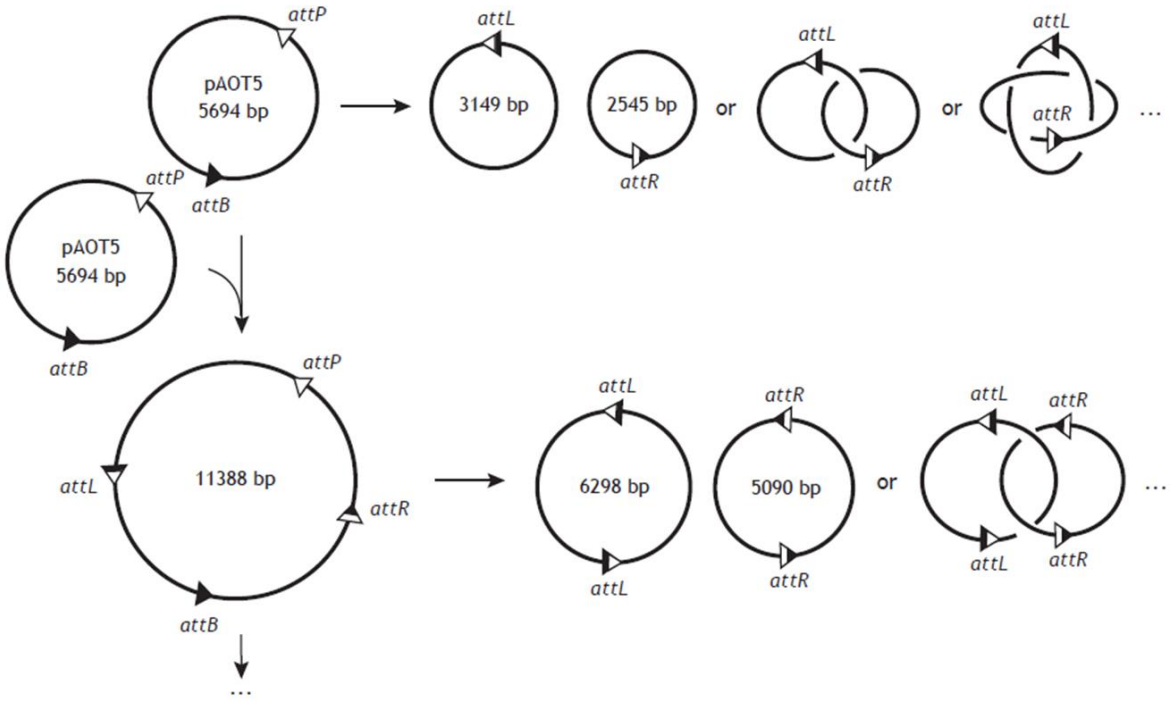

Figure 3.4 – Possible recombination products for a circular substrate with directly repeated *attP* and *attB* sites. Intramolecular recombination of pAOT5 (5694 bp) leads to circular products of 3149 bp and 2545 bp, which can be unlinked, or in the form of torus catenanes with even numbers of crossings. If the recombination is intermolecular, that is, between the *attB* on one plasmid with *attP* on a second plasmid, the product is a plasmid dimer of 11388 bp. The unrecombined *attP* and *attB* sites can then undergo intramolecular recombination to form products of 6298 bp and 5090 bp, which are dimers of the two circular products formed by intramolecular recombination on pAOT5. These two dimer products could be catenated as shown. When the 11388 bp plasmid recombines with another 5694 bp plasmid the final products are trimers of the 3149 bp and 2545 bp circles, and so on.

3.5 Detection of catenanes formed on plasmids *in vivo*

Since Int mediated recombination *in vitro* produced catenanes (Figure 3.3), it was expected that catenanes would also be formed by recombination *in vivo*. To test this, an experiment was designed to determine in which conditions bacteria would accumulate catenanes. A possible complication of an *in vivo* experiment is the presence of type II topoisomerases. Although Topo IV and DNA gyrase have been shown to unlink catenanes *in vitro*, Topo IV is the major decatenase *in vivo* (Peng and Marians, 1993; Ullsperger and Cozzarelli, 1996; Zechiedrich and Cozzarelli, 1995).

In the following two sections the role of both type II topoisomerases was tested *in vivo*. The role of these two topoisomerases in decatenation was studied using the drug norfloxacin. First, catenane formation was studied when both enzymes were inhibited (DS941) and second, when just Topo IV was inhibited (C600SN) (see Chapter 2, section 2.1).

3.5.1 Catenanes can be detected when DNA gyrase and Topo IV are inhibited

To test catenane formation when DNA gyrase and Topo IV were inhibited, the experiment was performed in DS941 *in vivo*. In DS941 both enzymes are sensitive to norfloxacin, therefore treating this strain with norfloxacin inhibits any decatenation reaction. The catenanes were produced by site-specific recombination on pAOT5 mediated by Int, encoded by pZJ7m.

DS941 containing pAOT5 and pZJ7m were grown at 37°C until OD of 0.6 was reached. Time point 0 was taken and arabinose was added to the remaining culture to induce Int expression. In a separate culture, norfloxacin was added 2 minutes after arabinose to inhibit type II topoisomerases. In a third control culture, cells were treated with norfloxacin alone. Samples were taken at 10, 20 and 30 minutes timepoints, the cells pelleted by centrifugation, and plasmid DNA extracted as fast as possible using QIAprep Spin Miniprep Kit. Plasmid DNA obtained from all the timepoints was nicked with Nb.BbvCI and separated by agarose gel electrophoresis. The results were detected by Southern hybridization using the kanamycin resistance gene as probe.

During the experiment, it was observed that norfloxacin was interfering with cell growth. The optical density measurements of the cultures taken before and after norfloxacin treatment showed almost no cell growth after norfloxacin addition (Figure 3.5A). This is consistent with the fact that norfloxacin inhibits DNA gyrase, an enzyme that introduces negative supercoiling into the DNA and is essential for DNA replication and cell growth. This way, bacterial DNA supercoiling is impaired in the presence of norfloxacin, which interferes with DNA replication, causing decrease in bacterial growth. Upon treatment with just arabinose the cells continued to grow (Figure 3.5A). In the samples treated with

arabinose and norfloxacin, addition of norfloxacin led to almost complete inhibition of cell growth, just as observed for the sample treated with norfloxacin alone (Figure 3.5A).

When bacteria were treated with norfloxacin in the absence of arabinose, no recombination occurred, as expected (Figure 3.5B lanes 1-4). Norfloxacin does not induce Int expression so no recombination should occur (Figure 3.6A).

Upon treatment with just arabinose recombination occurred (Figure 3.5B lanes 5-8). Arabinose induces Int expression which recombines the *att* sites on pAOT5 (Figure 3.6B). The 0 minutes sample was taken just before arabinose addition, so only one band corresponding to pAOT5 substrate was observed. After 10 minutes of integrase expression, recombination products started to appear, the main ones being the free 3149 bp and 2545 bp circles. Dimers of these circles, as seen in *in vitro* reaction, also formed, migrating on the gel just above and below pAOT5 substrate. Some faint bands were observed at the 10 minutes time point migrating between the 2545 bp circle dimer and 3149 bp circle, which co-migrated with the catenanes formed on the same substrate plasmid by recombination *in vitro* (Figure 3.5B lanes 6 and L). However, the bands seemed to disappear after 20 minutes of treatment (Figure 3.5B lanes 7 and 8). In this sample, Topo IV and DNA gyrase were active, therefore any formed catenane would be a substrate for decatenation by those enzymes (Figure 3.6B).

When bacteria were treated with arabinose and norfloxacin, similar results were observed as for cells treated with arabinose. However, in this case the ladder of topologies which resembled catenanes did not disappear with increasing time (Figure 3.5B lanes 10-12). This suggested that norfloxacin was inhibiting DNA gyrase and Topo IV, which in turn were not able to decatenate recombination products, allowing catenanes to accumulate over time (Figure 3.6C).

A

	OD_{600} at 0 min	OD_{600} at 30 min
Norfloxacin	0.56	0.57
Arabinose	0.56	0.74
Both	0.57	0.58

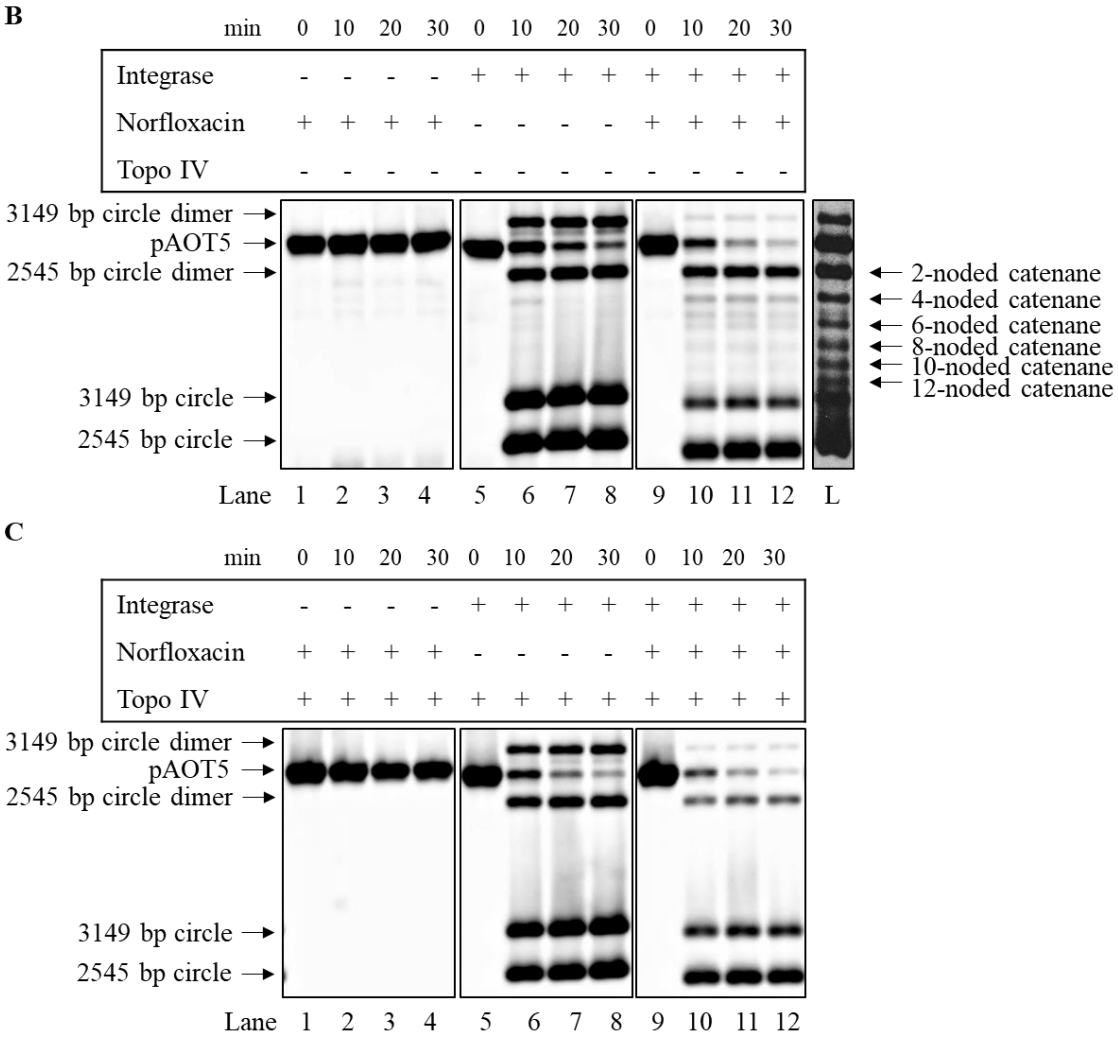

Figure 3.5 – Analysis of *in vivo* site-specific recombination by ΦC31 integrase on plasmids in DS941. Southern hybridization of samples separated on a 0.7% agarose gels run at 35V. **A)** Table with values for optical density measured at 600 nm. The bacterial growth was measured just before treatment with norfloxacin, arabinose or both (0 min) and after 30 minutes of treatment. **B)** Cells treated with 10 µg/ml norfloxacin, 0.2% arabinose or both as indicated by table above gel, in a time course experiment. Plasmid DNA was extracted from cells at the indicated timepoints and nicked with Nb.BbvCI. The gel was Southern blotted, and DNA detected by hybridization with the kanamycin resistance gene probe. Lane L was the ladder of catenanes made by *in vitro* recombination on pAOT5. **C)** Samples as in B) but treated with Topo IV *in vitro* before nicking.

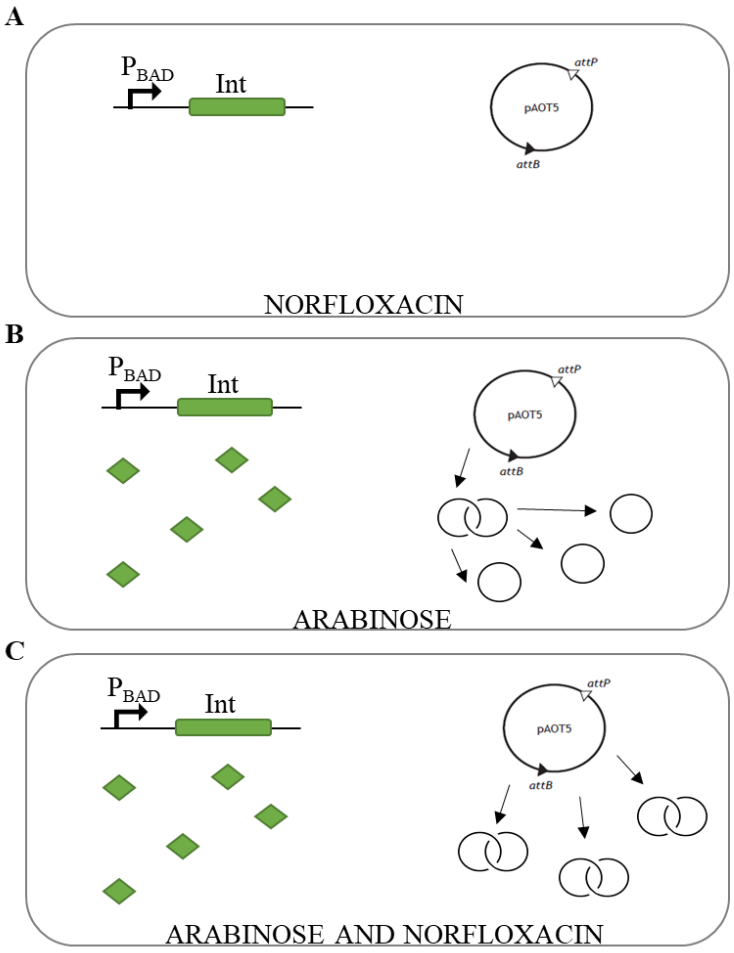

Figure 3.6 – Expected results of catenanes formation in DS941. A) Cells treated with just norfloxacin are expected to have the type II topoisomerases inhibited, but no recombination. **B)** In cells treated with just arabinose, recombination and decatenation are expected. **C)** In cells treated with arabinose and norfloxacin, recombination but no decatenation are expected. P_{BAD} is the arabinose inducible promoter; green diamonds represent ΦC31 integrase protein.

A difference observed during the results analysis was the amount of large circle (3149 bp) compared to the small one (2545 bp), or the large circle dimer compared to small circle dimer. In the absence of norfloxacin, the 3149 bp circle was proportional to the 2545 bp circle and the same was observed for their dimers (Figure 3.5B lanes 6-8). In the presence of norfloxacin, the 3149 bp circle and its dimer were present in lower quantity, compared to the 2545 bp circle and its dimer (Figure 3.5B lanes 10-12). Norfloxacin inhibits DNA gyrase by trapping the cleavage complex. Since the big circle has a segment of DNA from

pSC101 specific for DNA gyrase activity (the pSC101 *par* locus) (Wahle and Kornberg, 1988), once gyrase cleaves the DNA, it would be linearized and degraded by nucleases in the cell. Also, it would not be recovered after the alkaline lysis used for plasmid extraction.

The results discussed above suggested that catenanes are formed *in vivo* by recombination on pAOT5. If those topologies indeed corresponded to catenanes, they should be decatenated by treatment with Topo IV *in vitro*, and this could be detected by gel electrophoresis. To test this hypothesis, the samples from the time course were treated with Topo IV *in vitro*, nicked to remove supercoiling and separated on an agarose gel. The DNA was again detected by Southern hybridization using the kanamycin resistance gene as probe.

Interestingly, all the bands co-migrating with catenanes disappeared after Topo IV treatment (Figure 3.5C lanes 6-8 and 10-12), supporting the conclusion that those bands do indeed correspond to catenanes. The band corresponding to the 2-noded catenane did not disappear completely after Topo IV treatment, suggesting that the 2-noded catenane co-migrates with the 2545 bp circle dimer on the gel, as previously observed for *in vitro* reactions.

Altogether, these results show catenane formation by ΦC31 integrase mediated recombination on pAOT5 *in vivo*, in the presence of arabinose. Norfloxacin allows catenane accumulation by inhibiting type II topoisomerases. These catenanes were easily detected by Southern hybridization.

3.5.2 Catenane detection when just Topo IV is inhibited

Catenanes were observed from recombination on pAOT5 when Int expression was induced with arabinose in DS941 in the presence of norfloxacin. In DS941, norfloxacin inhibits both type II topoisomerases leading to inhibition of cell growth and poor recovery of circular DNA with pSC101 *par* locus. Also, from the results described above, it is impossible to tell which of the topoisomerases was responsible for decatenation. Is it DNA gyrase or Topo IV that decatenates the site-specific recombination products *in vivo*?

One way to answer this question was to use a strain in which only one topoisomerase would be inhibited by norfloxacin, for example Topo IV. C600SN is a strain that carries a mutation in one of the DNA gyrase genes (*gyrA*) making the protein resistant to norfloxacin. Since gyrase is norfloxacin resistant, it is expected that upon antibiotic treatment, the DNA will remain supercoiled and the replication proceed as usual. This in turn will not impair cell growth, unlike in DS941. Also, the recovery of DNA containing the pSC101 *par* locus is expected to increase since gyrase can exit the DNA-protein cleavage complex.

The experiment carried out with C600SN was exactly as explained for DS941 (see section 3.5.1 in this chapter).

In C600SN, the cell growth was not inhibited by addition of norfloxacin during the time course experiment. The optical density measurement showed that cells continued to grow after addition of norfloxacin (Figure 3.7A).

As expected, in C600SN treated with norfloxacin and no arabinose, almost no recombination occurred (Figure 3.7B lanes 1-4).

Arabinose allowed ΦC31 integrase expression and recombination on pAOT5 yielding products like those seen for DS941 (Figure 3.7B lanes 5-8). The products of recombination were the free 3149 bp and 2545 bp circles and their dimers. The only difference in products formed between the two strains was that catenanes were not detected in C600SN after 10 minutes of induction with arabinose (Figure 3.7B lane 6).

After integrase expression in the presence of norfloxacin, the catenanes were seen to form in the beginning of time course, but also to disappear during the time course (Figure 3.7B lanes 9-12). This result differed from the one observed for DS941. In DS941 treated with arabinose and norfloxacin the catenanes remained present over the time course. This suggested that in C600SN the catenanes could still be decatenated by DNA gyrase. The amount of the 3149 bp circle and its dimer was more proportional to the 2545 bp circle and its dimer in C600SN, when compared to DS941. Suggesting that in C600SN the gyrase was not being trapped in the cleavage complex with the DNA, thus stopping the large circle and its dimer from being linearized and degraded.

To test whether the bands of the agarose gel corresponded to catenanes, the samples were treated with Topo IV *in vitro*, nicked to remove supercoiling and the DNA was again detected by Southern hybridization using kanamycin resistance gene as probe.

The bands corresponding to catenanes were no longer detected on the gel after Topo IV treatment (Figure 3.7C lanes 9-12). This confirmed that the products seen in Figure 3.7B lanes 10-12 were catenanes, formed from site-specific recombination on pAOT5 in C600SN, and that they could be decatenated *in vitro* by Topo IV. The band corresponding to the 2-noded catenane did not disappear completely after Topo IV treatment, showing again that the 2545 bp circle dimer is present and co-migrates with 2-noded catenane on the gel.

A

	OD_{600} at 0 min	OD_{600} at 30 min
Norfloxacin	0.51	0.55
Arabinose	0.53	0.58
Both	0.49	0.56

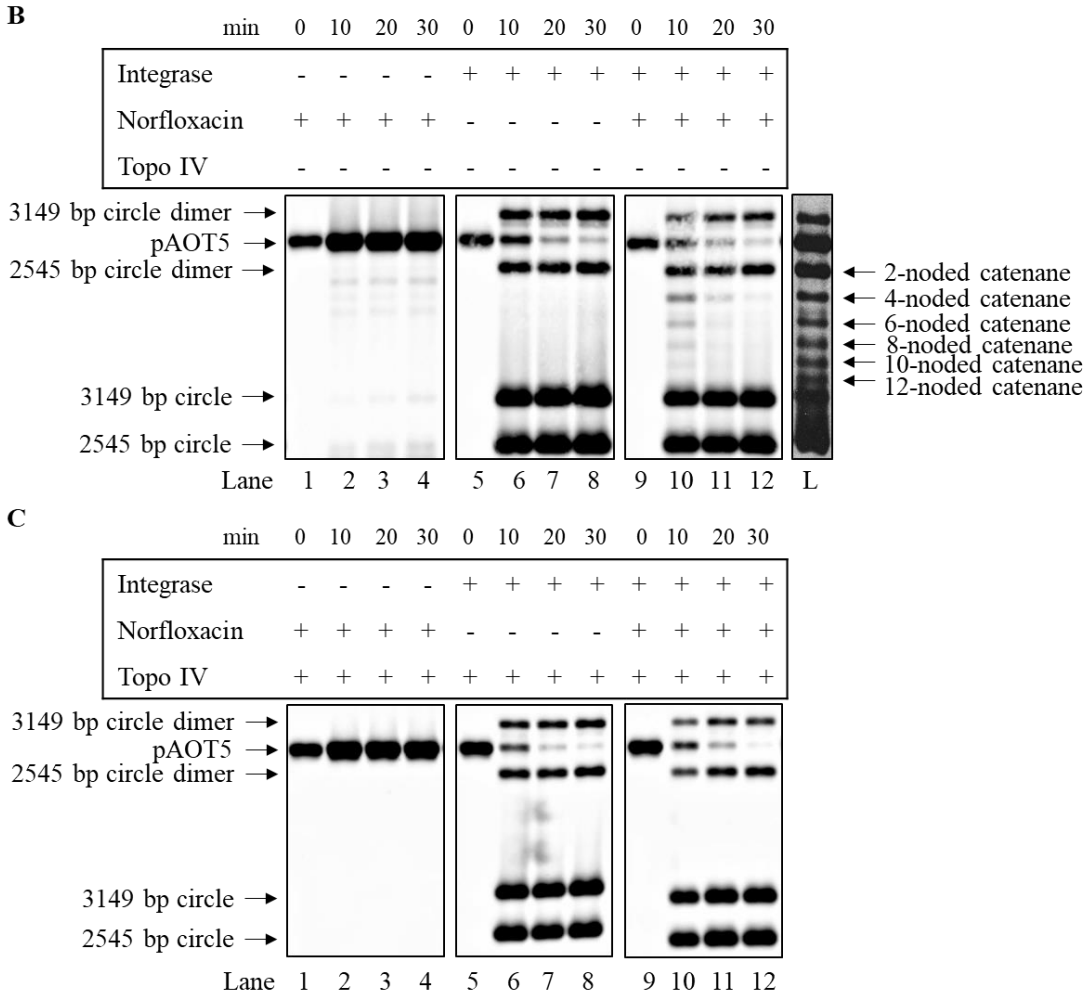

Figure 3.7 – Analysis of *in vivo* site-specific recombination by ΦC31 integrase on plasmids in C600SN. Southern hybridization of samples separated on a 0.7% agarose gels run at 35V. **A)** Table with values for optical density measured at 600 nm. The bacterial growth was measured just before treatment with norfloxacin, arabinose or both (0 min) and after 30 minutes of treatment. **B)** Cells treated with 10 µg/ml norfloxacin, 0.2% arabinose or both as indicated by table above gel, in a time course experiment. Plasmid DNA was extracted from cells at the indicated timepoints and nicked with Nb.BbvCI. The gel was Southern blotted, and DNA detected by hybridization with the kanamycin resistance gene probe. Lane L was the ladder of catenanes made by *in vitro* recombination on pAOT5. **C)** Samples as in B) but treated with Topo IV *in vitro* before nicking.

3.6 Conclusion

ΦC31 integrase mediated site-specific recombination between two directly repeated *att* sites on a plasmid produced smaller circles, which were unlinked, or catenated with even number of nodes (2, 4, 6, etc). The more nodes there is between two circles the higher the complexity of the catenane. The topology of the products of *in vitro* recombination by ΦC31 integrase has been previously studied (Olorunniji *et al*, 2012).

The *in vitro* recombination was used in this work to verify the activity of Int on pAOT5, and to create a ladder of catenanes used to compare the migration of topologies formed during *in vivo* site-specific recombination assays.

Formation and detection of catenanes *in vivo* was more a challenge, since bacteria have type II topoisomerases which decatenate them (Peng and Marians, 1993; Ullsperger and Cozzarelli, 1996). For this reason, cells were treated with norfloxacin to inhibit both type II topoisomerases (DS941) or just Topo IV (C600SN).

When both Topo IV and gyrase were inhibited in DS941, it was found that simultaneous addition of arabinose and norfloxacin led to poor expression of Int possibly from inability to remove positive supercoiling ahead of RNA polymerase. Therefore, in all experiments in this thesis, arabinose was added two minutes before norfloxacin. In C600SN, Int expression was not impaired by simultaneous addition of arabinose and norfloxacin, showing that the problem observed in DS941 was in fact due to inhibition of gyrase.

Catenanes were observed when cells were treated with arabinose for Int expression and norfloxacin for type II topoisomerases inhibition. The bands which were thought to be catenanes, co-migrated with the catenanes of the ladder obtained *in vitro* on an agarose gel. After Topo IV treatment those bands disappear, confirming their identities as catenanes.

The results obtained in the two strains, DS941 and C600SN, showed that catenanes produced from site-specific recombination on plasmid are not only removed by Topo IV, but also by DNA gyrase (more slowly), which is thought to be a very poor decatenase (Zechiedrich and Cozzarelli, 1995; Ullsperger and Cozzarelli, 1996; Zechiedrich *et al*, 1997).

It would be interesting to perform this experiment in a strain with Topo IV resistant and DNA gyrase sensitive to norfloxacin but unfortunately, we did not have access to this strain.

In conclusion, the results of this chapter show that conditions have been developed that allow detection of catenanes produced *in vivo*. These conditions could therefore be used to detect any catenanes produced in our assays to detect precatenation on chromosome.

4. Using *terE* to produce replication intermediates and a model system for the detection of precatenanes

4.1 Introduction

Ter sites are replication termination sites that occur naturally in the *E. coli* chromosome (Hill *et al*, 1988). Five *ter* sites stall replication forks moving in the clockwise direction and another five stall forks moving in the counterclockwise direction. This allows both forks to fuse and replication to terminate. However, the speed with which the clockwise and counterclockwise forks travel can be different (Breier *et al*, 2005). Also, one fork might be stalled by lesions in the DNA, such as nicks and gaps (Khan and Kuzminov, 2011). This means that one fork is going to reach the *ter* site first and remain there until the second fork arrives. While the fork at the *ter* site is waiting on the second fork to arrive, it can form precatenanes by rotating the replication machinery, to relieve the positive supercoiling produced between the two forks. Precatenation is associated with replication termination, in other words, precatenanes are thought to occur when replication is in its final steps (Sundin and Varshavsky, 1981). For example, precatenanes are thought to be the product of replication of the last couple of hundred of base pairs. In this way, *ter* sites, replication termination and precatenation could be connected.

To create a replication intermediate, a *ter* site can be inserted into a plasmid with a unidirectional origin of replication. When choosing a *ter* site, it is important to consider the efficiency of that site in stalling the replication fork. For example, if a Tus-*ter* complex stops 100% of the forks, the plasmid is not able to replicate, and it can be lost. However, Tus-*terE* does not stop all the replication forks and this allows enough replication to maintain the plasmid (Gottlieb *et al*, 1992; Cebrián *et al*, 2015) and to accumulate RIs.

In a replication intermediate, after the replication termination at *terE* site, the plasmid is partially replicated (Figure 4.1A). That is, part of the plasmid is replicated and part unreplicated. According to previous observations, the unreplicated region should be supercoiled and the replicated sister duplexes should be precatenated (Peter *et al*, 1998; Wang *et al*, 2008). However, *in vivo*, DNA gyrase resolves all the positive supercoiling in the unreplicated region and Topo IV the precatenanes in the replicated region. Moreover, DNA gyrase will continue to introduce negative supercoiling into the unreplicated portion which can result in replication fork swivel and formation of left-handed precatenanes in the replicated portion, substrate for Topo IV decatenation (Cebrián *et al*, 2015). It might be expected that using a strain with inactive Topo IV could result in accumulation of RIs with

negatively supercoiled unreplicated portion and precatenated replicated portion (Figure 4.1B).

Here, the *terE* site was used to our advantage, to create a plasmid model that would mimic precatenane occurrence *in vivo* on the bacterial chromosome. We wanted to create replication intermediates on plasmid that contained *terE* site and which could be used as a model for studying precatenane formation. Also, it was tested whether site-specific recombination can be used to entrap and detect this precatenation.

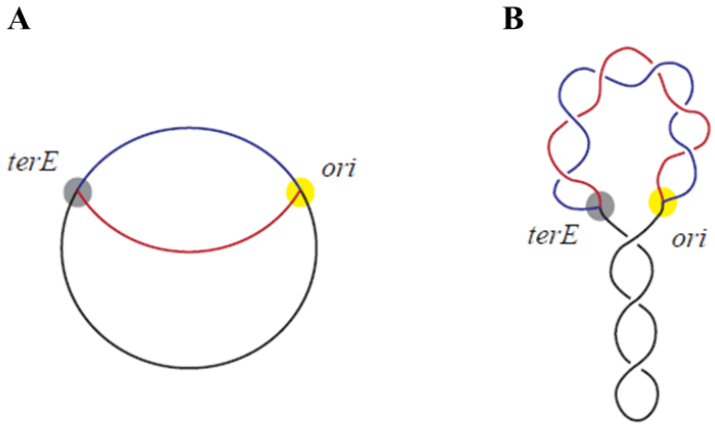

Figure 4.1 – Replication intermediate model. A) Relaxed RI containing *terE* site and unidirectional origin of replication (*ori*). **B)** RI with negatively supercoiled unreplicated region and precatenated replicated region. The negative supercoiling in the unreplicated region is free to equilibrate with the left-handed precatenation in the replicated region. The replicated regions cannot maintain supercoiling as these regions are free to rotate around the nicks at the forks. The two replicated duplexes are in blue and red, and the unreplicated portion is in black.

In our model, a plasmid was constructed with a unidirectional ColEI origin of replication, a *terE* site, and *attP* and *attB* sites. The *att* sites were positioned in the plasmid so they would end up in the replicated region of the RI (Figure 4.2). Once the RI has formed, it is expected to have supercoiling in the unreplicated region and precatenation in the replicated regions produced by fork and maybe even *ori* rotation. Each sister duplex has a copy of *attP* and *attB* sites, recombination by ΦC31 integrase should result in two circles, which could be catenated if precatenation was entrapped (Figure 4.2).

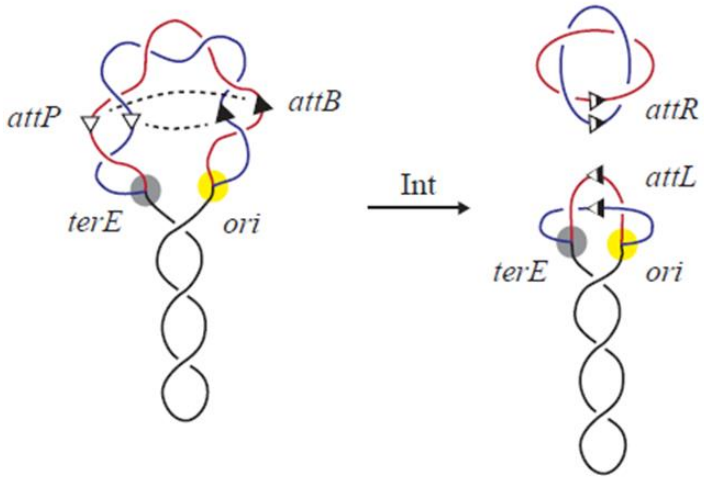

Figure 4.2 – Approach for precatenane entrapment through site-specific recombination on RI. The *att* sites were positioned between the origin of replication (*ori*) and *terE* site. After replication terminated at *terE* each duplex had a pair of *att* sites. After recombination by ΦC31 integrase the products are a catenane if precatenation is trapped and the rest of the RI. Dotted lines represent site-specific recombination between *attP* and *attB* sites on the same duplex.

4.2 Construction of plasmids containing *attP* and *attB* sites and replication termination site *terE*

To obtain RIs, two different plasmids were constructed. These plasmids had to have a unidirectional origin of replication, in other words only one replication fork proceeding in one direction replicates the full plasmid. A cassette containing the *attP* and *attB* sites was inserted after the *ori*, so it can be replicated. The two *att* sites were spaced by 2.5 kb and in between them is the kanamycin resistance and *lacI* genes. The kanamycin resistance gene was used as a selective marker in this chapter, while the *lacI* gene was used as a spacer to maintain the distance between the *att* sites at 2.5 kb. The *terE* was inserted after the cassette.

The difference between the two plasmids was the copy number and the ratios between the replicated and unreplicated regions. pAOT10 had a pBR322 origin of replication and the *rop* gene, which gave plasmid a low/medium-copy number. pAOT12 had a pUC18 origin of replication which lacks the *rop* gene, and therefore this plasmid had a higher-copy number. For pAOT10 the unreplicated (1537 bp) region was 3.3x smaller than the

replicated region (5095 bp). For pAOT12 the difference in size was approximately two times, the unreplicated portion was 1689 bp and replicated portion was 3402 bp.

First, pBR322 was digested with EcoRI and HindIII and the 4330 bp fragment was ligated to a synthetic nucleotide that also introduced a NcoI site, forming pBR322-*terE*-NcoI (Figure 4.3A). Then, pBR322-*terE*-NcoI was digested with BamHI and NcoI and the 4013 bp fragment was ligated to 2619 bp fragment containing the cassette, obtained by digestion of pAOT3 with the same enzymes. This plasmid was named pAOT10 (Figure 4.3B). To construct pAOT12, *terE* was simply inserted into pAOT3 digested with NgoMIV and BamHI (Figure 4.3C).

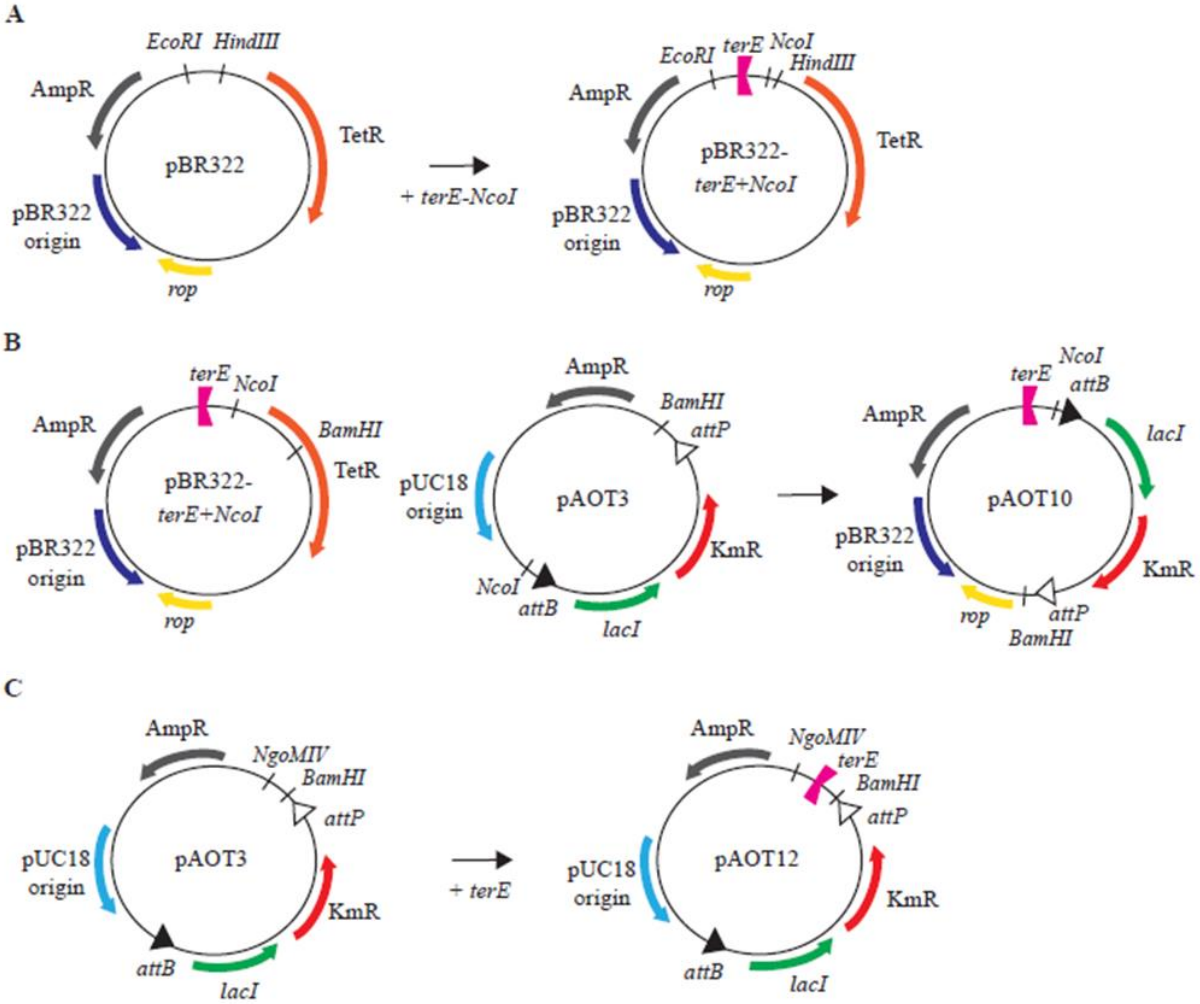

Figure 4.3 – Construction of pAOT10 and pAOT12. The distance between the origins, genes, *att* sites and *terE* site are not to scale. **A)** Construction of pBR322-*terE*-NcoI, a pBR322-based plasmid with *terE* site inserted between EcoRI and HindIII sites. **B)** Construction of pAOT10 with the pBR322 origin, *rop* gene, ampicillin resistance gene, *terE* site, *attP*, *attB*, kanamycin resistance, and *lacI* genes. The *attB* site is 13 bp away from the *terE*, and *attP* site is 1529 bp away from the *rop* gene. **C)** Construction of pAOT12 with the pUC18 origin, ampicillin resistance gene, *terE* site, *attP*, *attB*, kanamycin resistance, and *lacI* genes. The *attP* site is 12 bp away from the *terE* site, and *attB* site is 449 bp away from the origin.

4.3 Formation of RI *in vivo*

After construction of plasmids containing the *terE* site, it was important to test if RIs would form. When extracting RIs from bacteria, two methods were used. A standard alkaline lysis method, where the double-strands are denatured and renatured; and a non-denaturing one. In the former, when two replicated sister duplexes (represented in red and blue in Figure 4.1) are denatured, two single-strands are not topologically attached. They can dissociate apart from the parent singe-strands which served as template during DNA replication. During renaturation, the two parent single-strands renature together because of their proximity and complementarity, which results in the original plasmid, without RI topology. For this reason, a non-denaturing method (preparation of crude lysate by Triton lysis) was also used to maintain the RI topology formed in the cells.

The presence of the RI was studied by digestion of DNA extracted by alkaline and Triton lysis. XbaI and ScaI each cut once in pAOT10 and pAOT12, therefore it is expected that the plasmids are going to be linearized upon digestion with one of those enzymes (Figure 4.4A). In the RI, XbaI cuts in the replicated region, while ScaI cuts in the unreplicated portion (Figure 4.4A). Digesting the RI with XbaI results in a double Y-shape and digesting with ScaI in a bubble-like shape (Figure 4.4A).

Cultures of DS941 containing pAOT10 or pAOT12 were grown overnight at 37°C with shaking. Then, these cultures were diluted 40-fold into fresh LB containing kanamycin and grown at 37°C with shaking until OD_{600} of 0.6 was reached. DNA was extracted using alkaline lysis or a non-denaturing method by Triton lysis. Then DNA was digested with XbaI or ScaI at 37°C for 1 h. Samples were separated by agarose gel electrophoresis and DNA detected by staining with ethidium bromide.

For pAOT10, when DNA was extracted using alkaline lysis, only supercoiled circular plasmid was present (Figure 4.4B lane 1). When Triton lysis was used, supercoiled pAOT10 was present and numerous bands migrating as a smear were observed (Figure 4.4B lane 2). These bands could correspond to RIs since these have a higher mass compared to the circular pAOT10, which caused their slower migration on the gel. After DNA digestion with XbaI, pAOT10 was linearized and the RIs migrated mainly as a band (Figure 4.4B lanes 3 and 4). Upon DNA treament with ScaI, pAOT10 was linearized and

the RIs migrated as a single band again (Figure 4.4B lanes 5 and 6), but this band migrated slower than the RI band that had been treated with XbaI (Figure 4.4B lanes 4 and 6).

Similar results were observed for pAOT12. Alkaline lysis only allowed extraction of supercoiled circular DNA (Figure 4.4B lane 7), while Triton lysis allowed extraction of circle and RIs, with the RIs migrating on the gel as a band instead of a smear (Figure 4.4B lane 8). Upon digestion with XbaI, circular pAOT12 was linearized, and the RIs migrated as one band (Figure 4.4B lanes 9 and 10). Upon digestion with ScaI, circular pAOT12 was linearized, while the RIs migrated as one slower band (Figure 4.4B lanes 11 and 12).

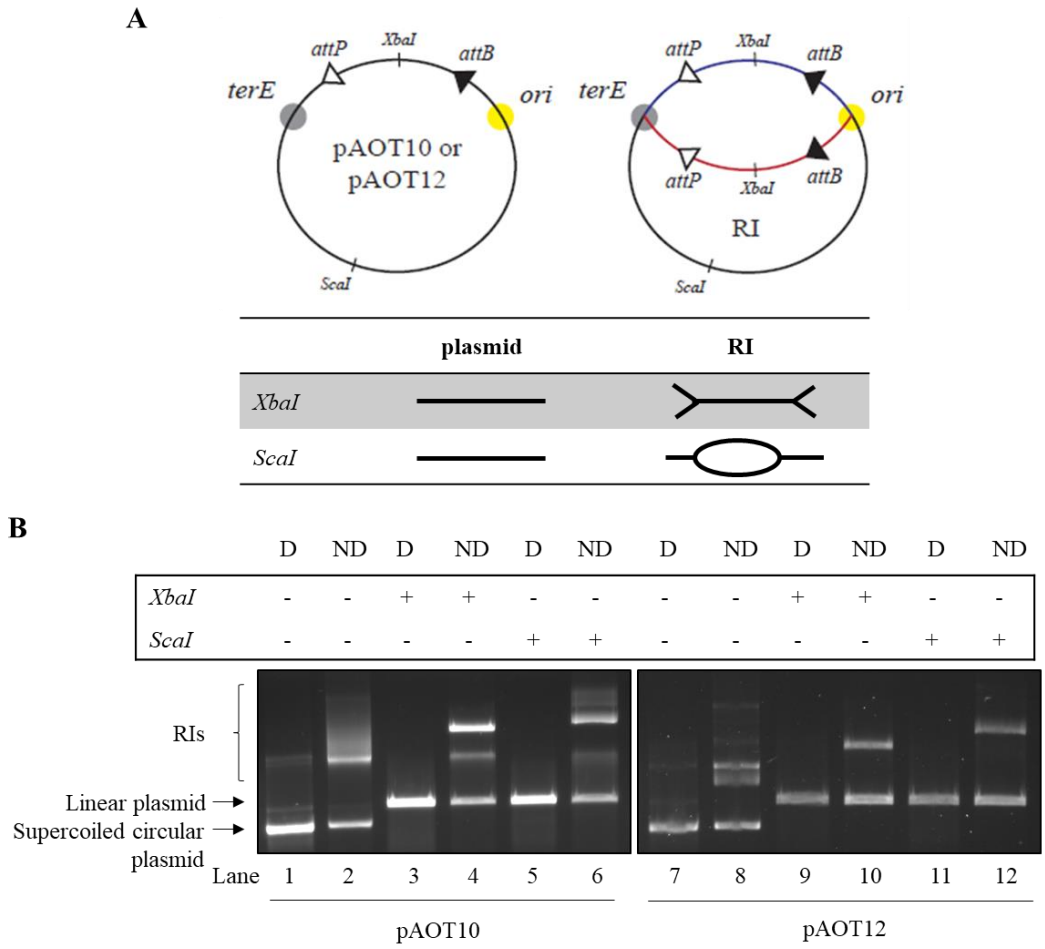

Figure 4.4 – Digestion of DNA obtained by alkaline and Triton lysis. A) Schematic representation of the circular plasmids pAOT10 and pAOT12 and their RIs. Localization of the restriction sites recognized by XbaI and ScaI are shown. The unreplicated region is represented in black and the replicated regions are in red and blue. The table shows the expected topologies after plasmid and RI digestion with XbaI or ScaI. The circular plasmids are expected to be linearized with XbaI and ScaI. The RIs are expected to acquire a double Y-shape after digestion with XbaI, and a bubble-like shape after digestion with ScaI. **B)** 1% agarose gel run at 90V showing the migration of DNA in untreated samples, or DNA digested with XbaI or ScaI. *ori*, origin of replication; RI, replication intermediate; D, denaturing method (alkaline lysis); ND, non-denaturing method (Triton lysis).

Altogether, these results show presence of RIs, which could be extracted by the non-denaturing Triton lysis method.

4.4 Studying the topology of RIs

The RIs formed from both, pAOT10 and pAOT12, were studied for topological complexity. In other words, this study allowed us to see how supercoiled the RIs were. The more supercoiled they are, higher the chance of precatenane formation. Therefore, the higher the chance of obtaining catenanes with trapped precatenation after Int recombination. As mentioned above, pAOT10 and pAOT12 differ in the plasmid copy-number and in the ratios between the unreplicated and replicated regions. Therefore, any difference in results regarding RIs topology could be explained by those.

DNA was extracted as described in section 4.3 and then nicked with DNase I in the presence of ethidium bromide for removal of supercoiling. DNA was treated with Topo I (calf thymus) which relaxes supercoiled DNA in the absence of ethidium bromide. To supercoil the DNA, this was added to a mixture containing ethidium bromide (6 µg/ml) and Topo I. The intercalator decreases Lk_0 of the molecule, and Topo I introduce a single-stranded nick. Therefore, after strand re-ligation and ethidium bromide removal, the final product is negatively supercoiled. The samples were then separated by agarose gel electrophoresis, the gel stained with ethidium bromide and DNA detected by fluorescence scanning (Typhoon).

As observed earlier, when analysing the results obtained for pAOT10 it was observed that upon DNA extraction via alkaline lysis (denaturing method (D)) only circular pAOT10 was extracted, and no RIs (Figure 4.5 lane 1 and 2). When DNA was extracted via the non-denaturing method (ND), some circular pAOT10 was present and an extensive ladder of bands was observed, which were thought to correspond to RIs with different level of supercoiling (Figure 4.5 lane 3). After nicking this sample to eliminate supercoiling, most of the RIs seem to disappear but the bands present at the top of the gel remained, suggesting that the top bands represent the nicked RIs (Figure 4.5 lane 4). When the sample from lane 3 was treated with Topo I in absence of ethidium bromide, a ladder of pAOT10 circle topoisomers was observed migrating below the band corresponding to the

nicked plasmid, and a brighter band was present at the top of the gel (Figure 4.5 lane 5). The pAOT10 topoisomers are more widely spread than the RI topoisomers, suggesting that the bands in lane 3 are different from topoisomers of circular pAOT10. Furthermore, the RI topoisomers ladder extends all the way back to the presumed nicked RI position, while the slowest circular topoisomers migrate at about the position of the nicked circle. Treating the sample from lane 3 with Topo I in presence of ethidium bromide showed two major differences compared to untreated sample. First, the circular pAOT10 was more supercoiled, migrating slightly faster than the untreated circular pAOT10 (Figure 4.5 lane 6). Second, the RIs migrated closer to each other in a smear-like way, with no visible ladder of bands. Also, the RIs migrated faster than the ones observed in the untreated sample. This suggested that the extracted RIs of pAOT10 had a low level of supercoiling.

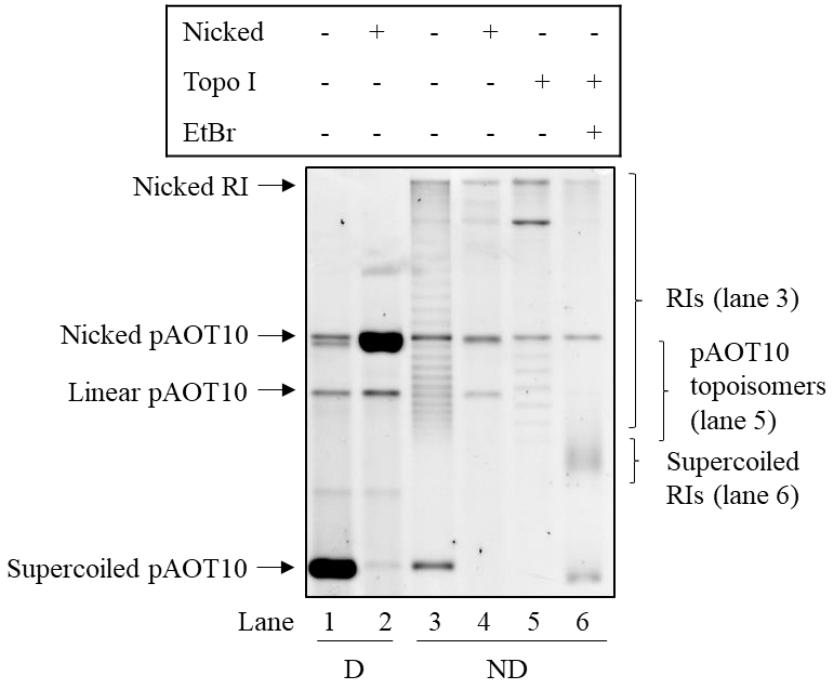

Figure 4.5 – pAOT10 RI extraction and supercoiling. 1% agarose gel run at 35V. The DNA was extracted using alkaline lysis (denaturing (D)) and a non-denaturing (ND) method. The samples were nicked with DNase I in presence of ethidium bromide (EtBr) for removal of supercoiling; treated with Topo I for DNA relaxation and with Topo I in presence of 6 µg/ml EtBr for DNA supercoiling.

The same results were observed for DNA extracted by the two different methods for pAOT12. The DNA extracted using the denaturing method (alkaline lysis) gave only circular pAOT12 (Figure 4.6 lanes 1 and 2). When the DNA was extracted using the non-denaturing method, pAOT12 and RIs were present (Figure 4.6 lane 3). However, the RIs of pAOT12 migrated as a more compact ladder apparently more supercoiled, compared to

those observed for pAOT10 where the ladder was spread over the lane. The nicking reaction was not efficient since some of the supercoiled pAOT12 and RIs remained present (Figure 4.6 lane 4). Treating the sample from lane 3 with Topo I in the absence of ethidium bromide resulted in topoisomers of circular pAOT12, migrating just below the band corresponding to the nicked circle (Figure 4.6 lane 5). In this sample, the RIs migrated much slower, appearing at the top of the gel. The bright band at the top of the gel in lane 5 might indicate the migration of the relaxed RI. When the sample from lane 3 was treated with Topo I in the presence of ethidium bromide, circular pAOT12 was more supercoiled and migrated on the gel slightly faster than the one in the untreated sample (Figure 4.6 lane 3 and 6). RIs migrated as a more compacted ladder but not that much faster than the untreated RIs. This suggested that the RIs of pAOT12 had higher level of supercoiling, than those of pAOT10.

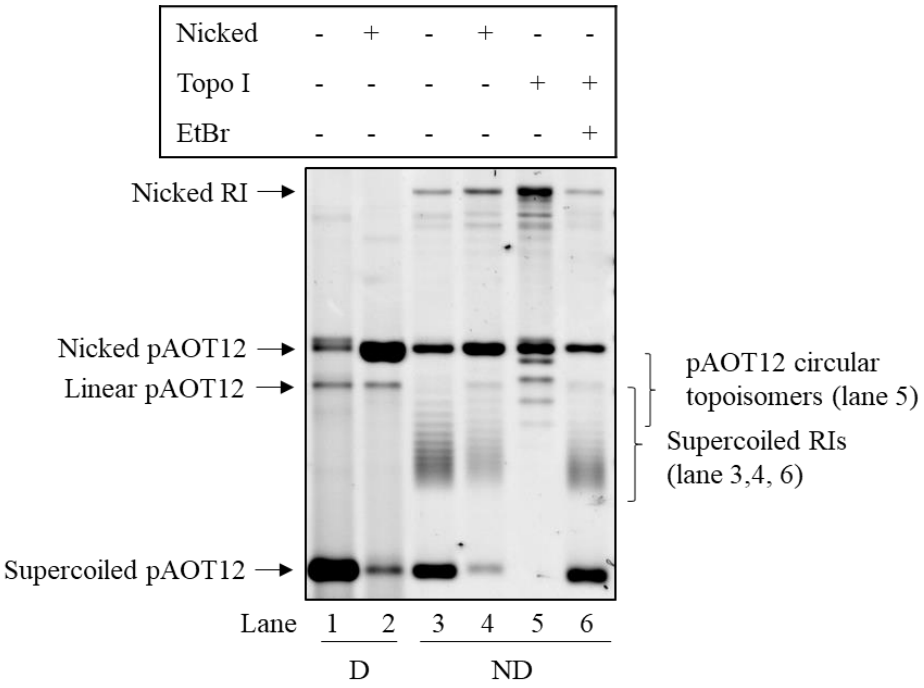

Figure 4.6 – pAOT12 RI extraction and supercoiling. 1% agarose gel run at 35V. The DNA was extracted using alkaline lysis (denaturing (D)) and a non-denaturing (ND) method. The samples were nicked with DNase I in the presence of ethidium bromide (EtBr) for removal of supercoiling; treated with Topo I for DNA relaxation and with Topo I in the presence of 6 µg/ml EtBr for DNA supercoiling.

In conclusion, it was observed that the pAOT12 RI could be easily purified at higher concentration than pAOT10 RI, probably due to the higher-copy number of pAOT12. Furthermore, the RIs from pAOT12 were more supercoiled than the RIs from pAOT10. One reason for this could be the ratios in the unreplicated and replicated regions. pAOT10

had an unreplicated portion 3.3x smaller than the replicated one, whereas that of pAOT12 was 2x smaller than the replicated region. Possibly, the smaller the unreplicated region, less supercoils it can accommodate and therefore less precatenanes are going to form. On the other hand, if the unreplicated region is equivalent or bigger than the replicated region, more supercoiling can be introduced in the unreplicated portion and more precatenanes can form between the replicated duplexes. In a study by Peter and co-workers, they also found in their *in vitro* system that the smaller the replicated region of RI, the less precatenation it can accommodate (Peter *et al*, 1998). Since pAOT12 RIs were found to be more supercoiled than those of pAOT10 (Figure 4.7), and more supercoiling should lead to more precatenation, pAOT12 was chosen for further experiments in detection of precatenation.

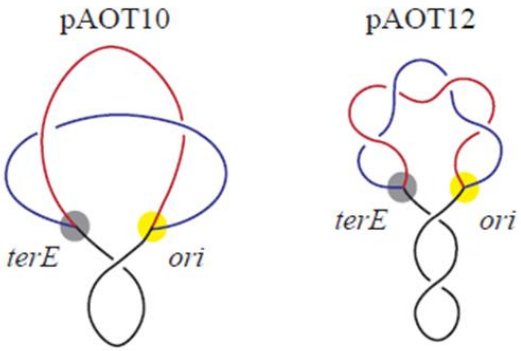

Figure 4.7 – Schematics illustrating RIs of pAOT10 and pAOT12. pAOT10 has an unreplicated region of 1537 bp (23%) and two replicated segments of 5095 bp (77%). pAOT12 has an unreplicated region of 1689 bp (33%) and two replicated segments of 3402 bp (67%). RIs from pAOT12 were more supercoiled than those from pAOT10. The replicated duplexes are in red and blue, and unreplicated region is in black. o*ri*, origin of replication.

4.5 *In vivo* site-specific recombination between *attP* and *attB* sites on RIs

Site-specific recombination was performed on replicating pAOT12 *in vivo* mediated by arabinose induction of ΦC31 integrase from pZJ7m. Recombination of the circular pAOT12 will produce two circular products: one of 2545 bp containing *lacI* and kanamycin resistance genes, and the other 2546 bp circle containing the rest of the plasmid. Recombination on RI produces two of the 2545 bp circles containing each *lacI* and kanamycin resistance genes, and a replication bubble structure containing the rest of

the RI. It might also be possible to delete just one 2545 bp circle instead of two. If precatenation has been trapped by site-specific recombination, the two 2545 bp cassettes produced from the RI will be catenated. To see the topology of these catenanes, they had to be nicked to remove supercoiling. The enzyme used to do this, Nb.BbvCI, is a nicking endonuclease that has one recognition site in the cassette between the *attP* site and the kanamycin resistance gene (Figure 4.8).

The cassettes, catenated or not, might be linked to the rest of the RI (Figure 4.8B), therefore they can be freed by cleaving the RI with BamHI. BamHI has one restriction site in pAOT12 and its RI between *terE* and the *attP* site, just outside the 2545 bp cassette (Figure 4.8). Digestion with this enzyme linearizes pAOT12 and the second circular product (2546 bp) (Figure 4.8A) and cleaves the RI and its recombination product to double Y-shaped products (Figure 4.8B).

Any catenane of the 2545 bp circles (5090 bp) will be quite similar in size to the unrecombined pAOT12 (5091 bp) and catenanes produced from this. In an agarose gel, the nicked 2-noded catenane migrates very close to the linearized pAOT12. Therefore, pAOT12 and the remaining RI were cleaved with AlwNI. AlwNI has one restriction site in pAOT12 and RI in the origin of replication (Figure 4.8). Digestion with this enzyme and BamHI leads to fragments smaller than 5090 bp, which do not co-migrate with the nicked 2-noded catenane.

Treating the DNA with Nb.BbvCI, BamHI and AlwNI simultaneously, allowed nicking the circular cassettes (catenated or not) and removing all the bands that co-migrate with catenanes on the agarose gel.

DS941 and C600SN containing pAOT12 and pZJ7m were grown overnight in LB with glucose at 37°C with shaking. Then, the culture was diluted 25-fold into fresh LB containing kanamycin, chloramphenicol and glucose, and grown at 37°C with shaking until OD_{600} of 0.6 was reached. Bacteria were collected by centrifugation and resuspended in fresh LB containing chloramphenicol. 10 ml of culture were taken, cells were pelleted, and DNA was extracted. This DNA was used as timepoint 0. Arabinose or arabinose and norfloxacin were added to the remaining culture and incubation continued at 37°C. 10 ml samples were taken at timepoints 10, 20 and 30 minutes and the DNA extracted using a QIAprep Spin Miniprep Kit. Although this treatment will destroy any RI present, any 2545 bp covalently closed circles and their catenanes should be purified intact. The extracted

DNA was treated with BamHI, AlwNI and Nb.BbvCI in a single reaction. The samples were separated by agarose gel electrophoresis and the DNA detected by Southern hybridization by using the kanamycin resistance gene as probe.

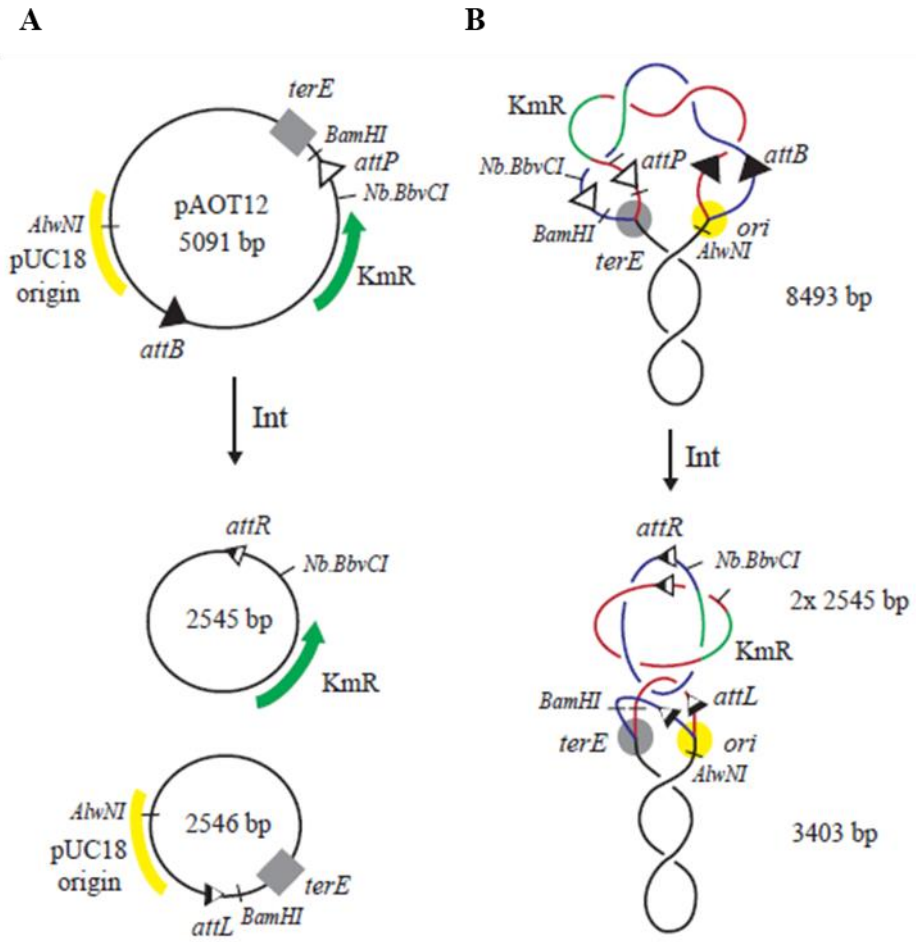

	pAOT12	RI
Unrecombined	3423 bp (linear; Km) 1668 bp (linear)	6823 bp (Y-shape; Km) 1670 bp (Y-shape)
Recombined	2545 bp (nicked circle; Km) 1668 bp (linear) 878 bp (linear)	5090 bp (nicked catenane; Km) 1733 bp (Y-shape) 1670 bp (Y-shape)

Figure 4.8 – Schematic diagram illustrating pAOT12 and its RI before and after recombination by ΦC31 integrase. This diagram shows where each enzyme cuts or nicks in the unrecombined and recombined pAOT12 and RI. **A)** Treating pAOT12 with BamHI, AlwNI and Nb.BbvCI produces two linear fragments of 3423 bp and 1668 bp when the plasmid has not recombined. If pAOT12 has recombined, the treatment produces two linear fragments of 1668 bp and 878 bp from the 2546 bp circle, and a nicked circle of 2545 bp. **B)** Treating the RI with the same enzymes produces two Y-shaped fragments of 6823 bp and 1670 bp. After recombination, two Y-shaped fragments of 1733 bp and 1670 bp and two 2545 bp nicked circles, which may be catenated are produced. The 2545 bp circles could also be linked to the remaining RI molecule as shown. KmR, kanamycin resistance gene; *ori*, origin of replication; Int, ΦC31 integrase.

After alkaline lysis, the expected topologies present in the samples were the circular substrate pAOT12, the circular products of recombination of 2545 bp and 2546 bp and any 5090 bp catenane produced from RI (Figure 4.8). Dimers of the 2545 bp and 2546 bp circles produced by intermolecular recombination would also be extracted. After treatment with Nb.BbvCI, BamHI and AlwNI, not all of those topologies were expected to be detected by Southern hybridization with the kanamycin resistance gene probe. The expected fragments to be seen on the blot were the linear 3423 bp fragment produced by digestion of unrecombined pAOT12; the nicked 2545 bp circle produced by recombination on pAOT12; and the nicked 5090 bp dimer and any catenanes of two 2545 bp circles produced by recombination on the RI.

When the unrecombined pAOT12 was treated with BamHI, AlwNI and Nb.BbvCI, the fragment of 3423 bp containing the kanamycin resistance gene was detected by Southern hybridization (Figure 4.9 lane 1 and Figure 4.10 lane 1). In DS941, at 0 minutes the brightest band corresponded to the linear 3423 bp fragment from the unrecombined pAOT12, as expected (Figure 4.9 lane 2). After 10 minutes of Int expression the 3423 bp fragment decreased in intensity while the 2545 bp open circle started to appear, suggesting that recombination was occurring (Figure 4.9 lane 3). With the increasing incubation time, the linear 3423 bp fragment kept on gradually disappearing while the nicked 2545 bp circle continued to increase in amount (Figure 4.9 lanes 4 and 5). The nicked 5090 bp circle accumulated with the time. Interestingly, a fragment of approximately 6 kb appeared after 10 minutes of treatment of bacteria with arabinose. This 5973 bp fragment is formed when a dimer of pAOT12 is produced by intermolecular recombination (see Chapter 3 section 3.3) and cleaved with BamHI and AlwNI. Furthermore, the 2545 bp circle dimer is produced by recombination between *attP* and *attB* sites of the pAOT12 dimer. Therefore, appearance of the linear 5937 bp fragment at the early timepoint, and appearance of the nicked 5090 bp fragment at the later timepoints, suggests that the 5090 bp fragment corresponds to the dimer rather than a catenane. The 2545 bp circle dimer can also be formed from recombination on RI between *attP* on one sister duplex and *attB* on the second duplex. This was an experiment made *in vivo* and catenanes probably would not accumulate with time due to Topo IV activity.

When the experiment was carried out in presence of norfloxacin to inhibit type II topoisomerases, the 3423 bp fragment band intensity did not decrease as much as it did in the experiment with just arabinose. The 2545 bp fragment only formed after 30 minutes of

induction and at a very low level (Figure 4.9 lanes 6-9). This suggests that once the supercoiling level altered, the Int could not be expressed and recombination would be impaired. Lack of supercoiling in the ΦC31 integrase substrate would not inhibit recombination, since Int can recombine linear or relaxed substrates (Colloms *et al*, 2014).

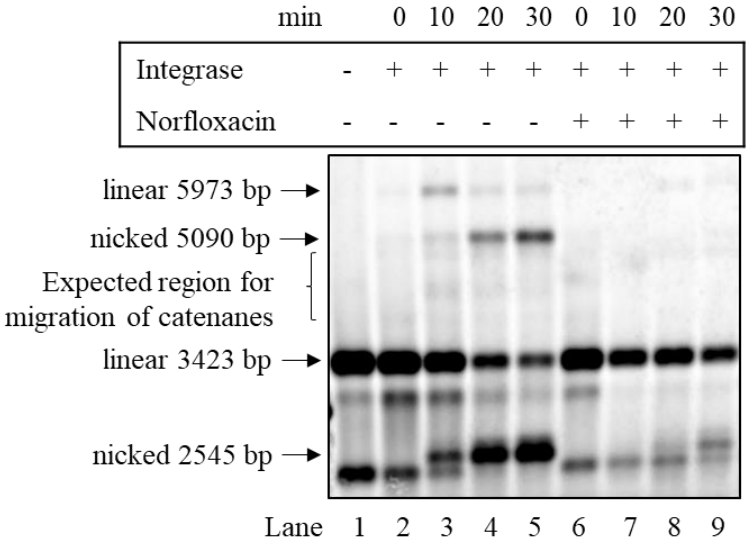

Figure 4.9 – Analysis of *in vivo* site-specific recombination on RI in DS941. Southern hybridization of samples separated on a 0.7% agarose gel run at 35V. DS941 containing pAOT12 and pZJ7m was treated with 0.2% arabinose or 0.2% arabinose and 10 µg/ml norfloxacin in a time-course experiment. At the 0, 10, 20 and 30 minutes timepoints the DNA was extracted and treated with BamHI, AlwNI and Nb.BbvCI. The samples were then separated by agarose gel electrophoresis and DNA detected by Southern hybridization using kanamycin resistance gene as probe. As a control, unrecombined pAOT12 was treated with BamHI, AlwNI and Nb.BbvCI to obtain the 3423 bp fragment marker (lane 1).

In C600SN, a strain with DNA gyrase resistant to norfloxacin, the 0 minutes timepoint showed presence of the 3423 bp fragment, as expected (Figure 4.10 lane 2). Upon arabinose addition for Int expression, the 3423 bp fragment was mostly gone in first 10 minutes, and the 2545 bp fragment appeared at the same time, showing recombination occurred quickly (Figure 4.10 lanes 3, 4 and 5). The 5090 bp circle formed after 10 minutes of incubation and continued to accumulate with time. As described for DS941, the 5090 bp circle formed in C600SN was thought to be a dimer of the 2545 bp circle.

When C600SN was treated with arabinose in the presence of norfloxacin, recombination was observed, in contrast to DS941 where little recombination was seen. At 0 min, the 3423 bp fragment was observed, suggesting no recombination had yet occurred, as expected (Figure 4.10 lane 6). At 10 minutes of treatment with arabinose and norfloxacin

the 3423 bp fragment largely gone away while the 2545 bp circle started to form, as well as the 5090 bp one (Figure 4.10 lane 7). As the time progressed, both circles accumulated (Figure 4.10 lanes 8 and 9). In C600SN, just Topo IV was inhibited by addition of norfloxacin, therefore the band corresponding to the 5090 bp circle could be the dimer or the 2-noded catenane. The region expected for catenane observation appeared clear on the blot (Figure 4.10 lanes 7, 8 and 9), suggesting no complex catenanes were formed during recombination.

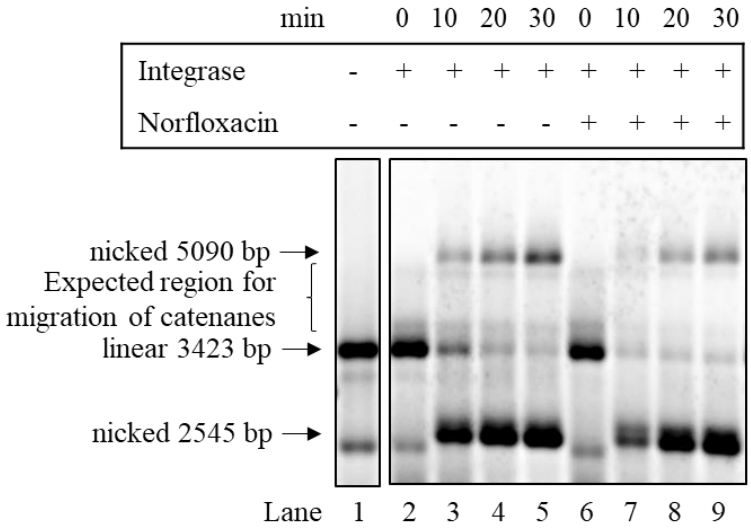

Figure 4.10 – Analysis of *in vivo* site-specific recombination on RI in C600SN. Southern hybridization of samples separated on a 0.7% agarose gel run at 35V. C600SN containing pAOT12 and pZJ7m was treated with 0.2% arabinose or 0.2% arabinose and 10 µg/ml norfloxacin in a time-course experiment. At the 0, 10, 20 and 30 minutes timepoints the DNA was extracted and treated with BamHI, AlwNI and Nb.BbvCI. The samples were then separated by agarose gel electrophoresis and DNA detected by Southern hybridization using kanamycin resistance gene as probe. As a control, unrecombined pAOT12 was treated with BamHI, AlwNI and Nb.BbvCI to obtain the 3423 bp fragment marker (lane 1).

In summary, the *in vivo* recombination on pAOT12 and presumably its RI occurred. The 2545 bp circle could have formed from recombination on pAOT12 or on RI, if the sister duplexes were not precatenated or if recombination does not capture the precatenation. Linear 3423 bp fragment can only form from unrecombined substrate pAOT12. The 5090 bp could have formed from recombination on pAOT12 dimer, producing a 2545 bp circle dimer. It also could have formed from intermolecular recombination between *att* sites on sister duplexes of the RI. However, if the replicated duplexes had few precatenanes, intramolecular recombination might have resulted in a catenane with few crossings, like a 2-noded catenane. Although the 2-noded catenane is expected to run ahead of the

unknotted dimer, they do migrate close to each other and it is difficult to draw any definite conclusions from these gels.

4.6 Topo IV treatment for verification of catenane formation

If site-specific recombination on RIs of pAOT12 was producing a 2-noded catenane and a dimer of the same size, one way to distinguish between them would be to treat the recombination products with Topo IV. If 2-noded catenane was present, then after Topo IV treatment the band on the blot corresponding to it should have decreased, and the one corresponding to nicked 2545 bp increased. Recombination products obtained from C600SN were chosen for this experiment because DS941 did not formed any dimer or 2-noded catenane when treated with arabinose and norfloxacin.

The same recombination products described in section 4.5 were treated with BamHI, AlwNI and Nb.BbvCI in a single reaction as before. Then, half of the digestion volume was loaded on the gel without Topo IV treatment, and the other half was treated with Topo IV prior to loading on the gel. The samples were separated by agarose gel electrophoresis and the DNA detected by Southern hybridization using kanamycin resistance gene as probe.

As described earlier, the nicked 5090 bp circle formed when bacteria were treated with arabinose in absence of norfloxacin most likely corresponded to the dimer of the 2545 bp circle and not catenane, as Topo IV should rapidly unlink catenanes *in vivo* as they are produced (Figure 4.11 lanes 1-4). Regardless, these samples were treated with Topo IV *in vitro* and used to check any bands intensity variations which are not caused by catenane decatenation by Topo IV (Figure 4.11 lanes 9-12). As can be observed, all bands had reduced intensity after Topo IV treatment, suggesting that lower bands intensity was due to other reason than the Topo IV decatenation, such as loss of DNA during processing. The recombination products obtained by C600SN treatment with arabinose and norfloxacin, also showed decrease in bands intensity after Topo IV treatment (Figure 4.11 lanes 5-8, 13-16). The decrease in bands intensity of all samples seemed to be due to DNA loss during Topo IV reactions rather than to decatenation of catenanes. Therefore, the results presented here suggested that 2-noded catenane was not formed during site-specific recombination on RIs.

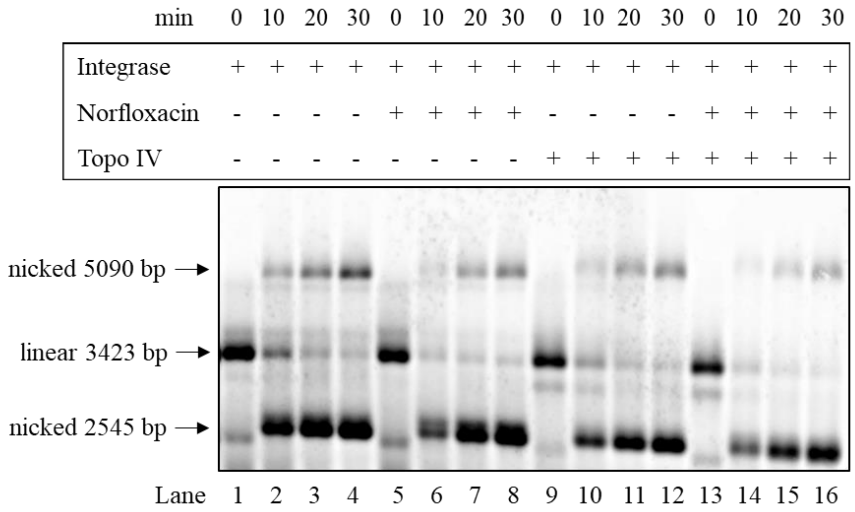

Figure 4.11 – Analysis of *in vivo* site-specific recombination on RI in C600SN and treatment with Topo IV. Southern hybridization of samples separated on a 0.7% agarose gel run at 35V. C600SN containing pAOT12 and pZJ7m was treated with 0.2% arabinose or 0.2% arabinose and 10 µg/ml norfloxacin in a time-course experiment. At the 0, 10, 20 and 30 minutes timepoints the DNA was extracted and treated with BamHI, AlwNI and Nb.BbvCI. Half of the volume was treated with Topo IV. The samples were separated by agarose gel electrophoresis and DNA detected by Southern hybridization using kanamycin resistance gene as probe. Lanes 1-8 are the same as lanes 2-9 from Figure 4.10.

4.7 Conclusion

Cloning a replication termination site into a plasmid is an efficient method to create RIs. RI in turn should be a good model for precatenane formation and could be used for their entrapment.

In this chapter, two plasmids were produced, and both were able to form RI *in vivo*. The RI produced from pAOT12 were more supercoiled than those from pAOT10, possibly due to a larger unreplicated region in pAOT12. *In vivo*, site-specific recombination by ΦC31 integrase on *att* sites, positioned on the replicated region of the RI, should lead to formation of the 2545 bp product and its dimer. However, both these products can form from the circular form of pAOT12 as well. The presence of catenanes was not confirmed, maybe because pAOT12 was not supercoiled enough for generation of precatenanes. Also, absence of catenanes might indicate that rotation at fork or *ori* has not occurred and no precatenanes were formed. However, if both, fork and *ori* are free to rotate the density of

supercoiling and precatenation should be independent of the length of the replicated and unreplicated domains.

Constructing a new plasmid, with the unreplicated and replicated regions more proportional (half of plasmid replicated and half unreplicated) maybe would increase the chances of precatenation. Also, in pAOT10 and pAOT12 the closest *att* sites to *terE* are 13 and 12 bp away, respectively. The Tus binding to *terE* site might be preventing the recombination from occurring. Therefore, positioning the *att* sites further from the *ter* site would be advantageous.

One problem was encountered during the results analysis for precatenanes formation on RI. This problem was presence of higher concentration of pAOT12 than of RI in the extracted samples. A way of solving this problem would be transforming the strains, already containing pAOT12, with a plasmid coding for Tus protein with inducible expression (Peter *et al*, 1998). Like this, overexpression of Tus might increase the rate of formation of Tus-*terE* complex, which could stall more forks and produce more RI than fully replicated pAOT12. Using a stronger *ter* site instead of *terE* might also increase production of RI.

In a different experiment the RIs were extracted by Triton lysis from an exponentially growing culture of DS941. This sample was used in site-specific recombination *in vitro*. Unfortunately, the recombination reaction was not efficient and catenane detection was not clear. Also, the extracted sample was a mixture of RI and fully replicated pAOT12 and it would be better if only RI was present. As future work, the RI should also be extracted by Triton lysis from C600SN in presence of norfloxacin. Inhibition of Topo IV should result in RI with higher level of supercoiling and thus higher chance of precatenation between the replicated regions (Cebrián *et al*, 2015), increasing the chances of catenane formation by recombination. Additionally, the extracted RIs could be supercoiled *in vitro* by Topo I in the presence of ethidium bromide, therefore increasing the level of precatenation (see Chapter 1 section 1.1.1).

5. Precatenane entrapment on the bacterial chromosome

5.1 Introduction

Precatenation is the intertwining of replicated sister chromosomes behind the replication fork (Champoux and Been 1980; Peter *et al*, 1998). Early studies using electron microscopy showed partially replicated molecules with the replicated regions not intertwined, indicating that precatenation does not occur (Sebring *et al*, 1971; Bourgaux and Bourgaux-Ramoisy, 1972; Fuke and Inselburg, 1972). However, a study by Cozzarelli's group in 1998 showed that precatenation does form by analysing the RIs produced *in vitro* and *in vivo*. They showed that the replication fork is free to rotate *in vitro*, allowing segregation of supercoiling on either side of the fork. By presenting electron microscopy data, they suggested that the previous results obtained by electron microscopy were misleading, since the sample preparation method altered the original DNA conformation (Peter *et al*, 1998). *In vivo* studies in budding yeast have shown that fork rotation and precatenation occur specifically at replication termination (Schalbetter *et al*, 2015). A more recent study in *E. coli* has shown evidence of precatenanes formation in replicating plasmid (Cebrián *et al*, 2015). After extracting RIs from actively replicating bacteria, they analysed their torsional tension by 2D agarose gels. The three RIs tested had different proportions between the replicated and unreplicated portions, and they were constructed by positioning the *ter* site at different distances from the unidirectional origin of replication. Despite the studies on precatenation formation, this topology has not been detected or directly observed on the chromosome *in vivo* (Joshi *et al*, 2013; Bermejo *et al*, 2008).

The work presented in this chapter was carried out to try and answer the following question: does precatenation occurs on the *E. coli* chromosome *in vivo*?

A DNA cassette with selective markers surrounded by site-specific recombination sites *attP* and *attB* for the large serine recombinase ΦC31 integrase, one at each end, were inserted into the bacterial chromosome through homologous recombination. After the replication fork passes through this cassette, each sister chromosome will be left with one copy of the cassette (Figure 5.1). In a situation where no precatenation is present, site-specific recombination is expected to excise the cassettes from the sister duplexes as unlinked circles (Figure 5.1A). However, if precatenation is present, the circular products of recombination are expected to be catenated (Figure 5.1B). The number of nodes between the two catenated circles will depend on the number of precatenation nodes

entrapped between the *att* sites. Therefore, detection of catenanes in this assay would support the idea that precatenation is present in the bacterial chromosome *in vivo*.

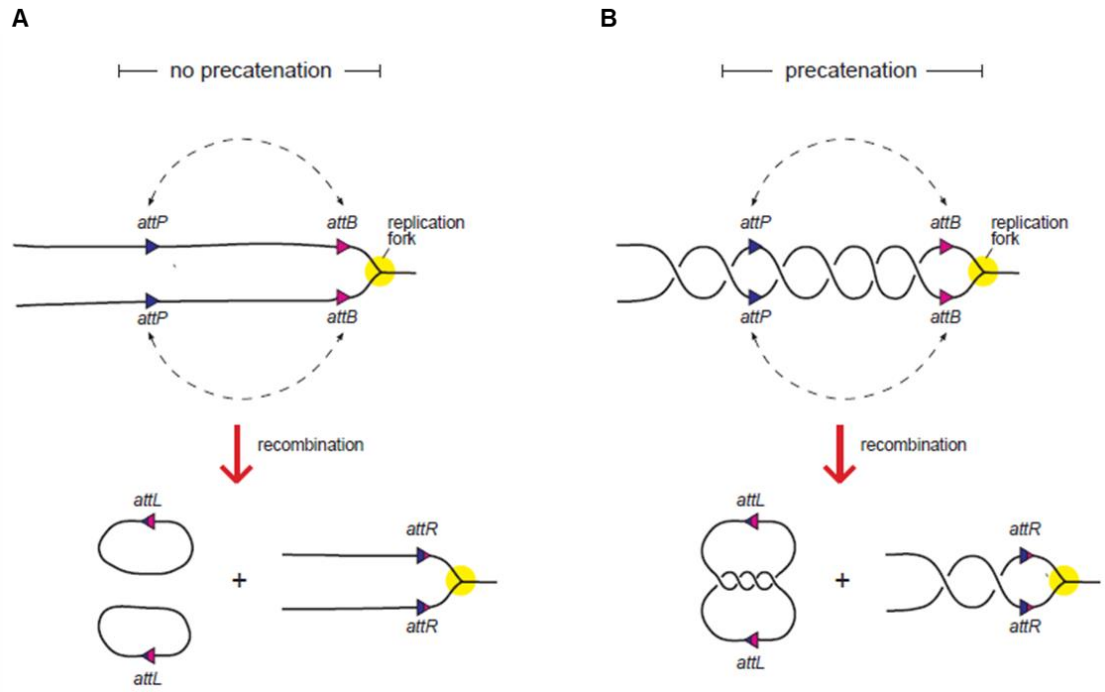

Figure 5.1 – Approach for precatenane entrapment and detection using ΦC31 integrase mediated site-specific recombination. **(A)** DNA cassette containing *attP* and *attB* sites is inserted into bacterial chromosome. After the replication fork had passed, both sister chromosomes have a copy of the cassette. When there is no precatenation at this region, inducing site-specific recombination (dashed lines) leads to separate product circles and the rest of chromosome. **(B)** On the other hand, when the two newly replicated chromosomes are precatenated, site-specific recombination can produce two catenated circles.

Curiously, with this assay catenation between fully replicated sister chromosomes could also be detected. That is, if the replication finishes at the terminus region of the chromosome, but the DNA remains catenated for significant amount of time before decatenation by Topo IV or XerCD-*dif*-FtsK (see Chapter 1 section 1.2.2 and 1.6). Sherratt's group studied the time that two *loci* in bacterial chromosomes take to segregate after replication (Wang *et al*, 2008). By labelling the origin of replication with fluorescent dye they observed by fluorescent microscopy that the two *ori* were separated approximately 15 minutes after replication. This time decreased upon Topo IV overexpression and increased with Topo IV inhibition. Therefore, they concluded that precatenation is responsible for sister chromosomes cohesion after replication.

If precatenation can be detected *in vivo*, positioning the cassette at different locations on the chromosome could help understand if precatenation occurs randomly or is specific to certain regions of the chromosome. In this work, the precatenation was studied near *dif* and near *terC* (Figure 5.2).

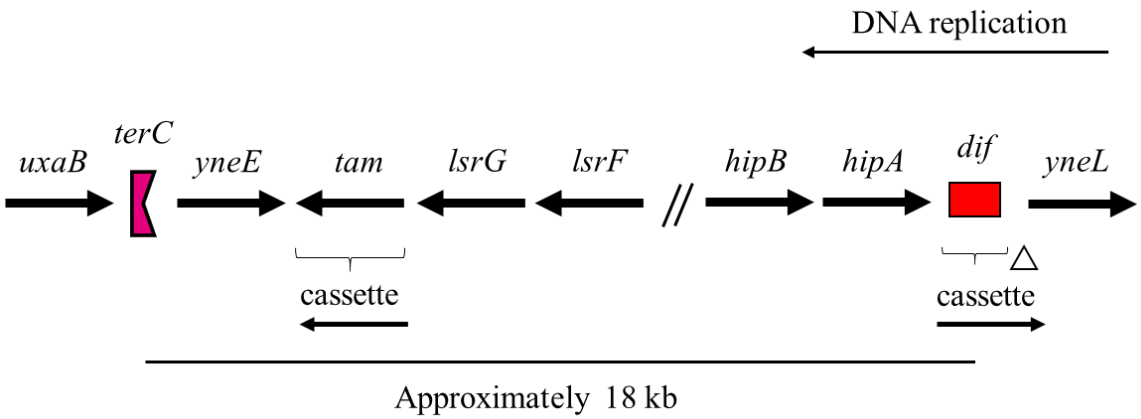

Figure 5.2 – Bacterial chromosome region where the cassette was inserted. The thick black arrows represent the organization of the genes present in the bacterial chromosome between *terC* (pink) and *dif* (red). The *terC* site halts forks progressing from right to left, which already passed through *dif*. In CP100 *dif*$^{+}$, the *attP*-Km^{R}-*lacI*-*attB* cassette was inserted between *dif* and *yneL* (represented by a white triangle). In CP100 *Δdif*, the cassette was inserted instead of *dif* (represented by the right bracket). However, this strain was not used in this thesis. In DS941 and C600SN, the cassette was inserted instead of *tam* gene (represented by the left bracket). The double forward slash indicates that the DNA sequence between *lsrF* and *hipB* is not represented.

5.2 Insertion of *attP*-Km^{R}-*lacI*-*attB* cassette into the chromosome

The *attP*-Km^{R}-*lacI*-*attB* cassette was constructed in pMTL23, as explained in Chapter 3, and the plasmid was named pAOT3 (Figure 5.3). The cassette was designed to be amplified by PCR using pAOT3 as template. Homologous recombination could then be used to insert the cassette at chosen location in the chromosome. To do this, 50 nucleotides of DNA sequence homologous to the target were added to the 5´ ends of the primers used for cassette amplification (Figure 5.3).

The *attP*-Km^{R}-*lacI*-*attB* cassette (2545 bp) was amplified in a PCR using Phusion High-Fidelity DNA Polymerase. Then the reaction was treated with DpnI for pAOT3 degradation and the cassette purified using QIAquick PCR purification kit. The purified

cassette was used in electroporation of electrocompetent strains, with the λ red system proteins provided from the temperature sensitive pKOBEGC.

Using this method, the cassette could be amplified from pAOT3 and targeted to any chosen genomic location simply by changing the homology tails on the PCR primers.

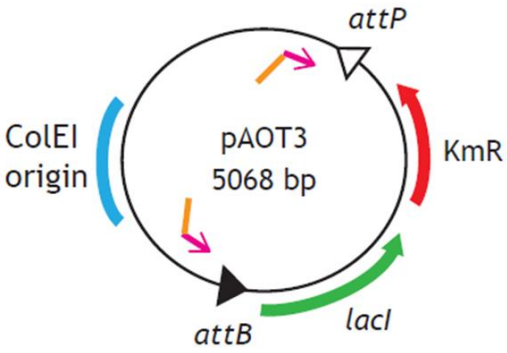

Figure 5.3 – Cassette amplification from pAOT3. The primers used for cassette amplification are in pink and the 50 bp tails homologous to *E. coli* chromosome are in orange.

5.3 Investigating whether precatenation is present near *dif*

Precatenation occurrence was first studied in the region of the *dif* site (Figure 5.2). The region in which *dif* is found is thought to be where replication generally terminates and is last to be segregated at cell division (Hendrickson and Lawrence, 2007). Furthermore, it has been suggested that recombination at *dif* by XerCD recombinases could be involved in removing final catenation prior to chromosome segregation and cell division (Ip *et al*, 2003; Shimokawa *et al*, 2013). Therefore, testing catenanes accumulation in strains depleted of *dif*, XerC or XerD could help us understand if site-specific recombination at *dif* is involved in decatenation.

The kanamycin resistance gene present between *attP* and *attB* sites was used to select for initial insertion of cassette into the chromosome, and to check it was still present. The *lacI* gene made it possible to measure recombination efficiency by blue and white screening in *ΔlacI* strains like CP100.

In this chapter, the cassette insertion into the chromosome, the efficiency and products of recombination are described.

5.3.1 Verifying insertion of the *attP*-Km^R-*lacI*-*attB* cassette in the *E. coli* chromosome near *dif*

Homologous recombination was used to insert the cassette 60 bp from *dif*, between *dif* and the *yneL* pseudogene, using λ red recombination as described above and deleting a 130 bp fragment (Figure 5.4) (The DNA sequence where the cassette was inserted is shown in Appendix A). Correct insertion of the cassette was verified by PCR of colonies formed on kanamycin plates. Different colonies were picked and resuspended in 10 µl of water each. These suspensions were used as templates in the PCRs. Specific sets of primers were designed to distinguish between the wild-type chromosome and the cassette insertion near *dif*. P2 and P3 are outward facing in the cassette and can be used with flanking genomic primers P1 and P4, respectively (Figure 5.4). P5 is in the region of the chromosome deleted when the cassette is integrated and can be used with P4 to amplify a fragment from wild-type but not cassette integrated DNA (Figure 5.4). One of the colonies that showed cassette insertion was chosen for a second PCR.

Comparison of expected sizes and the PCR products obtained confirmed successful cassette insertion (Figure 5.4). When the wild-type (no cassette) and the recombinant (cassette) strains were used in PCR with primers P1 and P2 only the recombinant strain gave a product of 694 bp (Figure 5.4). Similarly, with P3 and P4, no product was seen for the wild-type strain, but the recombinant strain gave a fragment of 914 bp. Primers P1 and P4 gave products in both strains, a band of 532 bp for the wild-type, and a faint band just above the 3000 bp for the recombinant strain. Primers P5 and P4 just amplified the 277 bp fragment in the wild-type strain. Altogether, these results show that the homologous recombination between the 50 bp tails of the cassette and the *E. coli* chromosome was successful.

Similarly, a strain was made in which *dif* was completely replaced with the *attP*-Km^R-*lacI*-*attB* cassette using the same right homology tail near *yneL* but a left homology tail just to the left of *dif*, in *hipA* gene (Figure 5.2). (The DNA sequence where the cassette was

inserted is shown in Appendix B). This strain was not studied further in this thesis but could in the future be used to study the role of *dif* in precatenane or catenane removal.

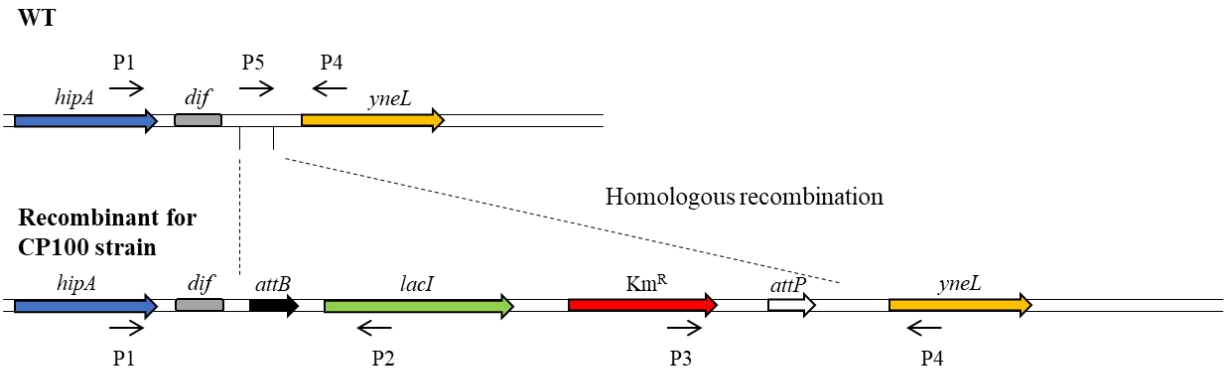

Set of primers	Wild-type strain products	Recombinant strain products
P1+P2	No product	694 bp
P3+P4	No product	914 bp
P1+P4	532 bp	3031 bp
P5+P4	277 bp	No product

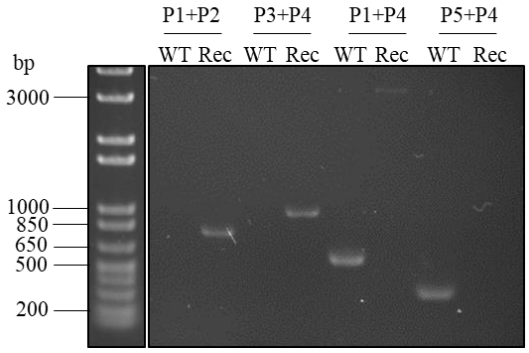

Figure 5.4 – Verification of the *attB-lacI*-Km^R-*attB* cassette integration near *dif*. The primers P1 (dif-flank-F), P4 (dif-flank-R) and P5 (dif-out-F) are complementary to the chromosome, while P2 (lac-mid-R) and P3 (kan-mid-F) are complementary to the cassette. The table shows the expected products when wild-type or recombinant strains were used as template for each set of primers. The 1% agarose gel run at 90V shows the results of PCR for both strains. WT, wild-type; Rec, recombinant strain.

5.3.2 Recombination between *attP* and *attB* sites on chromosome

Next it was important to determine if site-specific recombination between the *att* sites on the chromosome would occur and if the circular 2.5 kb product of recombination could be detected. If those could be detected, they could then be further investigated to see if they were catenated as a test of precatenation at this region of the chromosome. In this experiment recombination was mediated by ΦC31 integrase encoded by pZJ7. Therefore, upon arabinose addition, Int should be expressed and the cassette should be excised from the chromosome.

Plasmid pZJ7 was introduced into the *ΔlacI* CP100 strain containing the *attP*-Km^R-*lacI*-*attB* cassette in the chromosome near *dif* (CP100 *dif*$^+$ *attP*-Km^R-*lacI*-*attB*). Bacteria were grown overnight at 37°C with shaking in glucose, thymidine and chloramphenicol. Then the culture was diluted 40-fold into fresh media containing chloramphenicol and thymidine and grown at 37°C for 2, 3 and 4 h. Then, arabinose was added to each flask and the cells grown further for 15, 30 and 60 min. For a control, cells were grown for 5 hours without addition of arabinose. At each time point 10 ml of culture were taken, the cells collected by centrifugation and covalently closed circular DNA was extracted using a QIAprep Spin Miniprep Kit. The samples were separated by agarose gel electrophoresis and DNA detected by staining with ethidium bromide.

As expected, all the time course samples contained pZJ7 (Figure 5.5). It was also observed presence of the 2.5 kb circle, suggesting that the cassette was being excised from the chromosome. The amount of circle produced increased with higher incubation times of bacteria at 37°C. In the control cells grown for 5 hours, some supercoiled cassette produced from recombination on chromosome (Figure 5.5 lane 2) was observed. Since this sample was not treated with arabinose, the cassette was not expected to produce. However, comparing the amount of 2.5 kb circle in lane 2 and lane 11 (Figure 5.5), shows that presence of arabinose is leading to an increase of excised cassette.

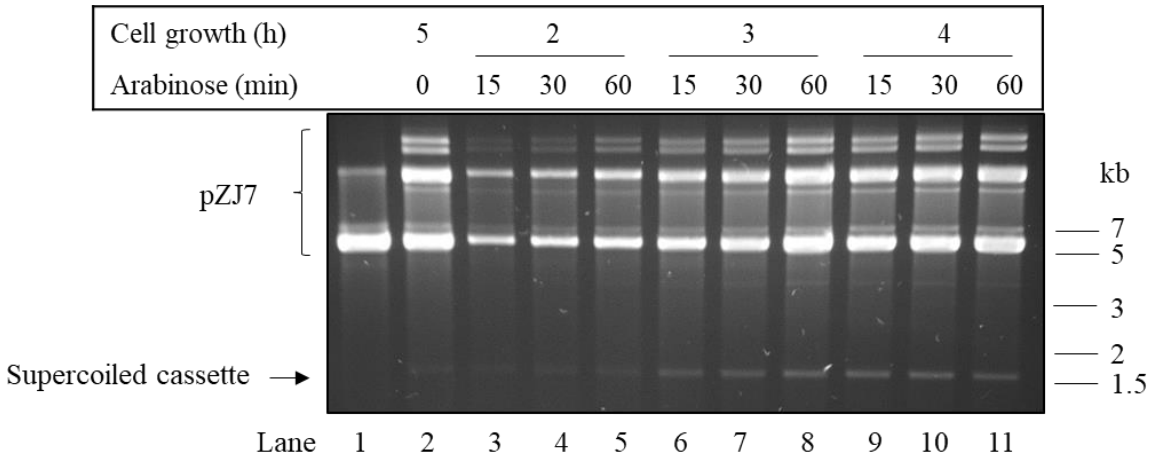

Figure 5.5 – Recombination between *att* sites on chromosome in CP100. 1% agarose gel run at 90V. CP100 dif$^+$ *attP*-Km^R-*lacI*-*attB* containing pZJ7 was grown for 2, 3 and 4 h. Then arabinose was added, and the cells were incubated for a further 15, 30 and 60 min. In a control sample, cells were grown for the full duration of the experiment (5 h) without arabinose. As a control and marker, pZJ7 was loaded in lane 1.

Altogether, these results show that recombination between the *att* sites was occurring. It also showed to be efficient, since after 15 minutes of incubation with arabinose the amount of cassette observed was similar to the amount obtained after 60 minutes (for each cell growth period). Staining the gel with ethidium bromide allowed visualization of the 2.5 kb product of recombination. However, since cassette was detected when no arabinose was added, the result suggests that a leakage in Int expression was occurring.

To confirm that the band on gel corresponded to the circular cassette of 2545 bp (Figure 5.5), two samples were chosen to be digested. The samples were the DNA extracted from cells grown for 3 hours and induced with arabinose for 15 minutes (Figure 5.6 (A)) and from cells grown for 4 hours and induced for 60 minutes (Figure 5.6 (B)). These samples were digested with BamHI which cleaves once in pZJ7, BsrGI which cleaves once in the cassette or EcoRV which cleaves once in each, pZJ7 and cassette (Figure 5.6).

After digesting the samples with BamHI, the band that corresponded to the supercoiled cassette remained present while most of the band corresponding to pZJ7 merged into one, representing the linear pZJ7 (Figure 5.6 lanes 4 and 5). Digesting with BsrGI did not alter the migration of bands corresponding to pZJ7, however, the cassette migrated slower on the gel, suggesting that it was linearized (Figure 5.6 lanes 6 and 7). When the sample were treated with EcoRV, only two bands were observed for each sample, which corresponded to the linear forms of pZJ7 and the cassette (Figure 5.6 lanes 8 and 9).

In summary, this result shows that the 2.5 kb cassette is excised by site-specific recombination after induction of Int expression and can be detected by agarose gel electrophoresis.

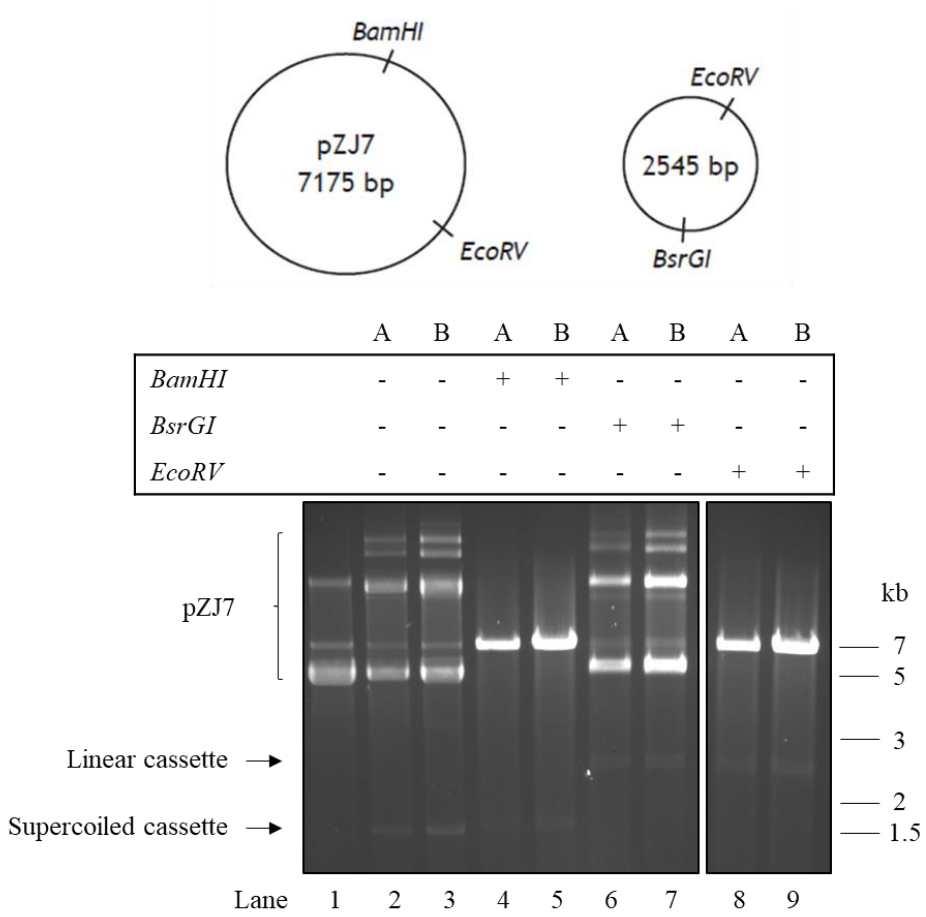

Figure 5.6 – Presence of products of site-specific recombination. 1% agarose gel run at 90V. DNA extracted from cells grown for 3 hours and incubated with arabinose for 15 minutes (A) and from cells grown for 4 hours and induced for 60 minutes (B) was digested with BamHI, BsrGI or EcoRV. pZJ7 can be linearized by BamHI or EcoRV. The 2.5 kb supercoiled cassette can be linearized by BsrGI or EcoRV. As a control and marker, pZJ7 was loaded in lane 1. Lanes 2 and 3 represent the untreated samples.

5.3.3 Site-specific recombination efficiency

Although pZJ7 was giving inducible cassette excision, the background excision in the absence of arabinose might cause problems. Therefore, pZJ7m was tested instead. As explained earlier, in pZJ7m the Int gene has a mutated start codon (GTG instead of ATG) which makes its expression weaker. Therefore, the leakage in Int expression was expected to decrease. Second, glucose works as a repressor of the P_{BAD} promoter. So, its use was tested as a repressor of Int expression. We also wanted to test what happens if arabinose and glucose are both present, as might be the case when arabinose is added to a culture where glucose is already present.

A fast and accurate experiment to determine how controlled and efficient the recombination was by taking advantage of the *lacI* gene in the cassette and the *Δlac* mutation in the *lac* operon of CP100. The cassette-encoded *lac* repressor binds to the *lac* operator upstream of the *lacZ* gene in the bacterial chromosome and represses the expression of the *lacZ* gene required for X-gal metabolism (Figure 5.7A). Therefore, if recombination has not occurred, *lacI* repressor represses *lacZ*, and the colonies are white (Figure 5.7A). If recombination occurs, and the cassette is deleted from the chromosome, *lacI* is lost and the colonies formed will be blue (Figure 5.7A). Thus, the number of blue and white colonies formed on plates containing X-gal allowed the efficiency of recombination to be directly observed.

Plasmid pZJ7m was introduced into the CP100 *dif*$^{+}$ *attP*-Km^{R}-*lacI*-*attB*. Colonies were selected for resistance to kanamycin and chloramphenicol on plates containing thymidine, 0.2% glucose and X-gal. A white colony was picked and grown overnight at 37°C with shaking in glucose, thymidine, kanamycin and chloramphenicol. Then the culture was diluted 40-fold into fresh media containing glucose, thymidine, kanamycin and chloramphenicol and grown for another 4 h. The bacteria were pelleted by centrifugation to remove any remaining glucose and resuspended in fresh media containing thymidine and chloramphenicol with glucose, arabinose or both and incubated for 30 minutes with shaking. Finally, bacteria from each condition were diluted (10^{-5}) and plated on plates containing thymidine, chloramphenicol and X-gal, and the number of blue and white colonies counted.

The results showed that some degree of recombination was already happening during overnight growth (Figure 5.7B I – 14.1% of bacteria) and the 30 minutes incubation with glucose (II – 18.7%), probably due to leakage in integrase expression from pZJ7m. Nonetheless, most recombination was seen upon arabinose addition in the absence of glucose (IV – 100%). In contrast, arabinose did not efficiently induce recombination if glucose was present (III – 29.8%).

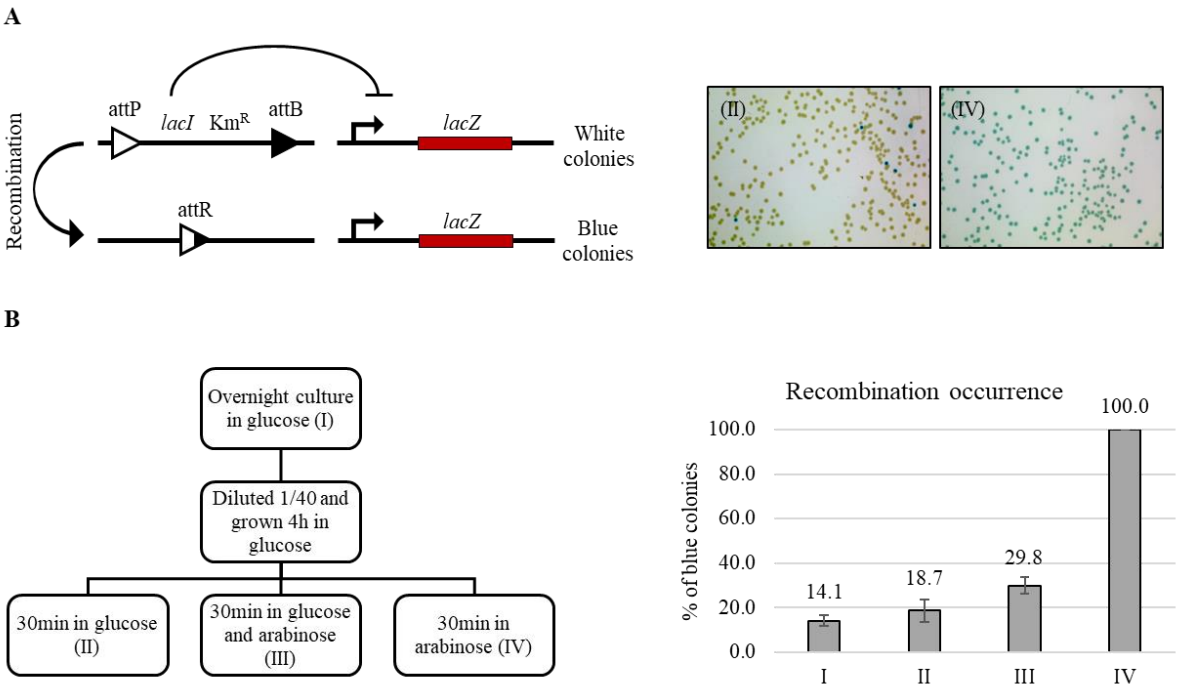

Figure 5.7 – Efficiency of site-specific recombination on the chromosome. **A)** Upon *lacI* expression from cassette, lac repressor stops *lacZ* from being expressed, leading to white colonies on X-gal (II). When recombination occurs, the cassette is deleted and *lacZ* can be transcribed, leading to blue colonies (IV). **B)** The diagram represents the methodology used for site-specific recombination assay, and the chart for recombination efficiency represented by the % of blue colonies formed during the assay. Error bars represent the standard deviation from three independent repeats.

Altogether, these results show that recombination between the *att* sites on the chromosome was occurring and efficient and could be controlled by addition of arabinose or glucose. Curiously, glucose must be absent so recombination can occur. Despite using pZJ7m, leakage in Int expression still occurred. Therefore, minimizing the time that pZJ7m is present in the cells before induction and changing further the Int gene (for instance using alternative RBS for Int) could prevent the leakage in Int expression. Maintaining kanamycin selection before induction with arabinose for as long as possible during the experiment might also help prevent build-up of bacteria that have deleted the cassette.

5.3.4 Site-specific recombination products

Once the successful induction of recombination with arabinose in absence of glucose was established, the samples were studied for the topology of site-specific recombination products. It was already observed that one product of recombination was the supercoiled 2545 bp cassette, but are there other topologies that we were not able to see on the gel?

Plasmid pZJ7m was introduced into CP100 *dif*+ *attP*-Km^R-*lacI*-*attB* strain and colonies were selected on plates containing thymidine, chloramphenicol, kanamycin, X-gal and 0.2% glucose. A white colony was picked and inoculated into fresh media containing thymidine, kanamycin, chloramphenicol, and glucose and grown overnight. Then, the culture was diluted 40-fold into fresh media containing thymidine, kanamycin, chloramphenicol and glucose and grown for 4 hours at 37°C with shaking. Bacteria were collected by centrifugation and resuspended in new media containing thymidine and chloramphenicol but no kanamycin. Then, arabinose to induce Int, or norfloxacin to inhibit type II topoisomerases, or both (when both were used, norfloxacin was added 2 minutes after arabinose) were added. The cultures were incubated for another 30 minutes at 37°C with shaking. Then bacteria were collected, and the covalently closed circular DNA was extracted using a QIAprep Spin Miniprep Kit. The DNA was run untreated on an agarose gel to examine supercoiling levels and singly nicked with DNase I in the presence of ethidium bromide to remove supercoiling and reveal any catenation. The detection was made by Southern hybridization using the *lacI* gene as probe.

As expected, in the control sample grown without arabinose or norfloxacin (Figure 5.8 lane 1) no recombination products were formed, although there was a low level of cross hybridization of the *lacI* probe to pZJ7m. When bacteria were treated with arabinose for induction of Int expression, recombination occurred yielding supercoiled cassette monomer (Figure 5.8 lane 2). Supercoiled cassette dimer was also observed. Cassette dimer can form in a two-step process (Figure 5.9). First, intermolecular recombination between *attP* on one sister chromosome and *attB* on the other sister leads to deletion of the cassette from one sister, and a tandem duplication of the cassette on the other. The two cassettes in this tandem duplication are separated by an *attL* site and flanked by *attP* and *attB* sites. Further recombination between this *attP* and *attB* will produce a cassette dimer. After the sample from lane 2 was treated with DNase I in the presence of ethidium bromide to eliminate supercoiling, two bands formed, corresponding to the nicked forms of the monomer and

dimer (Figure 5.8 lane 3). As expected, the control treated with norfloxacin alone gave no excised cassette (Figure 5.8 lane 4 and 5). When the cells were treated with arabinose to induce Int expression and norfloxacin to inhibit DNA gyrase and Topo IV excised circle was observed (Figure 5.8 lane 6). This circle had a much lower level of supercoiling compared to the sample produced with arabinose alone, consistent with inhibition of DNA gyrase. All the topoisomers merged into one band after nicking the sample (Figure 5.8 lane 7). Nicking of this sample demonstrated that much less dimer was produced in presence of norfloxacin than in its absence, relative to monomer. This might be a consequence of inhibition of DNA gyrase as well. As explained earlier, norfloxacin acts by not allowing gyrase to detach itself from the DNA. Like this, linearized DNA can be degraded in cells by nucleases or not extracted by the denaturing method used here. DNA gyrase not only binds the dimer, it also binds the monomer and the amount of monomer extracted from cells treated with arabinose and norfloxacin was less compared to bacteria treated with arabinose (Figure 5.8 lanes 3 and 7).

If catenanes containing two circles of 2.5 kb were present, they would have the same mass as the dimer but would run ahead of the nicked dimer in lanes 3 and 7 (Figure 5.8) due to compaction caused by catenation. The higher the number of nodes in the catenane, the faster they would run relative to the nicked circular dimer.

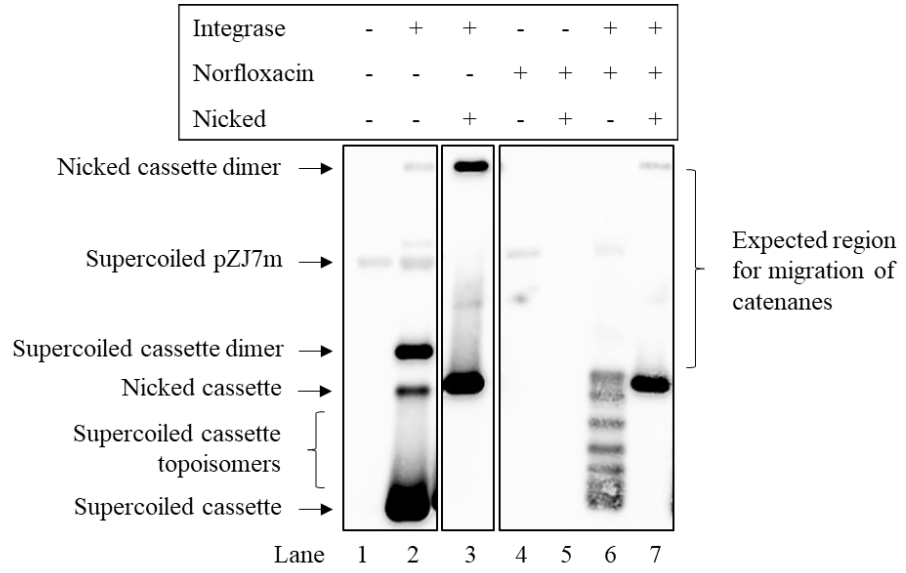

Figure 5.8 – Analysis of *in vivo* site-specific recombination on chromosome in CP100 with the cassette near *dif*. Southern hybridization of samples separated on a 1% agarose gel run at 35V. CP100 containing the cassette and pZJ7m were treated with 0.2% arabinose or 10 µg/ml norfloxacin or arabinose followed by norfloxacin. The covalently closed circular DNA was extracted, nicked with DNase I in presence of ethidium bromide, resolved by agarose gel electrophoresis and detected by Southern hybridization using the *lacI* gene as probe. pZJ7m corresponds to the ΦC31 integrase expression plasmid.

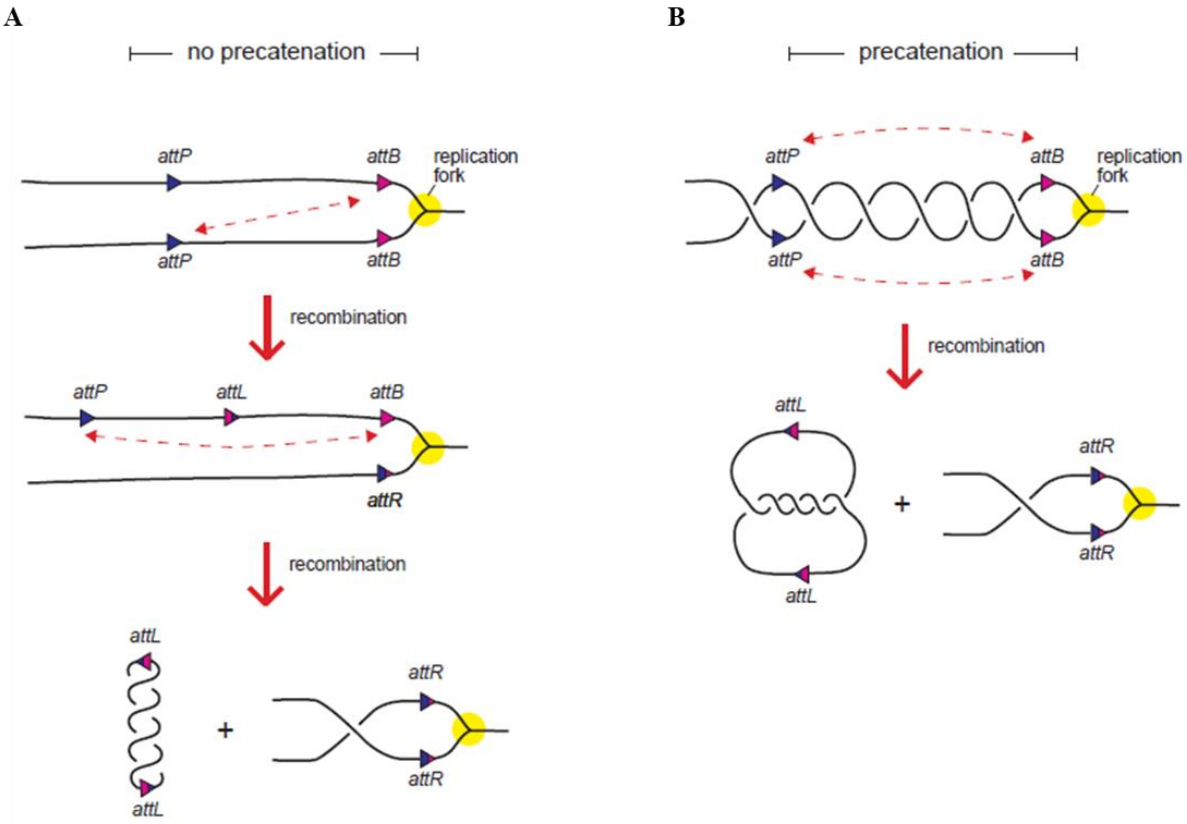

Figure 5.9 – Cassette dimer is produced by intermolecular recombination. A) First, intermolecular recombination yields a tandem duplicate of the cassette in one sister chromosome. Second, intramolecular recombination produces a dimer. If no precatenation is trapped, this will be an unknotted circle. **B)** If precatenation is trapped, this circle will be a knot (5-noded knot in the picture), belonging to the torus family.

Altogether, these results show that site-specific recombination between *attP* and *attB* sites of cassette was occurring efficiently and controllably. Norfloxacin was inhibiting DNA gyrase as demonstrated by the lower supercoil levels observed in the excised circle. Presumably, Topo IV was also inhibited in this condition, preventing unlinking of any catenanes. However, no catenanes were observed.

5.4 Investigating whether precatenation is present near *terC*

The same strategy was then used to investigate precatenation and catenation near the *terC* site (Figure 5.2). This site is 18 kb from *dif* and it was first suggested to be a chromosomal replication termination site (Hidaka *et al*, 1988). Hidaka and co-workers used the "Ter assay" in which any DNA fragment can be studied for activity in replication termination by cloning that fragment into the pUC vector. By employing this assay, they discovered three sites in *E. coli* chromosome that acted as replication termination sites. Duggin and Bell were able to show the fraction of chromosomes that had the replication forks stalled at *terC* in a mid-exponential phase growing culture of bacteria (Duggin and Bell, 2009). Compared to the amount of linear DNA, 0.85% of chromosomes had replication forks stopped at *terC*.

Precatenation near *terC* was studied here in two different strains DS941 and C600SN, used earlier in detection of catenanes formed on plasmid *in vivo*. The same *attP*-Km^R-*lacI*-*attB* cassette designed above was inserted into the chromosome. As before, any precatenation formed in this region would be entrapped after recombination by ΦC31 integrase.

5.4.1 Verifying insertion of the *attP*-Km^R-*lacI*-*attB* cassette in the *E. coli* chromosome near *terC*

The *attP*-Km^R-*lacI*-*attB* cassette was inserted 1053 bp from *terC*, between *yneE* and *lsrG* (Figure 5.10). (The DNA sequence where the cassette was inserted is shown in Appendix C). In this way, the cassette replaced the *tam* gene, which is not essential for bacterial growth (Cai and Clarke, 1999). For verification of cassette insertion, the primers were designed as follows. Primers P1 and P2 only give product when cassette is present in the chromosome (Figure 5.10). Primers P3 and P4 amplify the *tam* gene, present in wild-type strain. Primer P5 is homologous to the chromosome in the *lsrG* gene.

The *attP*-Km^R-*lacI*-*attB* cassette was prepared and used to replace *tam* exactly as described in section 5.3.1 and the cassette was inserted by homologous recombination in DS941 and C600SN.

Comparison of expected sizes and PCR products obtained confirmed successful cassette insertion and *tam* knockout (Figure 5.10). When the wild-type (DS941) and the recombinant strains were used in PCR with primers P1 and P2 only the recombinant strain gave a product of 797 bp. On the other hand, when P3 and P4 were used, only the wild-type strain yielded a 475 bp fragment. Primers P1 and P5 amplified a 1646 bp fragment in both DS941 and C600SN with the cassette.

Altogether these results show that homologous recombination between the *attP*-Km^R-*lacI*-*attB* cassette and the *E. coli* chromosome occurred, and cassette has been successfully integrated near *terC* within the *tam* gene.

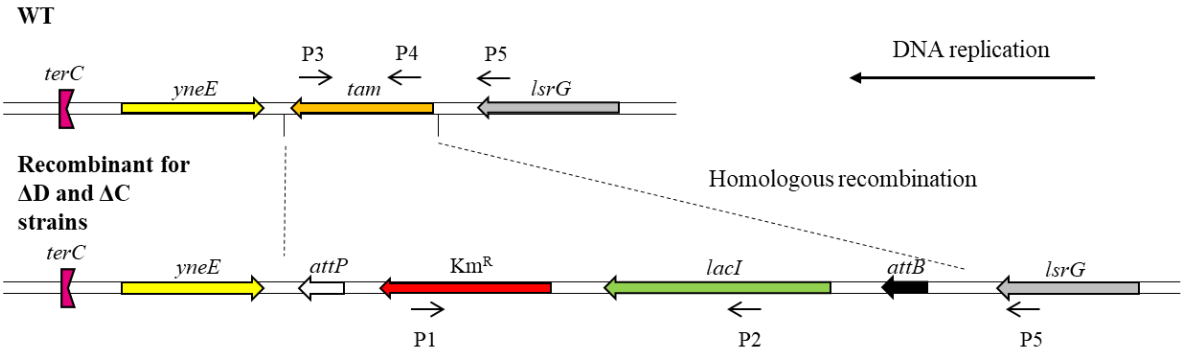

Set of primers	Wild-type strain products	ΔD and ΔC strains products
P1+P2	No product	797 bp
P3+P4	475 bp	No product
P1+P5	No product	1646 bp

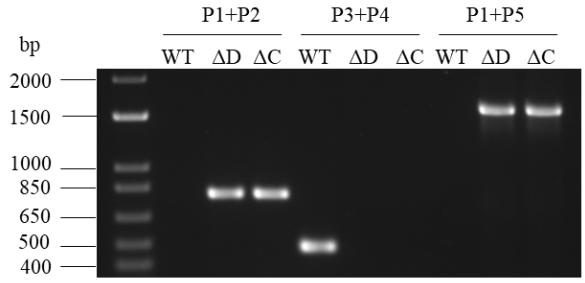

Figure 5.10 – Verification of the *attP*-Km^R-*lacI*-*attB* cassette integration near *terC*. The primers P3 (tam_fwd), P4 (tam_rev) and P5 (tam_flank_rev) are complementary to the chromosome, while P1 (incassette_kmR_rev) and P2 (incassette_lacI_fwd) are complementary to the cassette. The cassette was inserted 1053 bp from *terC*. The table shows the expected fragments when wild-type (WT), DS941 with the cassette (ΔD), or C600SN with the cassette (ΔC) strains were used as template for PCR, with the respective sets of primers. The 1% agarose gel run at 90V shows the results of PCR for all strains. The *terC* site stalls replication forks moving from right to left.

5.4.2 Site-specific recombination products

Once cassette insertion in the chromosome was confirmed, the samples were studied for topology of site-specific recombination products. As described earlier, the expected products were the monomeric cassette, the cassette dimer, and two cassettes intertwined with each other in form of catenanes or knots.

The recombination assay was performed exactly as described in section 5.3.4 except that DS941 and C600SN containing the *attP*-Km^R-*lacI*-*attB* cassette near *terC* were used, instead of cassette near *dif*. DNA was detected by Southern hybridization using kanamycin resistance gene as probe to minimize the cross hybridization of probe with pZJ7m.

The results obtained for DS941 are described here first. As expected, in the absence of arabinose no products were observed (Figure 5.11 lane 1). When Int expression was induced by addition of arabinose recombination took place and the supercoiled monomeric cassette and its dimer were detected (Figure 5.11 lane 2). A small amount of nicked cassette monomer was also observed. After nicking the sample, cassette monomer and dimer migrated slower on the gel as expected for nicked forms of these products (Figure 5.11 lane 3). As expected, in the control bacteria treated with just norfloxacin, no recombination products were seen (Figure 5.11 lane 4 and 5). Upon treatment with arabinose followed by norfloxacin, recombination occurred producing monomeric cassette (Figure 5.11 lane 6). Topoisomers were present indicating inhibition of DNA gyrase. Once the supercoiling of the sample was removed by nicking the DNA, all topoisomers of the cassette monomer merged into one band, which corresponded to the nicked form of the cassette (Figure 5.11 lane 7). Curiously, cassette dimer was not formed when cells were treated with arabinose and norfloxacin.

Results obtained for C600SN were similar to the ones just described for DS941. As expected, untreated cells showed no recombination products presence (Figure 5.11 lane 8). Arabinose alone allowed Int expression and recombination, which resulted in cassette monomer and dimer formation (Figure 5.11 lane 9). When the sample was nicked, both bands corresponding to cassette monomer and dimer migrated slower on the gel (Figure 5.11 lane 10). As expected, after cell treatment with norfloxacin no products were detected (Figure 5.11 lanes 11 and 12). Unlike in DS941, the cassette produced after treatment with arabinose and norfloxacin appeared fully supercoiled (Figure 5.11 lane 13). This is

consistent with the norfloxacin resistant gyrase in C600SN not being inhibited by norfloxacin. After nicking, cassette monomer and dimer migrated slower on the gel (Figure 5.11 lane 14). Interestingly, cassette dimer was detected in significant amounts in C600SN when treated with arabinose and norfloxacin.

Altogether, these results show that site-specific recombination between *attP* and *attB* sites of cassette was occurring efficiently. Norfloxacin was working via inhibition of DNA gyrase and Topo IV. The cassette dimer is either not produced or it is selectively degraded when gyrase is inhibited with norfloxacin. However, no topologies such as catenanes were detected.

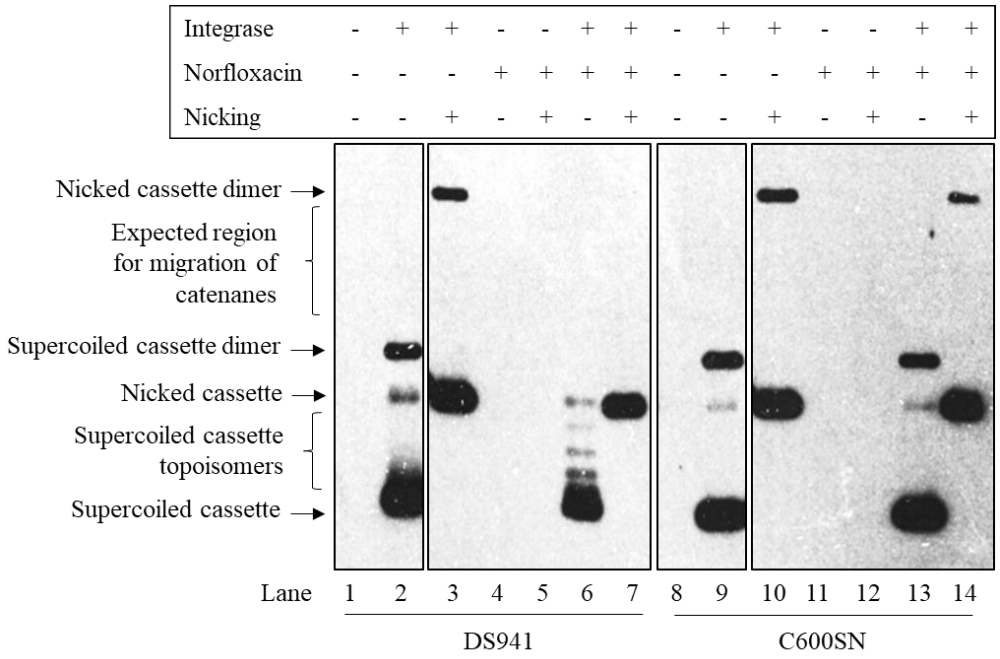

Figure 5.11 – Analysis of *in vivo* site-specific recombination on chromosome in DS941 and C600SN with cassette near *terC*. Southern hybridization of samples separated on 0.7% agarose gel run at 35V. DS941 and C600SN containing the cassette and pZJ7m were treated with 0.2% arabinose or 10 µg/ml norfloxacin or arabinose followed by norfloxacin. The covalently closed circular DNA was extracted, nicked with DNase I in presence of ethidium bromide, resolved by agarose gel electrophoresis and detected by Southern hybridization using the kanamycin resistance gene as probe.

5.5 Topo IV treatment for verification of catenane formation

One possibility to rule out was that the band assigned as cassette dimer could actually be 2-noded catenane. 2-noded catenane could be predominant product if precatenation is at a density of only 2 crossings in the 2.5 kb of the cassette.

Any catenane produced from chromosome has the same size as the dimer, but when the supercoiling is removed, the 2-noded catenane would migrate only slightly faster than the dimer on an agarose gel (as seen in Chapter 3). This made us question if the band assigned to the dimer could be 2-noded catenane or a mixture of dimer and 2-noded catenane. The easiest way to verify presence of 2-noded catenane would be to treat the sample with Topo IV and look for disappearance of 2-noded catenane as it is converted into free circles.

Since catenanes are removed by type II topoisomerases *in vivo*, samples that were treated with norfloxacin were selected for this experiment. Also, this could be tested only in C600SN because CP100 and DS941 strains showed very little or no presence of dimer/2-noded catenane when treated with norfloxacin.

DNA was obtained as described in section 5.4.2. The products obtained from recombination on C600SN were either treated with Topo IV or left untreated and then nicked with Nb.BbvCI to remove supercoiling. Samples were separated by agarose gel electrophoresis and DNA was then detected by Southern hybridization using the kanamycin resistance gene as probe.

When C600SN was grown without arabinose and norfloxacin no recombination was observed, as expected (Figure 5.12 lane 1). Upon treatment with arabinose, for Int expression, cassette monomer and dimer were produced just as seen previously (Figure 5.12 lane 2 and 3). However, the band corresponding to cassette dimer did not disappear or visibly reduced in intensity upon treatment with Topo IV (Figure 5.12 lane 4 and 5). This result was expected since these samples were prepared in C600SN without norfloxacin so that Topo IV would still be active and would unlink any 2-noded catenane.

As before, arabinose treatment in the presence of norfloxacin gave supercoiled cassette monomer and dimer (Figure 5.12 lanes 6). Nicking yields nicked cassette monomer and dimer (Figure 5.12 lane 7). Topo IV treatment of DNA extracted from bacteria treated with

arabinose and norfloxacin did not show evident result for presence of 2-noded catenane (Figure 5.12 lanes 8 and 9). Also, the order of DNA treatment by Topo IV and Nb.BbvCI did not make any difference.

In conclusion, the decrease in cassette dimer band intensity occurred for both, the ones treated with arabinose and the ones treated with arabinose and norfloxacin. This decrease upon Topo IV treatment cannot be justified by decatenation of 2-noded catenane, since this is not formed in samples treated with just arabinose. Moreover, if the band on the gel corresponded to 2-noded catenane extracted from bacteria treated with arabinose and norfloxacin, it would not appear after Topo IV treatment. For this reason, it can be concluded that 2-noded catenane is probably not present, and that the observed band corresponds to the cassette dimer.

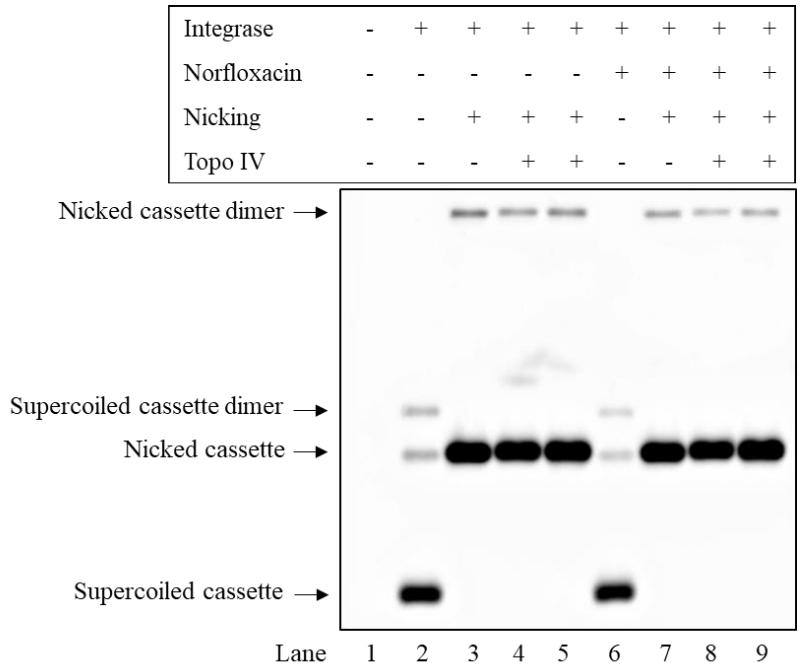

Figure 5.12 – Topo IV treatment of recombination products obtained from C600SN. 1% agarose gel run at 35V. Bacteria treated with 0.2% arabinose or with 0.2% arabinose and 10 µg/ml norfloxacin. The DNA was extracted, treated with Topo IV then nicked with Nb.BbvCI (lanes 4 and 8) or nicked first then treated with Topo IV (lanes 5 and 9). Then, DNA was separated by agarose gel electrophoresis and detected by Southern hybridization using kanamycin resistance gene as probe.

5.6 Conclusion

This study focused on precatenation formation near *dif* and *terC* sites. Precatenation is associated with replication termination, and both sites have been suggested to participate in it (Hendrickson and Lawrence, 2007; Duggin and Bell, 2009).

In this chapter, a new approach that could be used for precatenanes entrapment and detection was showed. It consisted of insertion of *attP* and *attB* sites, recognized by ΦC31 integrase, into the chromosome in a target location. The recombination between *att* sites occurred upon induction of integrase expression and showed to be efficient. Products of recombination were extracted by alkaline lysis method and were analysed by agarose gel electrophoresis and Southern hybridization.

Despite not being able to provide direct evidence for precatenanes formation we still showed some information that could indicate a possible interaction between the two replicated sister chromosomes. That information resides in formation of the cassette dimer upon recombination induction. As the dimer is formed when the recombination is intermolecular, this showed that after replication fork has passed the cassette, the two newly replicated sister chromosomes were remaining close enough for recombination to occur between them. Olivier Espeli and his group observed that sister chromatids colocalize following replication and even show cohesion during part of the colocalization, and that precatenation could be contributing for the observed (Lesterlin *et al*, 2012; Wang *et al*, 2008; Joshi *et al*, 2013). Our results support the findings by Espeli's group, which indicates that there is a possibility of finding precatenation.

Our results showed that the main product of recombination was the supercoiled cassette monomer. Dimer cassette can be formed as shown in Figure 5.9 and requires an initial inter-sister recombination followed by a second reaction that produces the dimer. If both sisters are present during the period in which recombination takes place, this could happen solely with addition of arabinose. However, the possibility that the first recombination takes place before arabinose is added, due to leakage expression of Int, cannot yet be ruled out.

Only a small percentage of chromosomes in a culture has replication forks stalled at *terC* (less than 1%, compared to linear DNA) (Duggin and Bell, 2009). The probability of those

being precatenated is even smaller. Maybe in order to detect precatenation a much bigger volume of cells had to be extracted. Synchronising the cells would help increase the number of forks trapped at the replication termination sites.

Maybe when norfloxacin is added to the culture and DNA gyrase is inhibited, the normal level of supercoiling in the cell is altered. This can result in decrease in Int expression from pZJ7m, which in turn results in decreased recombination. The decreased level of supercoiling could also position the cassettes in the sister chromosomes apart from each other, decreasing the chance of intermolecular recombination. These could explain the decrease in monomer and dimer formation observed in presence of norfloxacin in strains with DNA gyrase sensitive to norfloxacin.

Another consideration is the distance between the *att* sites on the cassette. Maybe 2.5kb is not length enough to entrap precatenation. Some work was made to increase the length between the *att* sites up to 6 kb. In this approach, one cassette containing the *attP* site was inserted near *terC*, and a second one containing *attB* was to be inserted approximately 6 kb apart. The insertion of the second cassette was difficult and the time left until the end of project was not enough to create a successful model. For this reason, in future, creating this model and maybe another with the distance between the sites even bigger, would be useful to study precatenation on bacterial chromosome.

The Sherratt group has been studying catenane decatenation by XerCD-*dif*-FtsK recombination (Ip *et al*, 2003; Grainge *et al*, 2007; Shimokava *et al*, 2013). They used catenated plasmid DNA containing *dif* sites to show that XerCD can unlink catenanes, suggesting that the same mechanism can occur *in vivo* in chromosome unlinking (see Chapter 1 Figure 1.22). What if precatenation could not be detected because Xer recombination was unlinking the sister chromosomes *in vivo*? We wanted to study precatenation in cells depleted from *dif*. A construct was made with *dif* deleted form chromosome and the cassette inserted instead of *dif*. However, no experiments were carried out using this Δ*dif*::*attP*-Km^R-*lacI*-*attB* construct due to time limitations.

6. Studying the linkage change of a 398 bp circle resulting from Xer site-specific recombination

6.1 Introduction

Recombination reactions can lead to change in linkage or supercoiling. The level of supercoiling in a DNA molecule can be defined as the difference between the absolute number of links in the molecule (Lk) and its relaxed linkage (Lk_0). Therefore, this level of supercoiling or linkage difference will be referred to as Lk-Lk_0 throughout this chapter. The linkage change of a recombination reaction (ΔLk_{xer} for example) can be defined as the difference between the total linkage of the products ($Lk_{products}$) and the substrates ($Lk_{substrates}$). However, the exact Lk of a DNA molecule is hard to measure. If $Lk_{0\ substrates}$ is equal to $Lk_{0\ products}$, then:

$$\Delta Lk = Lk_{products} - Lk_{substrates} = (Lk - Lk_0)_{products} - (Lk - Lk_0)_{substrates} \quad (1)$$

This is useful because Lk-Lk_0 in a circle can be measured by gel electrophoresis.

For example, Stark and co-workers (Stark *et al*, 1989) studied the linkage change of the recombination reaction catalysed by Tn3 resolvase. The ΔLk_{Tn3} of the reaction can be determined by the formula (1).

When recombination produces approximately equal sized circles, the supercoiling can partition into the two circles in different ways making it difficult to measure total Lk-Lk_0 of the products. However, if one of the product circles is much smaller than the other, it should be energetically favourable only to make one topoisomer. This means that the larger circle produced from a specific substrate topoisomer will have a specific Lk-Lk_0, allowing ΔLk of the reaction to de determined.

For this reason, they used as substrate a plasmid (3326 bp) with two closely spaced *res* sites (recognized by Tn3 resolvase) in direct repeat. The product of recombination is a 2-noded catenane in which the two circles are of 219 bp and 3107 bp. They showed that the Lk-Lk_0 of the small circle was always 0, in other words it was not supercoiled but in its relaxed state.

The group purified a specific topoisomer of the substrate plasmid and determined its Lk-Lk_0 to be -17. After incubation of this topoisomer with Tn3 resolvase, the Lk-Lk_0 of the

3107 bp circle was -13. When applying the values obtained to the formula (1), they concluded that the change of linkage associated with the deletion reaction is +4:

$$\Delta Lk_{deletion\ reaction} = 0 + (-13) - (-17) = +4$$

The linkage change determined above can be used to determine important information about the reaction mechanism using the formula (2):

$$\Delta \mathrm{Lg} = \Delta \mathrm{Lk} + \Delta \mathrm{Ca} = \mathrm{Xr} + \mathrm{Xtw} \qquad (2)$$

Where ΔLg represents the total linkage change of the reaction. ΔCa represents the change in catenation of the reaction and is known to be -2 because an unknotted circular substrate produces the -2-noded catenane in resolvase recombination (–2 – 0 = –2; Figure 6.1A). Xr represents the amount and sense of rotation during the strand exchange and was known to be +1 (Figure 6.1B).

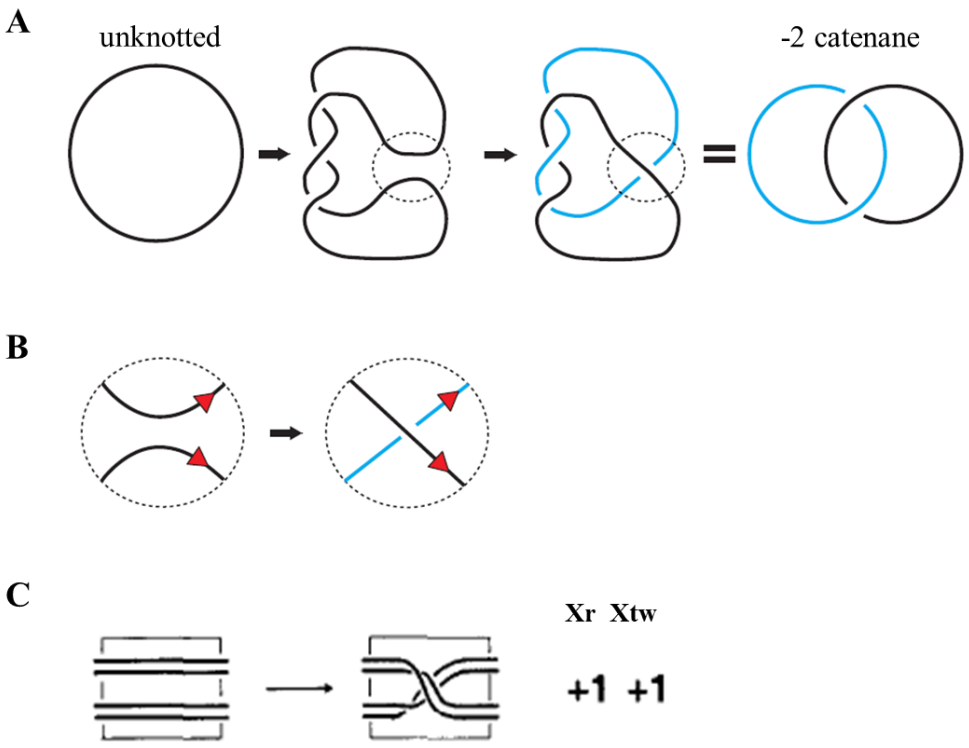

Figure 6.1 – Proposed strand exchange topology for Tn3 resolvase. A) By simple rotation mechanism, a serine recombinase like Tn3 resolvase produces a -2-noded catenane from an unknotted substrate. **B)** The recombination sites are aligned parallel (red arrow heads). After strand exchange, a positive crossing is introduced. **C)** Boxes represent the place where the strand exchange takes place. Right-handed 180° rotation of the half-sites introduces a +1 Xr and two half twists producing +1 Xtw. C) was adapted from Stark *et al* (1989) with permission. Order number 4505980761773.

Xtw represents the change in the total helical twist of the partners during the reaction and it was the unknown value to determine by applying formula (2):

$$\Delta Lg = +4 + (-2) = +1 + Xtw$$

This result allowed Stark and colleagues to deduce that Xtw = +1 in the reaction producing the -2-noded catenane. In other words, as well as a single positive crossing being introduced by the strand exchange mechanism (Xr = +1; Figure 6.1B), one positive (right-handed) twist is also added (Xtw = +1; Figure 6.1C). This is consistent with a simple rotation mechanism of strand exchange (right-handed 180° rotation of half-sites) and rules out other possible mechanisms.

Xer mediated recombination has its role in resolving chromosome dimers during chromosome replication (Sherratt *et al*, 1995). XerCD also play a role in converting plasmid multimers into monomers to assure their stability and inheritance. On the chromosome, XerCD act on the *dif* site, whereas on plasmids the enzymes recognize other naturally occurring sites such as *cer* or *psi* (Sherratt *et al*, 1995; Summers and Sherratt, 1984; Cornet *et al*, 1994) (Figure 6.2).

	XerC	central region	XerD
dif	GGTGCGCATAA	TGTATA	TTATGTTAAAT
psi	GGTGCGCGCAA	GATCCA	TTATGTTAAAC

Figure 6.2 – Core sites recognized by XerC and XerD recombinases. *dif* is present on the chromosome while *psi* is found in plasmids. The first 11 bp are recognized by XerC and the last 11 bp by XerD. A central region of 6 bp separates the two recognition sites.

The reaction at *psi* requires PepA and accessory sequences adjacent to core site to switch on and regulate recombination by XerCD (Figure 6.3A). The product of recombination from unknotted substrate is the 4-noded catenane (Colloms *et al*, 1997).

Studying the linkage change of a deletion recombination reaction by Xer at directly repeated *psi* sites, can reveal details of the mechanism of strand exchange by tyrosine recombinases.

In previous work done on ΔLk of a deletion recombination reaction by XerCD by Sean Colloms (unpublished work), he used as a substrate a plasmid containing two closely spaced *psi* sites in direct repeat. The product of recombination is a 4-noded catenane (Colloms *et al*, 1996; Bath *et al*, 1999) with the two circles of 398 bp and 3039 bp. As seen for resolvase, it was hoped that a single topoisomer of the small circle would be produced. He purified different topoisomers of the substrate and incubated them with XerC, XerD and PepA *in vitro*, and studied the Lk-Lk_0 of the substrate and the 3039 bp circle product. For example, a substrate with Lk-Lk_0 of -17, gave a 3039 bp product circle with Lk-Lk_0 of -12; a substrate with Lk-Lk_0 of -16 produced a 3039 bp circle with Lk-Lk_0 of -11, and so on. However, to calculate the ΔLk of the deletion reaction, the Lk-Lk_0 of both products is required (formula (1)).

The ΔLk_{xer} is unknown and we need to determine Lk-Lk_0 of small circle before linkage change of the deletion reaction can be calculated. Once ΔLk_{xer} is determined, the ΔLg can be calculated using formula (2) since ΔCa is known to be -4 (–4 – 0 = –4; Figure 6.3A). Xr is known to be -1 in reaction producing 4-noded catenane (Figure 6.3B). So, if ΔLg is known, Xtw can be determined, giving important information about the reaction mechanism by XerCD.

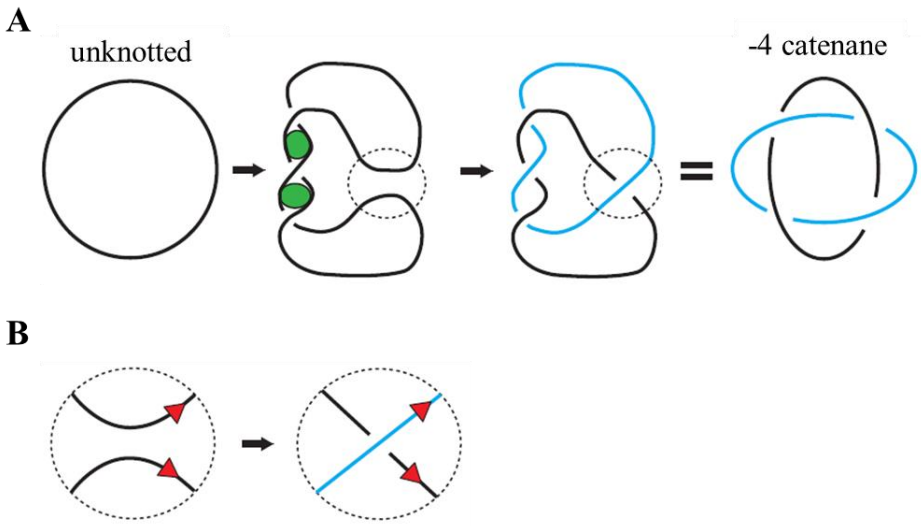

Figure 6.3 – Possible mechanism for formation of a 4-noded catenane by Xer recombinases. **A)** Xer recombination produces a -4-noded catenane from an unknotted substrate. Green circles represent PepA. **B)** After strand exchange, a negative crossing is introduced. Red arrow heads represent the recombination sites.

6.2 XerCD recombination on pSDC153 produced a 4-noded catenane

To study supercoiling of the small circle, this had to be produced first. Since the small circle is a product of site-specific recombination by XerC, XerD and PepA, a plasmid containing two *psi* sites in direct repeat (pSDC153) was used. The sites were separated by 398 bp, so after recombination two products of 398 bp and 3039 bp were formed. Also, the two products end up interlinked to form a 4-noded catenane (Figure 6.4). Elimination of supercoiling by nicking the sample allows clearer visualization of the catenane.

4-noded catenane was produced by incubating pSDC153 with XerC and XerD purified as described in sections 2.27 and 2.28, and PepA (provided by James Provan) in 1x *psi* reaction buffer and 10% glycerol. Reactions were carried at 37°C for 60 min. The reaction products were purified once by phenol:chloroform and once by chloroform:isoamyl alcohol extractions. Finally, the DNA was ethanol precipitated. The products of recombination were digested with EcoRI (cuts once in 3039 bp circle) and/or BamHI (cuts once in 398 bp circle), or treated with Nt.BsmAI to remove supercoiling. The samples were analysed by agarose gel electrophoresis.

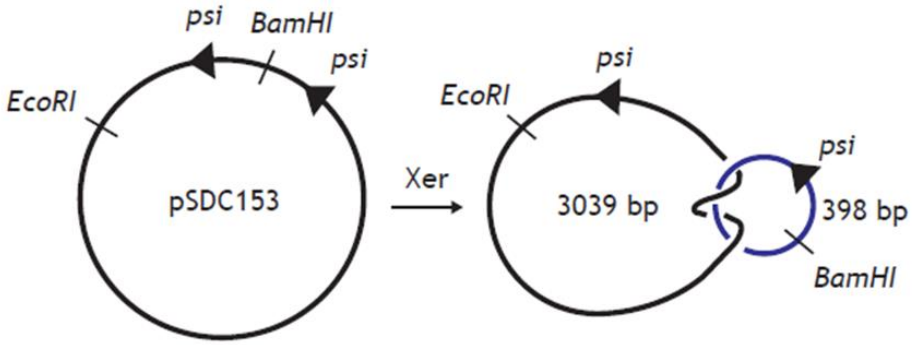

Figure 6.4 – Formation of 4-noded catenane by Xer recombination. pSDC153 was the substrate for XerCD recombination. The product of recombination is a right-handed 4-noded catenane, with the two sites oriented in an antiparallel way (Colloms *et al*, 1997).

When analysing the results, it was observed that the linear pSDC153 migrates slower than the nicked pSDC153 on the agarose gel (Figure 6.5 lanes 2 and 3). The 4-noded catenane produced by recombination migrated faster than the supercoiled pSDC153, as expected

(Figure 6.5 lanes 1 and 4). After digestion of sample from lane 4 with EcoRI, the expected 3039 bp linear fragment and 398 bp supercoiled circle were observed, as well as a band corresponding to linear pSDC153 (Figure 6.5 lane 5). After digestion of the same sample with BamHI, the supercoiled 3039 bp circle and linear 398 bp circle were observed, as well as a band corresponding to linear pSDC153 (Figure 6.5 lane 6). When the sample from lane 4 was nicked for elimination of supercoiling, some nicked pSDC153 and 4-noded catenane were detected (Figure 6.5 lane 7). The difference in migration between the catenane and pSDC153 was bigger when they were nicked, compared to when they were supercoiled.

In summary, this result show that the only product of site-specific recombination by XerCD on a plasmid with two *psi* sites in direct repeat was a 4-noded catenane. The efficient recombination reaction produced catenated circles with expected sizes.

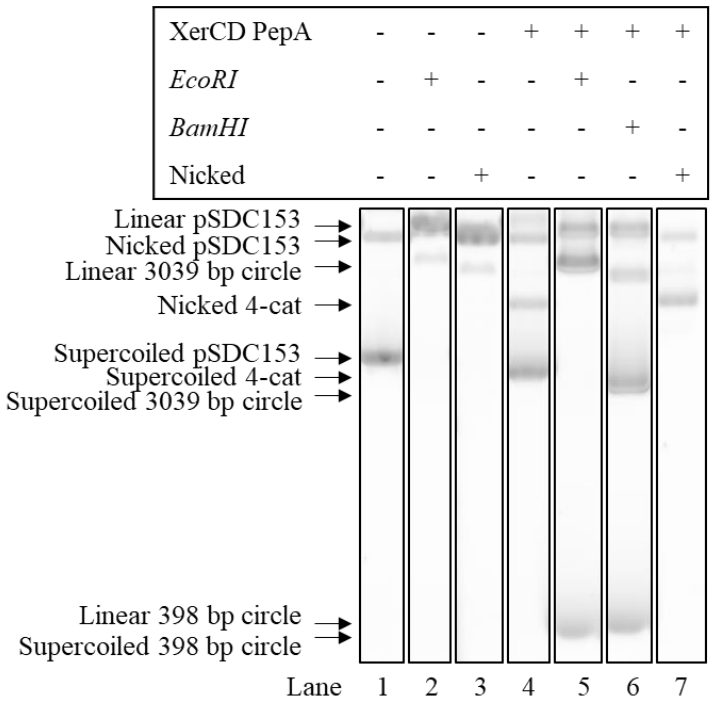

Figure 6.5 – Analysis of the products of recombination by Xer. 0.7% agarose gel run at 35V. Lane 1 shows the migration of supercoiled pSDC153 (3437 bp). Lane 2 shows the migration of EcoRI linearized pSDC153. Lane 3 shows the migration of nicked pSDC153. Lane 4 shows the migration of the supercoiled 4-noded catenane produced by recombination. Lane 5 shows the products of digestion of sample from lane 4 with EcoRI (linear 3039 bp circle, supercoiled 398 bp circle, linear pSDC153). Lane 6 shows the products of digestion of sample from lane 4 with BamHI (supercoiled 3039 bp circle, linear 398 bp circle, linear pSDC153). Lane 7 shows the products of nicking of sample from lane 4 (nicked 4-noded catenane and pSDC153).

6.3 Lk-Lk_0 of the 398 bp circle

To study the level of supercoiling (Lk-Lk_0) in the small circle resultant from site-specific recombination by XerCD and PepA on pSDC153, the 398 bp circle had to be free from the 3039 bp circle. Also, analysing supercoiling of small DNA circles on agarose gel is difficult and polyacrylamide gels have been used (Fogg *et al*, 2006; Irobalieva *et al*, 2015). Different topoisomers of the 398 bp circle were created so they could be used for migration comparison of the 398 bp circle.

First, the 4-noded catenane produced by Xer recombination was digested with EcoRI to linearize the large circle. After digestion, the sample was treated with lambda exonuclease and $RecJ^f$ to degrade the linear 3039 bp fragment. Lambda exonuclease recognizes linear double-strand and cleaves one strand from 5´ to 3´. Then, $RecJ^f$ degrades the remaining single-strand from 5´ to 3´ (Balagurumoorthy *et al*, 2008). Samples were digested with BamHI to obtain the linear 398 bp fragment, or with Nt.BsmAI to obtain the nicked form of the 398 bp circle (no supercoiling) as markers. Different topoisomers of the 398 bp supercoiled circle were created using Topo I from calf thymus in the presence of ethidium bromide. This topoisomerase removes any positive and negative supercoils and relaxes the DNA. However, if a DNA intercalator such as ethidium bromide is added to the reaction, the unwinding by the intercalator cannot be removed. When the ethidium bromide is removed by extraction with phenol, this under-winding is left behind as negative supercoiling (e.g. (Lk-Lk_0) < 0). A sample digested with EcoRI and treated with lambda exonuclease and $RecJ^f$, was treated with Topo I without ethidium bromide to create the relaxed 398 bp circle. Two other samples were treated with Topo I in presence of 1 and 3 µg/ml ethidium bromide to create molecules with -1, -2 and -3 supercoils. All the samples were separated in 5% PAGE, the gel was stained with SYBR Gold and DNA was detected using a Typhoon FLA 9500 scanner.

The 398 bp circle produced by Xer recombination *in vitro* consisted of one major species and a smaller amount of a second band on the gel (Figure 6.6 lane 1). These two bands are most likely two different topoisomers of the 398 bp circle. When the same DNA was digested with BamHI, only one band corresponding to linear 398 bp fragment was observed, migrating faster than the circular forms of the 398 bp circle (Figure 6.6 lane 2). Nicking the sample with Nt.BsmAI produced one band, which migrated slower than the circles produced by Xer recombination (Figure 6.6 lane 3). When the circle was relaxed by

Topo I in absence of ethidium bromide, only one band was observed, presumably corresponding to the relaxed circle, which migrated even slower than the nicked circle (Figure 6.6 lane 4). Treating the supercoiled circle with Topo I in presence of 1 µg/ml and 3 µg/ml ethidium bromide produced circles which were identified as having -1 and -2 supercoils (Figure 6.6 lane 5), and -2 and -3 supercoils (Figure 6.6 lane 6), respectively.

By comparing the migration of the two bands corresponding to the 398 bp circles produced by Xer recombination, to the topoisomers obtained by Topo I treatment in presence of ethidium bromide, it can be concluded that most (approx. 90%) of the 398 bp circle has one negative supercoil. A small portion (approx. 10%) of the circle has two negative supercoils. In conclusion, the Lk-Lk_0 of the majority of small circle is -1.

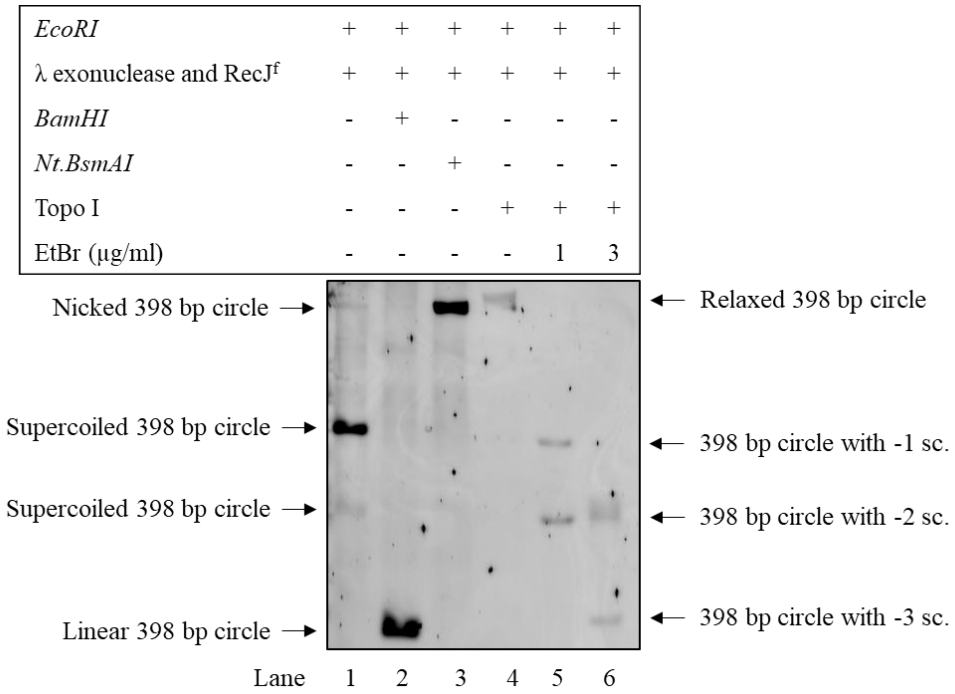

Figure 6.6 – Study of Lk-Lk_0 of the 398 bp circle. 5% polyacrylamide gel in TA-$CaCl_2$ run at 60V over 17 hours and stained with SYBR Gold. All the represented samples were treated with EcoRI, lambda exonuclease and $RecJ^f$. Lane 1 shows the migration of supercoiled 398 bp circle produced by Xer recombination from naturally supercoiled substrate. Lane 2 shows the migration of BamHI linearized 398 bp circle. Lane 3 shows the migration of the nicked 398 bp circle produced by treatment with Nt.BsmAI. Lane 4 shows the migration of the relaxed 398 bp circle produced by treatment with Topo I in the absence of ethidium bromide. DNA in lane 5 and 6 was relaxed with calf thymus topoisomerase I in the presence of 1 and 3 µg/ml ethidium bromide, respectively. Sc, supercoils.

In addition to the experiment described above, the topology of the 398 bp circle was also verified by atomic force microscopy (AFM). AFM was performed by Dr Alice Pyne, a Research Fellow in Biophysics at the London Centre for Nanotechnology. When analysing the pictures, it was observed that many of the molecules adopted a figure eight conformation (Figure 6.7A) as might be expected for a molecule with one negative supercoil (Irobalieva *et al*, 2015). In some cases, the sign of the crossings could be determined by examining the height trace (Figure 6.7B). The DNA appeared to adopt a right-handed plectonemic conformation as expected for negative supercoiling.

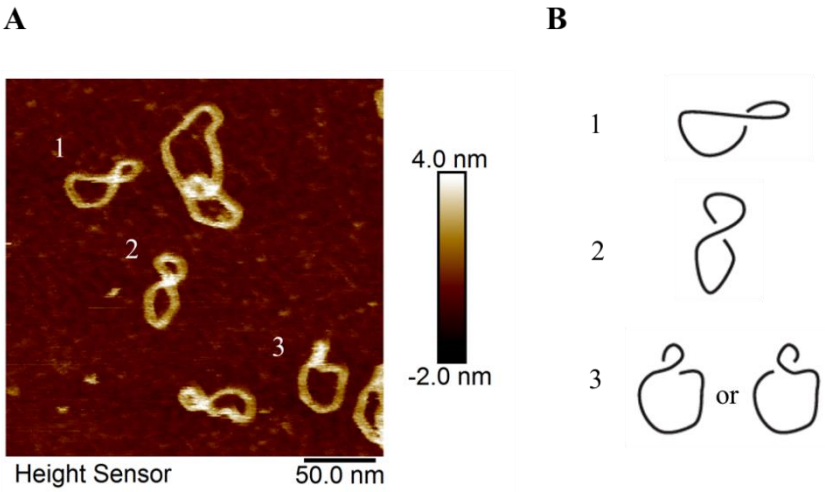

Figure 6.7 – AFM Hight Sensor image of 398 bp circle produced by recombination of pSDC153. A) Each pixel is colour coded, and each colour corresponds to a specific height. The lighter the colour, more height it represents. The picture shows four individual circles with one supercoil. The sample sent for microscopy contained the 4-noded catenane with the big circle (3039 bp) nicked with a nicking endonuclease. The big circle was nicked four or five times, which might have caused its linearization and freed the small circle. Therefore, the picture presented here is an amplification from a bigger picture. Scale bar = 50 nm; height bar = -2 to 4 nm. **B)** Interpretation of crossings in the 398 bp circle by examining the height trace. Circles 1 and 2 seemed to have right-handed crossings, while for circle 3 it was more difficult to discern the handedness of the crossing.

6.4 Conclusion

In this chapter the Lk-Lk_0 in the 398 bp circle formed by site-specific recombination by XerC, XerD and PepA at *psi* on a 3437 bp circle was studied. Previous studies by Sean Colloms (unpublished data) lacked this important piece of information and could not deduce the ΔLk of the Xer deletion reaction.

Here, we showed that Lk-Lk_0 of the small circle is -1. This circle formed from negatively supercoiled DNA obtained from *E. coli* with average supercoiling density of about -0.05 to -0.06 expected to range from approx. -14 to -20 supercoils. Previous work by S. Colloms showed that a substrate with Lk-Lk_0 of -16 produces a large circle with Lk-Lk_0 of -11. Therefore, ΔLk of the recombination reaction can be determined by applying formula (1):

$$\Delta Lk_{xer} = -1 + (-11) - (-16) = +4$$

Therefore, by knowing that ΔCa is -4, the ΔLg can be calculated by applying formula (2):

$$\Delta Lg = +4 + (-4) = 0$$

The total linkage change in the Xer reaction is 0, and this is fully consistent with Holliday junction strand exchange mechanism (Figure 6.8) and inconsistent with other models such as simple rotation (Figure 6.3) (Crisona et al, 1999).

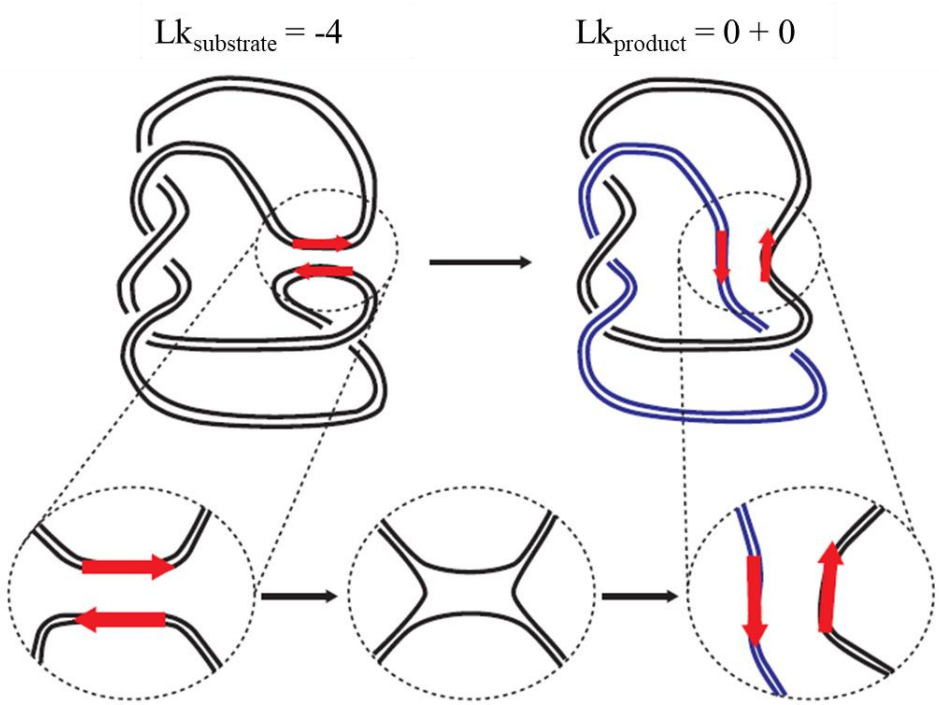

Figure 6.8 – Site-specific recombination by XerCD recombinases on *psi* sites. Synapsis brings the two *psi* sites (red arrows) together, which are recombined through formation of a Holiday junction. When the two sites are brought together supercoiling is trapped, which results in interlinks between the two circular products (blue and black circles) after recombination. Therefore, $\Delta Lk_{xer} = 0 + 0 - (-4) = +4$.

The presence of a small amount of the 398 bp circle with Lk-Lk_0 of -2 indicates that some of the substrate with Lk-Lk_0 of -16 may have produced large circle with Lk-Lk_0 of -10. However, the original gels of S. Colloms were not sensitive enough to see this small percentage of product with a different supercoiling level.

The Xer reaction will be made highly energetically favourable by loss of four negative supercoils, converted to four catenation crossings, driving the reaction to near completion (Figure 6.5 lanes 4-7).

7. Discussion and future work

Precatenation was first suggested to occur by Peter and co-workers (Peter *et al*, 1998), where they observed by electron microscopy a plasmid RI with the two partially replicated duplexes intertwined in a precatenane. More recent work, also on plasmids, concluded that precatenanes form during replication (Cebrián *et al*, 2015). Does precatenation occur on chromosome *in vivo*? Why is there no evidence for precatenation formation on chromosome?

To shed light into the field of precatenation occurrence, it was essential to develop a method which would enable us to produce, extract and detect catenanes (Chapter 3), before departing on our hunt for precatenanes detection on chromosome.

The method was based on the deletion reaction catalysed by ΦC31 integrase. This recombinase recognizes two *att* sites positioned in direct repeat in a plasmid and performs strand exchange, producing two smaller circles (Olorunniji *et al*, 2012). Olorunniji and co-workers studied this mechanism *in vitro* on different plasmid substrates and produced catenanes with different level of complexity. Our work focused on the ΦC31 integrase ability to generate catenanes *in vivo*. In our results, catenanes were produced by site-specific recombination, corroborating the results obtained by Olorunniji and co-workers *in vitro*, and extending them to the *in vivo* level.

Upon production of catenanes *in vivo*, new measures were required for catenane accumulation since bacterial Topo IV was decatenating them. Norfloxacin was used in this study for inhibition of Topo IV. However, this drug also inhibits DNA gyrase (Khodursky *et al*, 1995). The addition of norfloxacin allowed catenanes produced by ΦC31 integrase to be detected.

The unhealthy growth of DS941 in presence of norfloxacin led to the use of an additional strain for catenane production. In C600SN the DNA gyrase was norfloxacin resistant, and it showed healthy growth upon norfloxacin treatment. Additionally, by using C600SN our results showed that Topo IV is not the only decatenase that acts *in vivo*. According to previous decatenation studies *in vitro* and *in vivo* in *E. coli*, Topo IV is much more efficient in producing unlinked circles than DNA gyrase is, which still means that gyrase has decatenase activity, regardless of how low its rate (Peng and Marians, 1993; Ullsperger and Cozzarelli, 1996; Zechiedrich and Cozzarelli, 1995). In an *in vivo* study done by Zechiedrich and co-workers, they concluded that DNA gyrase's role in decatenation is by introducing negative supercoiling, which in turn produces a better substrate for Topo IV

(Zechedrich *et al*, 1997). However, if that was the case, in this work we would see accumulation of catenanes in C600SN upon Int expression and norfloxacin treatment. In other words, when site-specific recombination was induced in the presence of norfloxacin in a strain with DNA gyrase resistant to the drug, the catenanes formed would not be resolved due to Topo IV inhibition but would remain supercoiled due to the action of gyrase. After catenane extraction and nicking for supercoiling elimination, accumulation of catenanes over the time-course experiment would still be observed. That was not what was observed. Our results showed formation of catenanes at early timepoints of the experiment and their decatenation and disappearance at the later timepoints, which conflicts with the conclusion stated by Zechiedrich and colleagues.

In summary, a method for catenanes formation, extraction and detection was developed. In this *in vivo* method it was used a plasmid with *attP* and *attB* sites in direct repeat, ΦC31 integrase, norfloxacin, DNA extraction by alkaline lysis, DNA nicking for supercoiling elimination, agarose gel for samples separation and Southern hybridization for DNA detection.

Since this work intended to study precatenation formation on the chromosome, having a plasmid model which can mimic formation of precatenanes *in vivo* would allow us to study how efficient the method developed in Chapter 3 was.

The *terE* site was used as a tool by Schvartzman's group to study the topology of RIs (Olavarrieta *et al*, 2002; Cebrián *et al*, 2015), where they concluded that precatenation does form during plasmid replication.

Here the *terE* site was used to create those RIs which could precatenate the two replicated duplexes. In the region between the *ori* and *terE*, *attP* and *attB* sites were inserted 2.5 kb apart. In this way, any precatenation formed during plasmid replication could be trapped in the form of catenanes by simply inducing site-specific recombination by ΦC31 integrase. We used the method developed earlier (Chapter 3) on the precatenated replicated regions of a RI (Chapter 4).

Despite the successful RI production, no precatenanes were detected. Site-specific recombination between *att* sites on the replicated portions of the plasmid RI produced monomeric cassette (the region between the two *att* sites) and its dimer. A reason for us not seeing catenanes might be that the RI of pAOT12 was not supercoiled enough for

generation of precatenanes. Another approach to test our overall strategy for precatenation detection would be to carry out *in vitro* recombination on plasmid RIs.

Despite not being able to detect precatenation from a RI model on a plasmid, we still studied precatenane formation on the bacterial chromosome (Chapter 5). The study was made in two different regions of the chromosome, near *dif* and *terC*, and the same method was used as the one applied for precatenane detection from the RI model. The *attP* and *attB* were positioned on chromosome as a cassette with the kanamycin resistance and *lacI* genes between the *att* sites. The two sites were separated by 2.5 kb. Upon site-specific recombination between the *att* sites on the chromosome, the products detected were the monomer of cassette and its dimer.

Seeing recombination products indicated that recombination was occurring, and it was efficient (it only occurred when induced). A reason for absence of catenanes might be that the *att* sites were inserted into chromosome too close to each other, which might not be distance enough to entrap precatenation. Localization of the cassette insertion on the chromosome also might play its role. However, the cassette was inserted near sites associated with replication termination and thus precatenation formation.

A plausible reason for us not to see catenane formation from recombination on RI or chromosome *in vivo* might be presence of Topo III. This type I topoisomerase has been suggested to participate in catenane/precatenane unlinking (DiGate and Marians, 1988; Hiasa *et al*, 1994; Hiasa and Marians, 1994; Perez-Cheeks *et al*, 2012). Therefore, inhibiting Topo III might be a good test to see if this topoisomerase actually participates in precatenane unlinking and if precatenation levels are increased.

Perhaps when norfloxacin was used to inhibit both type II topoisomerases, or just Topo IV, any DNA bound by them was being degraded, since norfloxacin acts by trapping the cleaved protein-DNA complex. Therefore, repeating the experiments from chapters 3, 4 and 5 in strains with type II topoisomerases temperature sensitive (Topo IV, DNA gyrase or both sensitive) might result in higher concentration of DNA recovered, increasing the chances of detection of catenanes. Also, when using temperature sensitive strains, shifting them to a higher temperature would allow the build-up of precatenation. Then, induction of recombination would trap that precatenation in form of catenanes.

There are different confounding factors that might interfere with precatenane formation or detection. One of them is the positive supercoiling produced ahead of the fork during replication. If no or not enough positive supercoiling is formed, less chances there is for precatenane formation. Other factor is replication fork rotation. If replication forks cannot swivel due to attachment to cell membrane, for example, no precatenane can form. The third factor could be that at a given time in an exponentially growing culture of bacteria, less than 1% of the chromosomes are trapped at the *terC* site (Duggin and Bell, 2009). Therefore, the chance of trapping precatenation in a culture of non-synchronized cells is very low. For last, according to our approach, the site-specific recombination has to occur between the *attP* and *attB* sites on each chromosome for precatenation to be trapped in form of a catenane. As observed in the results, the recombination was occurring between the *att* sites on different molecules while these were co-localized. This also decreases the chance of precatenation entrapment.

Despite our results having not shown presence of precatenation we cannot conclude that they are not present. Work done during this project showed that it was not easy to get evidence for precatenanes formation on chromosome, probably why no study has showed it yet.

In Chapter 6 a different study was carried out, which did not focus on formation of precatenanes. Instead, the supercoiling level of a 398 bp circle produced by Xer site-specific recombination at *psi* sites was studied. This work was made to complement previous data obtained by Sean Colloms (unpublished data). Our results showed that ΔLk of the 398 bp circle was -1. Combined with the ΔLk values for the substrate plasmid and the second product of recombination, a 3039 bp circle, it was concluded that the deletion recombination reaction catalysed by XerC, XerD and PepA at *psi* proceeds with ΔLk of +4. This in turn allowed us to conclude that the total linkage change (ΔLg) of the reaction is 0 and this is consistent with the Holliday junction model of strand exchange by tyrosine recombinases (Nash and Pollock, 1983; Hsu and Landy, 1984; Gopaul *et al*, 1998; Crisona *et al*, 1999).

References

Abraham, J.M., Freitag, C.S., Clements, J.R. and Eisenstein, B.I. 1985. An invertible element of DNA controls phase variation of type 1 fimbriae of *Escherichia coli*. *PNAS*. **82**: 5724-5727.

Adams, D.E., Shekhtman, E.M., Zechiedrich, E.L., Schmid, M.B. and Cozzarelli, N.R. 1992. The Role of Topoisomerase IV in Partitioning Bacterial Replicons and the Structure of Catenated Intermediates in DNA Replication. *Cell*. **71**: 277-288.

Amann, E., Ochs, B. and Abel, K.J. 1988. Tightly regulated *tac* promoter vectors useful for the expression of unfused and fused proteins in *Escherichia coli*. *Gene*. **69**: 301-315.

Appleyard, R.K. 1954. Segregation of new lysogenic types during growth of a double lysogenic strain derived from *Escherichia coli* K12. *Genetics*. **39**: 440-452.

Arnold, D.A. and Kowalczykowski, S.C. 2001. RecBCD Helicase/Nuclease. *eLS, Wiley Online Library*. doi:10.1038/npg.els.0000586.

Asai, T., Bates, D.B. and Kogoma, T. 1994. DNA Replication Triggered by Double-Stranded Breaks in *E. coli*: Dependence on Homologous Recombination Functions. *Cell*. **78**: 1051-1061.

Aussel, L., Barre, F.X., Aroyo, M., Stasiak, A., Stasiak, A.Z. and Sherratt, D. 2002. FtsK Is a DNA Motor Protein that Activates Chromosome Dimer Resolution by Switching the Catalytic State of the XerC and XerD Recombinases. *Cell*. **108**: 195-205.

Austin, S., Ziese, M. and Sternberg, N. 1981. A Novel Role for Site-Specific Recombination in Maintenance of Bacterial Replicons. *Cell*. **25**: 729-736.

Balagurumoorthy, P., Adelstein, S.J. and Kassis, A.I. 2008. Method to eliminate linear DNA from mixture containing nicked-circular, supercoiled, and linear plasmid DNA. *Analytical Biochemistry*. **381**: 172-174.

Barre, F.X., Aroyo, M., Colloms, S.D., Helfrich, A., Cornet, F. and Sherratt, J. 2000. FtsK functions in the processing of a Holliday junction intermediate during bacterial chromosome segregation. *Genes & Development*. **14**: 2976-2988.

Barreiro, V. and Haggård-Ljungquist, E. 1992. Attachment Sites for Bacteriophage P2 on the *Escherichia coli* Chromosome: DNA Sequences, Localization on the Physical Map, and Detection of a P2-Like Remnant in *E. coli* K-12 Derivatives. *Journal of Bacteriology*. **174**: 4086-4093.

Bath, J., Sherratt, D.J. and Colloms, S.D. 1999. Topology of Xer Recombination on Catenanes Produced by Lambda Integrase. *Journal of Molecular Biology*. **289**: 873-883.

Berg, C.M. and Curtis III, R. 1967. Transposition derivatives of an Hfr strain of *Escherichia coli* K-12. *Genetics*. **56**: 503-525.

Berger, J.M. 1998. Structure of DNA topoisomerases. *Biochimica et Biophysica*, pp. 3-18.

Bermejo, R., Branzei, D. and Foiani, M. 2008. Cohesion by topology: sister chromatids interlocked by DNA. *Genes & Development*. **22**: 2297-2301.

Bianco, P.R., Tracy, R.B. and Kowalczykowski, S.C. 1998. DNA strand exchange proteins: a biochemical and physical comparison. *Frontiers in Bioscience*. **3**: 570-603.

Bigot, S., Saleh, O.A., Lesterlin, C., Pages, C., Karoui, M.E. Dennis, C., Grigoriev, M., Allemand, J.F., Barre, F.X. and Cornet, F. 2005. KOPS: DNA motifs that control *E. coli* chromosome segregation by orienting the FtsK translocase. *The EMBO Journal*. **24**: 3770-3780.

Blakely, G., May, G., McCulloch, R., Arciszewska, L.K., Burke, M., Lovett, S.T. and Sherratt, D.J. 1993. Two Related Recombinases Are Required for Site-Specific Recombination at *dif* and *cer* in *E. coli* K12. *Cell*. **75**: 351-361.

Blomfield, I.C., Vaughen, V., Rest, R.F. and Eisenstein, B.I. 1991. Allelic exchange in *Escherichia coli* using the *Bacillus subtilis sacB* gene and a temperature-sensitive pSC101 replicon. *Molecular Microbiology*. **5**: 1447-1457.

Boles, T.C., White, J.H. and Cozzarelli, N.R. 1990. Structure of Plectonemically Supercoiled DNA. *Journal of Molecular Biology*. **213**: 931-951.

Bolivar, F., Rodriguez, R.L., Greene, P.L., Betlach, M.C., Heyneker, H.L., Boyer, H.W. and Falkow, S. 1977. Construction and characterization of new cloning vector. II. A multipurpose cloning system. *Gene*. **2**: 95-113.

Bourgaux, P. and Bourgaux-Ramoisy, D. 1972. Unwinding of Replicating Polyoma Virus DNA. *Journal of Molecular Biology*. **70**: 399-413.

Branzei,D. and Foiani, M. 2010. Maintaining genome stability at the replication fork. *Nature Reviews in Molecular Cell Biology*. **11**: 208-219.

Breier, A.M., Weier, H.U.G. and Cozzarelli, N.R. 2005. Independence of replisomes in *Escherichia coli* chromosomal replication. *PNAS*. **102**: 3924-3947.

Brown, P.O. and Cozzarelli, N.R. 1979. A sign inversion mechanism for enzymatic supercoiling of DNA. *Science*. **206**: 1081-1083.

Brown, P.O. and Cozzarelli, N.R. 1981. Catenation and knotting of duplex DNA by type 1 topoisomerases: A mechanistic parallel with type 2 topoisomerases. *PNAS*. **78**: 843-847.

Buck, D. 2009. DNA Topology. *In*: Buck, D. and Flapan, E. (eds.) *Proceedings of Symposia in Applied Mathematics.* Volume 66: Applications of Knot Theory. American Mathematical Society, pp 47-82.

Cebrián, J., Castán, A., Martínez, V., Kadomatsu-Hermosa, M.J., Parra, C., Fernández-Nestosa, M.J., Schaerer, C., Hernández, P., Krimer, D.B. and Schvartman, J.B. 2015. Direct Evidence for the Formation of Precatenanes during DNA Replication. *Journal of Biological Chemistry*. **290**: 13724-13735.

Chambers, S.P., Prior, S.E., Barstow, D.A. and Minton, N.P. 1988. The pMTL nic-cloning vectors. I. Improved pUC polylinker regions to facilitate the use of sonicated DNA for nucleotides sequencing. *Gene*. **68**: 139-149.

Champoux, J.J. 2001. DNA Topoisomerases: Structure, Function, and Mechanism. *Annual Review of Biochemistry*. **70**: 369-413.

Champoux, J.J. and Been, M.D. 1980. In *Mechanistic Studies of DNA Replication and Genetic Recombination*. Alberts, B., ed., pp. 809-815, Academic Press, New York.

Chaveroche, M.K., Ghigo, J.M. and d'Enfert, C. 2000. A rapid method for efficient gene replacement in the filamentous fungus *Aspergillus nidulans*. *Nucleic Acids Research*. **28**: E97.

Colloms, S.D., Bath, J. and Sherratt, D.J. 1997. Topological Selectivity in Xer Site-Specific Recombination. *Cell*. **88**: 855-864.

Colloms, S.D., McCulloch, R., Grant, K., Neilson, L. and Sherratt, D.J. 1996. Xer-mediated site-specific recombination *in vitro*. *The EMBO Journal*. **15**: 1172-1181.

Colloms, S.D., Merrick, C.A., Olorunniji, F.J., Stark, W.M., Smith, M.C.M., Osbourn, A., Keasling, J.D. and Rosser, S.J. 2014. Rapid metabolic pathway assembly and modification using serine integrases site-specific recombination. *Nucleic Acids Research*. **42**: E23.

Colloms, S.D., Sykora, P., Szatmari, G. and Sherratt, D.J. 1990. Recombination at ColE1 *cer* Requires the *Escherichia coli xerC* Gene Product, a Member of the Lambda Integrase Family of Site-Specific Recombinases. *Journal of Bacteriology*. **172**: 6973-6980.

Corless, S. and Gilbert, N. 2016. Effects of DNA supercoiling on chromatin architecture. *Biophysical Reviews*. **8**: 245-258.

Cornet, F., Mortier, I., Patte, J. and Louran, J.M. 1994. Plasmid pSC101 Harbours a Recombination Site, *psi*, Which Is Able To Resolve Plasmid Multimers and To Substitute for the Analogous Chromosomal *Escherichia coli* Site *dif*. *Journal of Bacteriology*. **176**: 3188-3195.

Couturier, M., Bahassi, el-M. and Van Melderen, L. 1998. Bacterial death by DNA gyrase poisoning. *Trends in Microbiology*. **6**: 269-275.

Cozzarelli, N.R., Boles, T.C. and White, J.H. 1990. Primer on the Topology and Geometry of DNA Supercoiling. *In:* DNA Topology and Its Biological Effects, *Cold Spring Harbor Laboratory Press*, pp. 139-184.

Crisona, N.J., Weinberg, R.L., Peter, B.J., Sumners, D.W. and Cozzarelli, N.R. 1999. The Topological Mechanism of Phage λ Integrase. *Journal of Molecular Biology*. **289**: 747-775.

Datsenko, K.A. and Wanner, B.L. 2000. One-step inactivation of chromosomal genes in *Escherichia coli* K-12 using PCR products. *PNAS*. **97**: 6640-6645.

Deibler, R.W., Rahmati, S. and Zechiedrich, E.L. 2001. Topoisomerase IV, alone, unknots DNA in *E. coli*. *Genes & Development*. **15**: 748-761.

Deweese, J.E., Osheroff, M.A. and Osheroff, N. 2008. DNA Topology and Topoisomerases: Teaching a "Knotty" Subject. *Biochemistry and Molecular Biology Education*. **37**: 2-10.

DeWitt, S.K. and Adelberg, E.A. 1962. The occurrence of a genetic transposition in a strain of *Escherichia coli*. *Genetics*. **47**: 577-585.

DiGate, R.J. and Marians, K.J. 1988. Identification of a Potent Decatenating Enzyme from *Escherichia coli*. *Journal of Biological Chemistry*. **263**: 13366-13373.

DiNardo, S., Voelkel, K.A. and Sternglanz, R. 1982. *Escherichia coli* DNA Topoisomerase I Mutants Have Compensatory Mutations in DNA Gyrase Genes. *Cell*. **31**: 43-51.

Dixon, J.R., Selvaraj, S., Yue, F., Kim, A., Li, Y., Shen, Y., Hu, M., Liu, J.S. and Ren, B. 2012. Topological Domains in Mammalian Genomes Identified by Analysis of Chromatin Interactions. *Nature*. **485**: 376-380.

Drlica, K. 1999. Mechanism of fluoroquinolone action. *Current Opinion in Microbiology*. **2**: 504-508.

Dröge, P. and Cozzarelli, N.R. 1992. Topological Structure of DNA Knots and Catenanes. *Methods in Enzymology*. **212**: 120-129.

Duggin, I.G. and Bell, S.D. 2009. Termination Structures in the *Escherichia coli* Chromosome Replication Fork Trap. *Journal of Molecular Biology*. **387**: 532-539.

Duggin, I.G., Wake, R.G., Bell, S.D. and Hill, T.M. 2008. The replication fork trap and termination of chromosome replication. *Molecular Microbiology*. **70**: 1323-1333.

Finch, J.T. and Klug, A. 1976. Solenoidal model for superstructure in chromatin. *PNAS*. **73**: 1897-1901.

Fogg, J.M., Kolmakova, N., Rees, I., Magonov, S., Hansma, H., Perona, J.J. and Zechiedrich, E.L. 2006. Exploring writhe in supercoiled minicircle DNA. *Journal of Physics: Condensed Matter*. **18**:145-159.

Fournier, B., Zhao, X., Lu, T., Drlica, K. and Hooper, D.C. 2000. Selective Targeting of Topoisomerase IV and DNA Gyrase in *Staphylococcus aureus*: Different Patterns of Quinolone-Induced Inhibition of DNA Synthesis. *Antimicrobial Agents and Chemotherapy*. **44**: 2160-2165.

François, V., Louarn, J. and Louarn, J.M. 1989. The terminus of the *Escherichia coli* chromosome is flanked by several polar replication pause sites. *Molecular Microbiology*. **3**: 995-1002.

French, S. 1992. Consequences of Replication Fork Movement Through Transcription Units *in vivo*. *Science*. **258**: 1362-1365.

Fuke, M. and Inselburg, J. 1972. Electron Microscopic Studies of Replicating and Catenated Colicin Factor E1 DNA Isolated from Minicells. *PNAS*. **69**: 89-92.

Gartenberg, M.R. and Wang, J.C. 1992. Positive supercoiling of DNA greatly diminishes mRNA synthesis in yeast. *PNAS*. **89**: 11461-11465.

Gellert, M., Mizuuchi, K., O'Dea, M.H. and Nash, H.A. 1976. DNA gyrase: An enzyme that introduces superhelical turns into DNA. *PNAS*. **73**: 3872-3876.

Gopaul, D.N., Guo, F. and Duyne, G.D.V. 1998. Structure of the Holliday junction intermediate in Cre-*loxP* site-specific recombination. *The EMBO Journal*. **17**: 4175-4187.

Gottlieb, P.A., Wu, S., Zhang, X., Tecklenburg, M., Kuempel, P. and Hill, T.M. 1992. Equilibrium, Kinetic, and Footprinting Studies of the Tus-*Ter* Protein-DNA Interaction. *Journal of Biological Chemistry*. **267**: 7434-7443.

Grainge, I., Bregu, M., Vazquez, M., Sivanathan, V., Ip, S.C.Y. and Sherratt, D.J. 2007. Unlinking chromosome catenanes *in vivo* by site-specific recombination. *The EMBO Journal*. **26**: 4228-4238.

Grainge, I., Lesterlin, C. and Sherratt D.J. 2011. Activation of XerCD-*dif* recombination by the FtsK DNA translocase. *Nucleic Acids Research*. **39**: 5140-5148.

Grindley, N.D.F., Whiteson, K.L. and Rice, P.A. 2006. Mechanism of Site-Specific Recombination. *Annual Review of Biochemistry*. **75**: 567-605.

Guzman, L.M., Belin, D., Carson, M.J. and Beckwith, J. 1995. Tight Regulation, Modulation, and High-Level Expression by Vectors Containing the Arabinose P_{BAD} Promoter. *Journal of Bacteriology*. **177**: 4121-4130.

Hanahan, D. 1985. *In:* DNA Cloning: A Practical Approach. Glover, D. M. (ed.), Vol. 1, p. 109, IRL Press, McLean, Virginia.

Heilig, J.S., Elbing, K.L. and Brent, R. 1998. Large-Scale Preparation of Plasmid DNA. *In: Current Protocols in Molecular Biology*, 1.7.1-1.7.16.

Heisig, P. and Wiedemann, B. 1991. Use of a Broad-Host-Range *gyrA* Plasmid for Genetic Characterization of Fluoroquinolone-Resistant Gram-Negative Bacteria. *Antimicrobial Agents and Chemotherapy*. **35**: 2031-2036.

Hendrickson, H. and Lawrence, J.G. 2007. Mutational bias suggests that replication termination occurs near the *dif* site, not at *Ter* sites. *Molecular Microbiology*. **64**: 42-56.

Hiasa, H. and Marians, K.J. 1994. Topoisomerase III, but Not Topoisomerase I, Can Support Nascent Chain Elongation during Theta-type DNA Replication. *Journal of Biological Chemistry*. **269**: 32655-32659.

Hiasa, H. and Marians, K.J. 1996. Two Distinct Modes of Strand Unlinking during θ-Type DNA Replication. *Journal of Biological Chemistry*. **271**: 21529-21535.

Hiasa, H., DiGate, R.J. and Marians, K.J. 1994. Decatenating Activity of *Escherichia coli* DNA Gyrase and Topoisomerase I and III during *oriC* and pBR322 DNA Replication *in vitro*. *Journal of Biological Chemistry*. **269**: 2093-2099.

Hidaka, M., Akiyama, M. and Horiuchi, T. 1988. A Consensus Sequence of Three DNA Replication Terminus Sites on the *E. coli* Chromosome Is Highly Homologous to the *terR* Sites of the R6K Plasmid. *Cell*. **55**: 467-475.

Hidaka, M., Kobayashi, T. and Horiuchi, T. 1991. A Newly Identified DNA Replication Terminus Site, *TerE*, on the *Escherichia coli* Chromosome. *Journal of Bacteriology*. **173**: 391-393.

Hidaka, M., Kobayashi, T., Ishimi, Y., Seki, M., Enomoto, T., Abdel-Monem, M. and Horiuchi, T. 1992. Termination Complex in *Escherichia coli* Inhibits SV40 DNA Replication *in vitro* by Impeding the Action of T Antigen Helicase. *Journal of Biological Chemistry*. **267**: 5361-5365.

Hidaka, M., Kobayashi, T., Takenaka, S., Takeya, H. and Horiuchi, T. 1989. Purification of a DNA Replication Terminus (*ter*) Site-binding Protein in *Escherichia coli* and Identification of the Structural Gene. *Journal of Biological Chemistry*. **264**: 21031-21037.

Hill, T.M., Pelletier, A.J., Tecklenburg, M.L. and Kuempel, P.L. 1988. Identification of the DNA Sequences from the *E. coli* Terminus Region That Halts Replication Forks. *Cell*. **55**: 459-466.

Hill, T.M., Tecklenburg, M.L., Pelletier, A.J. and Kuempel, P.L. 1989. *tus*, the trans-acting gene required for termination of DNA replication in *Escherichia coli*, encodes a DNA-binding protein. *PNAS*. **86**: 1593-1597.

Hsu, P.L. and Landy, A. 1984. Resolution of synthetic *att*-sites Holliday structure by the integrase protein of bacteriophage λ. *Nature*. **311**: 721-726.

Ip, S.C.Y., Bregu, M., Barre, F.X. and Sherratt, D.J. 2003. Decatenation of DNA by FtsK-dependent Xer site-specific recombination. *The EMBO Journal*. **22**: 6399-6407.

Irobalieva, R.N., Fogg, J.M., Catanese, D.J., Sutthibutpong, T., Chen, M., Barker, A.K., Ludtke, S.J., Harris, S.A., Schmid, M.F., Chiu, W. and Zechiedrich, L. 2015. Structural diversity of supercoiled DNA. *Nature Communications*. **6**: 8440-8449.

Jayaram, M., Ma, C.H., Kachroo, A.H., Rowley, P.A., Guga, P., Fan, H.F. and Voziyanov, Y. 2014. An Overview of Tyrosine Site-Specific Recombination: From an Flp Perspective. Microbiology Spectrum. **3:** MDNA3-0021-2014.

Joshi, M.C., Magnan, D., Montminy, T.P., Lies, M., Stepankiw, N. and Bates, D. 2013. Regulation of Sister Chromosomes Cohesion by the Replication Fork Tracking Protein SeqA. *PloS Genetics*. **9**: e1003673.

Khan, S.R. and Kuzminov, A. 2011. Replication Forks Stalled at Ultraviolet Lesions Are Rescued via RecA and RuvABC Protein-catalyzed Disintegration in *Escherichia coli*. *Journal of Biological Chemistry*. **287**: 6250-6265.

Khodursky, A.B. and Cozzarelli, N.R. 1998. The Mechanism of Inhibition of Topoisomerase IV by Quinolone Antibacterials. *Journal of Biological Chemistry*. **273**: 27668-27677.

Khodursky, A.B., Zechiedrich, E.L. and Cozzarelli, N.R. 1995. Topoisomerase IV is a target of quinolones in *Escherichia coli*. *PNAS*. **92**: 11801-11805.

Kowalczykowski, S.C. 2000. Initiation of genetic recombination and recombination-dependent replication. *Trends in Biochemical Science*. **25**: 156-165.

Kratz, J., Schmidt, F. and Wiedemann, B. 1983. Characterization of Tn2411 and Tn2410, Two Transposons Derived from R-Plasmid R1767 and Related to Tn2603 and Tn21. *Journal of Bacteriology*. **155**: 1333-1342.

Kreuzer, K.N., Saunders, M., Weislo, L.J. and Kreuzer H.W.E. 1995. Recombination-Dependente DNA Replication Stimulated by Double-Strand Breaks in Bacteriophage T4. *Journal of Bacteriology*. **177**: 6844-6853.

Kuempel, P.L., Duerr, S.A. and Seeley, N.R. 1977. Terminus region of the chromosome in *Escherichia coli* inhibits replication forks. *PNAS*. **74**: 3927-3931.

Kuempel, P.L., Henson, J.M., Tecklenburg, M. and Lim, D.F. 1991. *dif*, a recA-independent recombination site in the terminus region of the chromosome of *Escherichia coli*. *New Biology*. **3**: 799-811.

Lederberg, E.M. and Lederberg, J. 1953. Genetic studies of lysogenicity in *Escherichia coli*. *Genetics*. **38**: 51-64.

Lee, J.Y. and Yang, W. 2006. UvrD Helicase Unwinds DNA One Base Pair at a Time by a Two-Part Power Stroke. *Cell*. **127**: 1349-1360.

Leslie, N.R. and Sherratt, D.J. 1995. Site-specific recombination in the replication terminus region of *Escherichia coli*: functional replacement of *dif*. *The EMBO Journal*. **14**: 1561-1570.

Lesterlin, C., Gigant, E., Boccars, F. and Espéli, O. 2012. Sister chromatid interactions in bacteria revealed by a site-specific recombination assay. *The EMBO Journal*. **31**: 3468-3479.

Levine, C., Hiasa, H. and Marians, K.J. 1998. DNA gyrase and topoisomerase IV: biochemical activities, physiological roles during chromosome replication, and drug sensitivities. *Biochimica et Biophysica*. pp. 29-43.

Lewis, P.J. 2001. Bacterial chromosome segregation. *Microbiology*. **147**: 519-526.

Lima, C.D., Wang, J.C. and Mondragón, A. 1994. Three-dimensional structure of the 67K N-terminal fragment of the *E. coli* DNA topoisomerase I. *Nature*. **367**: 138-146.

Lindsley, J.E. 2005. DNA Topology: Supercoiling and Linking. *eLS, Wiley Online Library*. doi:10.1038/npg.els.0003904.

Link, A.J., Phillips, D. and Church, G.M. 1997. Methods for Generating Precise Deletions and Insertions in the Genome of Wild-Type *Escherichia coli*: Applications to Open Reading Frame Characterization. *Journal of Bacteriology*. **179**: 6228-6237.

Liu, L.F. and Wang, J.C. 1987. Supercoiling of the DNA template during transcription. *PNAS*. **84**: 7024-7027.

Ljungman, M. and Hanawalt, P.C. 1995. Presence of negative torsional tension in the promoter region of the transcriptionally poised dihydrofolate reductase gene *in vivo*. *Nucleic Acid Research*. **23**: 1782-1789.

Lomovskaya, N.D., Mkrtumian, N.M., Gostimskaya, N.L. and Danilenko, V.N. 1972. Characterization of Temperate Actinophage ΦC31 Isolated from *Streptomyces coelicolor* A3(2). *Journal of Virology*. **9**: 258-262.

Lynn, R.M. and Wang, J.C. 1989. Peptide Sequencing and Site-Directed Mutagenesis Identify Tyrosine-319 as the Active Site Tyrosine of *Escherichia coli* DNA Topoisomerase I. *Proteins: Structure, Function and Genetics*. **6**: 231-239.

Mirkin, S.M. 2001. DNA Topology: Fundamentals. *eLS, Wiley Online Library*. doi:10.1038/npg.els.0001038.

Mondragón, A. and DiGate, R. 1999. The structure of *Escherichia coli* DNA topoisomerase III. *Structure*. **7**: 1373-1383.

Murphy, K.C. 1998. Use of Bacteriophage λ Recombination Functions To Promote Gene Replacement in *Escherichia coli*. *Journal of Bacteriology*. **180**: 2063-2071.

Muyrers, J.P.P., Zhang, Y., Testa, G. and Stewart, A.F. 1999. Rapid modification of bacterial artificial chromosomes by ET-recombination. *Nucleic Acids Research*. **27**: 1555-1557.

Nash, H.A. and Pollock, T.J. 1983. Site-specific Recombination of Bacteriophage Lambda. The Change in Topological Linking Number Associated with Exchange of DNA Strands. *Journal of Molecular Biology*. **170**: 19-38.

Nielsen, H.J., Ottesen, J.R., Youngren, B., Austin, S.J. and Hansen, F.G. 2006. The *Escherichia coli* chromosome is organized with the left and right chromosome arms in separate cell halves. *Molecular Microbiology*. **62**: 331-338.

Nitiss, J.L. 2009. DNA topoisomerase II and its growing repertoire of biological functions. *Nature Reviews Cancer*. **9**: 327-337.

Nolivos, S., Pages, C., Rousseau, P., Bourgeois, P.L. and Cornet, F. 2010. Are two better than one? Analysis of an FtsK/Xer recombination system that uses a single recombinase. *Nucleic Acids Research*. **38**: 6477-6489.

Ogawa, T., Yogo, K., Furuike, S., Sutoh, K., Kikuchi, A. and Kinosita Jr, K. 2014. Direct observation of DNA overwinding by reverse gyrase. *PNAS*. **112**: 7495-7500.

Olavarrieta, L., Martínez-Robles, M.L., Sogo, J.M., Stasiak, A., Hernández, P., Krimer, D.B. and Schvartzman, J.B. 2002. Supercoiling, Knotting and replication for reversal in partially replicates plasmids. *Nucleic Acids Research*. **30**: 656-666.

Olorunniji, F.J., Buck, D.E., Colloms, S.D., McEwan, A.R., Smith, M.C.M., Stark, W.M. and Rosser, S.J. 2012. Gated rotation mechanism of site-specific recombination by ΦC31 integrase. *PNAS*. **109**: 19661-19666.

Olorunniji, F.J., McPherson, A.L., Pavlou, H.J., McIlwraith, M.J., Brazier, J.A., Cosstick, R. and Stark, W.M. 2015. Nicked-site substrates for a serine recombinase reveal enzyme-DNA communication and an essential tethering role of covalent enzyme-DNA linkages. *Nucleic Acids Research*. **43**: 6134-6143.

Olorunniji, F.J., McPherson, A.L., Rosser, S.J., Smith, M.C.M., Colloms, S.D. and Stark, W.M. 2017. Control of serine integrase recombination directionality by fusion with the directionality factor. *Nucleic Acids Research*. **45**: 8635-8645.

Olorunniji, F.J., Rosser, S.J. and Stark, W.M. 2016. Site-specific recombinases: molecular mechanism for the Genetic Revolution. *Biochemical Journal*. **473**: 673-684.

Peng, H. and Marians, K.J. 1993. Decatenation activity of topoisomerase IV during *oriC* and pBR322 DNA replication *in vitro*. *PNAS*. **90**: 8571-8575.

Perez-Cheeks, B.A., Lee, C., Hayama, R. and Marians, K.J. 2012. A Role for Topoisomerase III in *Escherichia coli* Chromosome Segregation. *Molecular Microbiology*. **86**: 1007-1022.

Peter, B.J., Ullsperger, C., Hiasa, H., Marians, K.J. and Cozzarelli, N.R. 1998. The Structure of Supercoiled Intermediates in DNA Replication. *Cell*. **94**: 819-827.

Pettijohn, D.E. 1988. Histone-like Proteins and Bacterial Chromosome Structure. *Journal of Biological Chemistry*. **263**: 12793-12796.

Pollock, T.J. and Nash, H.A. 1983. Knotting of DNA Caused by a Genetic Rearrangement. Evidence for a Nucleosome-like Structure in Site-specific Recombination of Bacteriophage Lambda. *Journal of Molecular Biology*. **170**: 1-18.

Postow, L., Crisona, N.J., Peter, B.J., Hardy, C.D. and Cozzarelli, N.R. 2001. Topological challenges to DNA replication: Conformations at the fork. *PNAS*. **98**: 8219-8226.

Postow, L., Hardy, C.D., Arsuaga, J. and Cozzarelli, N.R. 2004. Topological domain structure of the *Escherichia coli* chromosome. *Genes & Development*. **18**: 1766-1779.

Povirk, L.F., Han, Y.H. and Steighner, R.J. 1989. Structure of Bleomycin-Induced DNA Double-Strand Breaks: Predominance of Blunt Ends and Single-Base 5´ Extensions. *Biochemistry*. **28**: 5808-5814.

Rausch, H. and Lehmann, M. 1991. Structural analysis of the actinophage ΦC31 attachment site. *Nucleic Acids Research*. **19**: 5187-5189.

Reshes, G., Vanounou, S., Fishov, I. and Feingold, M. 2008. Cell Shape Dynamics in *Escherichia coli*. *Biophysical Journal*. **94**: 251-264.

Rocha, E.P.C., Cornet, E. and Michel, B. 2005. Comparative and Evolutionary Analysis of the Bacterial Homologous Recombination Systems. *PLoS Genetics*. **1**: 247-259.

Schalbetter, S.A., Mansoubi, S., Chambers, A.L., Downs, J.A. and Baxter, J. 2015. Fork rotation and DNA precatenation are restricted during DNA replication to prevent chromosomal instability. *PNAS*. E4565-E4570.

Schvartzman, J.B. and Stasiak, A. 2004. A topological view of the replicon. *EMBO reports*. **5:** 256-261.

Sebring, E.D., Kelly Jr, T.J., Thoren, M.M. and Salzman, N.P. 1971. Structure of Replicating Simian Virus 40 Deoxyribonucleic Acid Molecules. *Journal of Virology*. **8**: 478-490.

Sharma, B. and Hill, T.M. 1992. *TerF*, the Sixth Identified Replication Arrest Site in *Escherichia coli*, Is Located within the rcsC Gene. *Journal of Bacteriology*. **174**: 7854-7858.

Sharma, P.C., Saneja, A. and Jain, S. 2008. Norfloxacin: a therapeutic review. *International Journal of Chemical Science*. **6**: 1702-1713.

Sheinin, M.Y., Li, M., Soltani, M., Luger, K. and Wang, M.D. 2013. Torque modulates nucleosome stability and facilitates H2A/H2B dimer loss. *Nature Communications*. **4**: 2579-2600.

Shen, L.L. and Pernet, A.G. 1985. Mechanism of inhibition of DNA gyrase by analogues of nalidixic acid: The target of the drugs is DNA. *PNAS*. **82**: 307-311.

Shen, L.L., Kohlbrenner, W.E., Weigl, D. and Baranowski, J. 1989. Mechanism of Quinolone Inhibition of DNA Gyrase. *Journal of Biological Chemistry*. **264**: 2973-2978.

Sherratt, D.J., Arciszewska, L.K., Blakely, G., Colloms, S., Grant, K., Leslie, N. and McCulloch, R. 1995. Site-specific recombination and circular chromosome segregation. *Philosophical Transactions of the Royal Society*. **347**: 37-42.

Shimokava, K., Ishihara, K., Grainge, I., Sherratt, D.J. and Vazquez, M. 2013. FtsK-dependent XerCD-*dif* recombination unlinks replication catenanes in a stepwise manner. *PNAS*. **110**: 20906-20911.

Sinden, R.R. and Pettijohn, D.E. 1981. Chromosomes in living *Escherichia coli* cells are segregated into domains of supercoiling. *PNAS*. **78**: 224-228.

Sivanathan, V., Allen, M.D., de Bekker, C., Baker, R., Arciszewska, L.K., Freud, S.M., Bycroft, M., Löwe, J. and Sherratt, D.J. 2006. The FtsK γ domain directs oriented DNA translocation by interacting with KOPS. *Nature Structural & Molecular Biology*. **13**: 965-972.

Spengler, S. J., Stasiak, A. and Cozzarelli, N.R. 1985. The Stereostructure of Knots and Catenanes Produced by Phage λ Integrative Recombination: Implications for Mechanism and DNA Structure. *Cell*. **42**: 325-334.

Stark, W.M. 2014. The Serine Recombinases. *Microbiology Spectrum*. **2**: MDNA3-0046-2014.

Stark, W.M., Sherratt, D.J. and Boocock, M.R. 1989. Site-Specific Recombination by Tn3 Resolvase: Topological Change in the Forward and Reverse Reactions. *Cell*. **58**: 779-790.

Steiner, W., Liu, G., Donachie, W.D. and Kuempel, P. 1999. The cytoplasmic domain of FtsK protein is required for resolution of chromosome dimers. *Molecular Microbiology*. **31**: 579-583.

Stirling, C.J., Stewart, G. and Sherratt, D.J. 1988. Multicopy plasmid stability in *Escherichia coli* requires host-encoded functions that lead to plasmid site-specific recombination. *Molecular Genetics and Genomics*. **214**: 80-84.

Summers, D.K. and Sherratt, D.J. 1984. Multimerization of High Copy Number Plasmids Causes Instability: ColE1 Encodes a Determinant Essential for Plasmid Monomerization and Stability. *Cell*. **36**: 1097-1103.

Summers, D.K. and Sherratt, D.J. 1988. Resolution of ColE1 dimers requires a DNA sequence implicated in the three-dimensional organization of the *cer* sites. *The EMBO Journal*. **7**: 851-858.

Sundin, O. and Varshavsky, A. 1981. Arrest of Segregation Leads to Accumulation of Highly Intertwined Catenated Dimers: Dissection of the Final Stages of SV40 DNA Replication. *Cell*. **25**: 659-669.

Thorpe, H.M. and Smith, M.C.M. 1998. *In vitro* site-specific integration of bacteriophage DNA catalysed by a recombinase of the resolvase/invertase family. *PNAS*. **95**: 5505-5510.

Toro, E. and Shapiro, L. 2010. Bacterial Chromosome Organization and Segregation. *Cold Spring Harbor Perspective in Biology*. **2**:a000349.

Ullsperger, C. and Cozzarelli, N.R. 1996. Contrasting Enzymatic Activities of Topoisomerase IV and DNA Gyrase from *Escherichia coli*. *Journal of Biological Chemistry*. **271**: 31549-31555.

Vieira, J. and Messing, J. 1982. The pUC plasmids, an M13mp7-derived system for insertion mutagenesis and sequencing with synthetic universal primers. *Gene*. **19**: 259-268.

Volkert, F.C. and Broach, J.R. 1986. Site-Specific Recombination Promotes Plasmid Amplification in Yeast. *Cell*. **46**:541-550.

Vologodskii, A.V., Crisona, N.J., Pieranski, B.L.P., Katritch, V., Dubochet, J. and Stasiak, A. 1998. Sedimentation and Electrophoretic Migration of DNA Knots and Catenanes. *Journal of Molecular Biology*. **278**: 1-3.

von Freiesleben, U. and Rasmussen, K.V. 1992. The level of supercoiling affects the regulation of DNA replication in *Escherichia coli*. *Research in Microbiology*. **143**: 655-663.

Wahle, E. and Kornberg, A. 1988. The partition locus of plasmid pSC101 is a specific binding site for DNA gyrase. *The EMBO Journal*. **7**: 1889-1895.

Wang, J.C. 1971. Interaction between DNA and an *Escherichia coli* Protein ω. *Journal of Molecular Biology*. **55**: 523-533.

Wang, J.C. 1998. Moving one DNA double helix through another by a type II DNA topoisomerase: the story of a simple molecular mechanism. *Quarterly Reviews of Biophysics*. **31**: 107-144.

Wang, J.C. 2002. Cellular roles of DNA topoisomerases: a molecular perspective. *Nature Reviews*. **3**: 430-440.

Wang, L. and Lutkenhaus, J. 1998. FtsK is an essential cell division protein that is localized to the septum and induced as part of the SOS response. *Molecular Microbiology*. **29**: 731-740.

Wang, X., Llopis, P.M. and Runder, D.Z. 2013. Organization and segregation of bacterial chromosomes. *Nature Reviews in Genetics*. **14**: 191-203.

Wang, X., Reyes-Lamonthe, R. and Sherratt, D.J. 2008. Modulation of *Escherichia coli* sister chromosomes cohesion by topoisomerase IV. *Genes & Development*. **22**: 2426-2433.

Wasserman, S.A. and Cozzarelli, N.R. 1984. Determination of the stereostructure of the product of Tn3 resolvase by a general method. *PNAS*. **82**: 1079-1083.

Wasserman, S.A., Dungan, J.M. and Cozzarelli, N.R. 1985. Discovery of a Predicted DNA Knot Substantiates a Model for Site-Specific Recombination. *Science*. **229**: 171-174.

Watson, J.D. and Crick, F.H.C. 1953a. The structure of DNA. *Cold Spring Harbor Symposia on Quantitative Biology*. **18**: 123-131.

Watson, J.D. and Crick, F.H.C. 1953b. Genetical implications of the structure of deoxyribonucleic acid. *Nature*. **171**: 964-967.

Weinfeld, M. and Soderlind, K.J.M. 1991. ^{32}P-Postlabeling Detection of Radiation-Induced DNA Damage: Identification and Estimation of Thymine Glycols and Phosphoglycolate Termini. *Biochemistry*. **30**: 1091-1097.

Wigley, D.B. 1995. Structure and mechanism of DNA topoisomerases. *Annual Review of Biophysics and Biomolecular Structure*. **24**: 185-208.

Witz, G. and Stasiak, A. 2009. DNA supercoiling and its role in DNA decatenation and unknotting. *Nucleic Acids Research*. **38**: 2119-2133.

Worcel, A. and Burgi, E. 1972. On the structure of the folded chromosome of *Escherichia coli*. *Journal of Molecular Biology*. **71**: 127-147.

Yates, J., Zhekov, I., Baker, R., Eklund, B., Sherratt, D.J. and Arciszewska, L.K. 2006. Dissection of a functional interaction between the DNA translocase, FtsK, and the XerD recombinase. *Molecular Microbiology*. **50**: 1754-1766.

Zakharova, S.S., Jesse, W., Beckendorf, C., Egelhaaf, S.U., Lapp, A. and van der Maarel, J.R. 2002. Dimensions of Plectonemically Supercoiled DNA. *Biophysical Journal*. **83**: 1106-1118.

Zechiedrich, E.L. and Cozzarelli, N.R. 1995. Roles of topoisomerase IV and DNA gyrase in DNA unlinking during replication in *Escherichia coli*. *Genes & Development*. **9**: 2859-2869.

Zechiedrich, E.L., Khodursky, A.B. and Cozzarelli, N.R. 1997. Topoisomerase IV, not gyrase, decatenates products of site-specific recombination in *Escherichia coli*. *Genes & Development*. **11**: 2580-2592.

Zechiedrich, E.L., Khodursky, A.B., Bachellier, S., Schneider, R., Chen, D., Lilley, D.M.J. and Cozzarelli, N.R. 2000. Roles of Topoisomerases in Maintaining Steady-state DNA Supercoiling in *Escherichia coli*. *Journal of Biological Chemistry*. **275**: 8103-8113.

Zhang, Y., Buchholz, F., Muyrers, J.P.P. and Stewart, A.F. 1998. A new logic for DNA engineering using recombination in *Escherichia coli*. *Nature Genetics*. **20**: 123-128.

Zhao, J. 2015. 'Engineering Serine Integrase-based Synthetic Gene Circuits for Cellular Memory and Counting', PhD thesis, University of Glasgow, Scotland.

Zhu, C.X. and Tse-Dinh, Y.C. 2000. The Acidic Triad Conserved in Type IA DNA Topoisomerases Is required for Binding of Mg(II) and Subsequent Conformational Change. *Journal of Biological Chemistry*. **275**: 5318-5322.

Zhu, C.X., Roche, C.J. and Tse-Dinh, Y.C. 1997. Effect of Mg(II) Binding on the Structure and Activity of *Escherichia coli* DNA Topoisomerase I. *Journal of Biological Chemistry*. **272**: 16206-16210.

Zieg, J., Silverman, M., Hilmen, M. and Simon, M. 1977. Recombinational switch for gene expression. *Science*. **196**: 170-172.

Appendix A

DNA sequence of the bacterial chromosome near *dif* where *attP*-Km^R-*lacI*-*attB* cassette was inserted in CP100 *dif*$^+$.

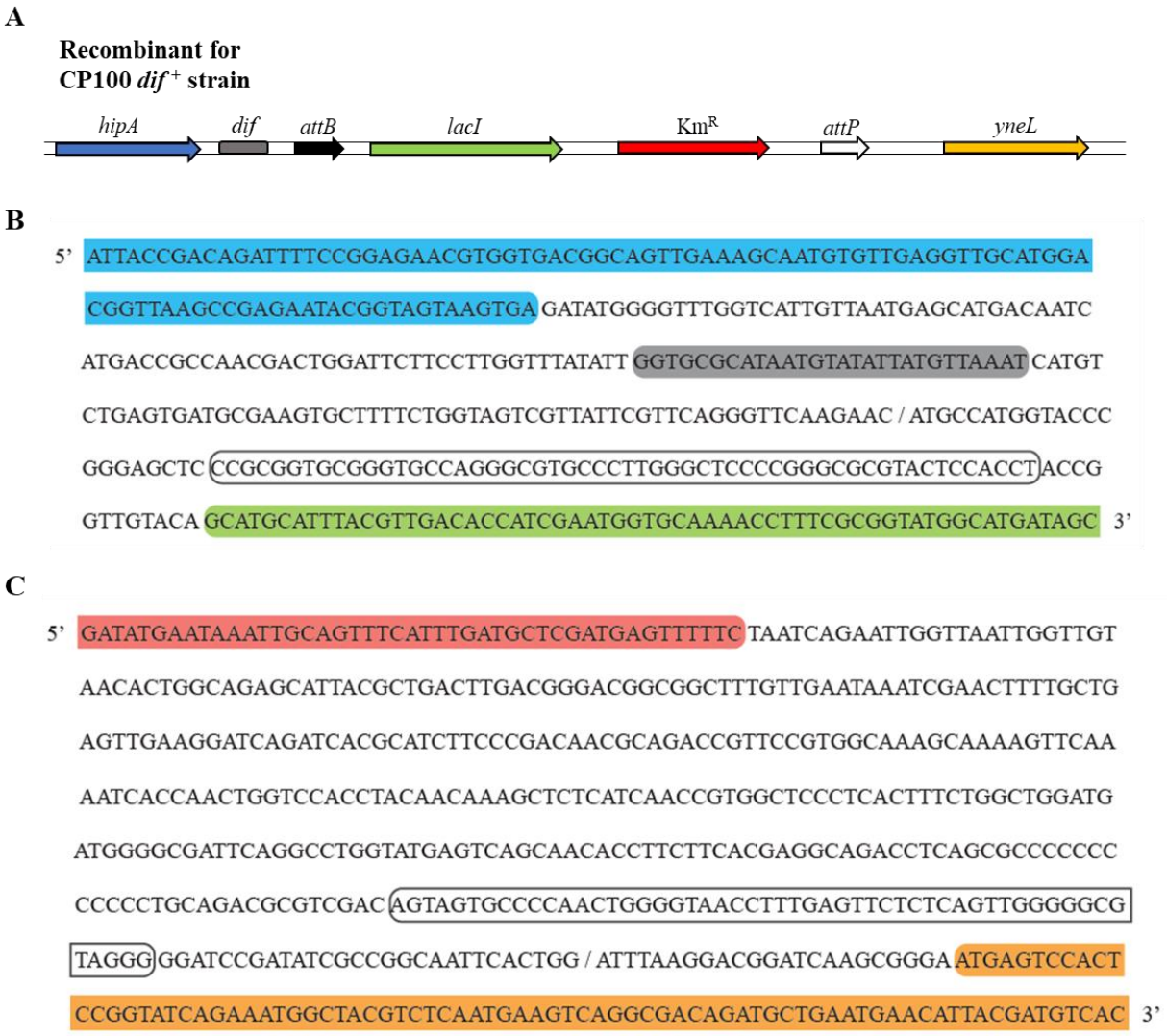

Figure 1 – *E. coli* chromosome sequence where *attP*-Km^R-*lacI*-*attB* cassette was inserted in CP100 *dif*$^+$ near *dif*. A) Diagram representing the orientation of the genes on the chromosome and cassette. The cassette was inserted between *dif* and *yneL*. **B)** DNA sequence from 5´ to 3´ representing the end of *hipA* gene in blue, the *dif* site in grey, the *attB* site in a white box and the start of *lacI* gene in green. The forward slash represents the end of the bacterial chromosome and the start of the cassette. **C)** DNA sequence from 5´ to 3´ representing the end of Km^R gene in red, the *attP* site in white box and the start of *yneL* gene in orange. The forward slash represents the end of the cassette and the start of the chromosome.

Appendix B

DNA sequence of the bacterial chromosome where *attP*-Km^R-*lacI*-*attB* cassette was inserted in the place of *dif* in CP100 Δ*dif*.

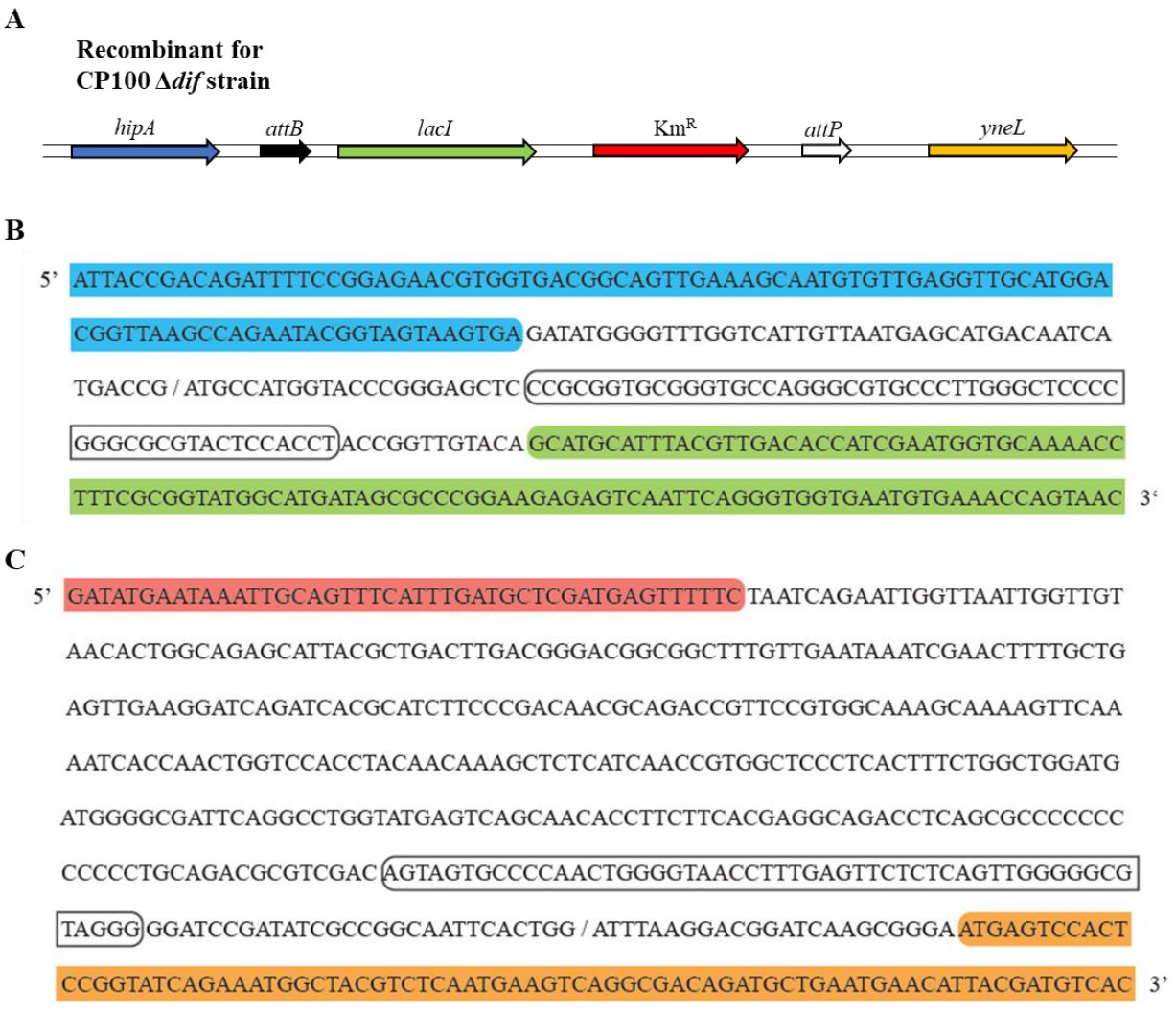

Figure 2 – *E. coli* chromosome sequence where *attP*-Km^R-*lacI*-*attB* cassette was inserted in the place of *dif* in CP100 Δ*dif*. A) Diagram representing the orientation of the genes on the chromosome and cassette. **B)** DNA sequence from 5´ to 3´ representing the end of *hipA* gene in blue, the *attB* site in a white box and the start of *lacI* gene in green. The forward slash represents the end of the bacterial chromosome and the start of the cassette. **C)** DNA sequence from 5´ to 3´ representing the end of Km^R gene in red, the *attP* site in white box and the start of *yneL* gene in orange. The forward slash represents the end of the cassette and the start of the chromosome.

Appendix C

DNA sequence of the bacterial chromosome where *attP*-Km^R-*lacI*-*attB* cassette was inserted in the place of *tam* near *terC* in DS941 and C600SN.

A

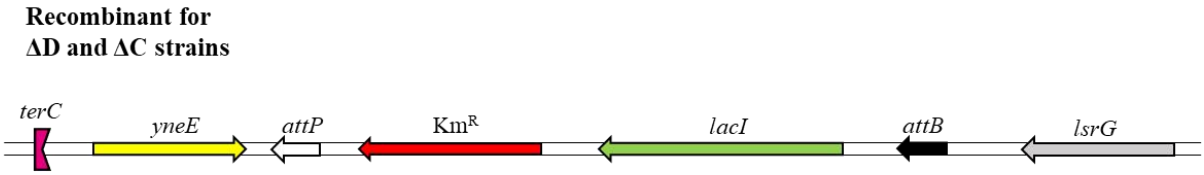

B

5' ACC ATATTAGTTACAACATCCTATAT GCCTTTATCATTAACAGGTGCCACATGCAGCGCCTGCTAAT
GTTGTAAGCTTGTAGGTAATTTGTAAGTAGCGTCTTGAGAATGTGATCGTAATCACGTTTAATAGG
GCGACTTTTCCACGCCTGAAGATAACC ATGATTGTTCGTCCACAACAACACTGGCTGCGCCGTAT
TTTTGTCTGGCACGGCTCAGTATTATCCAAGAT // AATTCCAGCAAAAATTCTTCCCGATCGTCATT
ACCAGCTGACGTGA TATT / CCAGTGAATTGCCGGCGATATCGGATCC CCCTACGCCCCCAACTGA
GAGAACTCAAAGGTTACCCCAGTTGGGGCACTACT GTCGACGCGTCTGCAGGGGGGGGGGGGCG
CTGAGGTCTGCCTCGTGAAGAAGGTGTTGCTGACTCATACCAGGCCTGAATCGCCCCATCATCCAG
CCAGAAAGTGAGGGAGCCACGGTTGATGAGAGCTTTGTTGTAGGTGGACCAGTTGGTGATTTTGA
ACTTTTGCTTTGCCACGGAACGGTCTGCGTTGTCGGGAAGATGCGTGATCTGATCCTTCAACTCAG
CAAAAGTTCGATTTATTCAACAAAGCCGCCGTCCCGTCAAGTCAGCGTAATGCTCTGCCAGTGTTA
CAACCAATTAACCAATTCTGATTA GAAAAACTCATCGAGCATCAAATGAAACTGCAATTTATTCATA 3'

C

5' CTCTCTTCCGGGCGCTATCATGCCATACCGCGAAAGGTTTTGCACCATTCGATGGTGTCAACGTAAA
TGCATGC TGTACAACCGGT AGGTGGAGTACGCGCCCGGGGAGCCCAAGGGCACGCCCTGGCACCC
GCACCGCGG GAGCTCCCGGGTACCATGGCAT / TTTTTTACTCCCGTCAGCGCGTTACCCCAATTGTA
GATAAAATTGATAAATTCGCC TCACGGCATCAAACCATTGAACAGACGTTTTTTACGCGGCCCGGTC
ATTAAAGATTCCAGTTTCGCGACACAGGTTTTGTAGTGGGGCGTGGTTTTATGGAACGCCACTGCGT 3'

Figure 3 – *E. coli* chromosome sequence where *attP*-Km^R-*lacI*-*attB* cassette was inserted in the place of *tam* in DS941 and C600SN. A) Diagram representing the orientation of the genes on the chromosome and cassette. The cassette was inserted near *terC*, deleting *tam*. **B)** DNA sequence from 5´ to 3´ representing the *terC* site in pink, the start and end of *yneE* gene in yellow, the *attP* site in a white box and the end of Km^R gene in red. The forward slash represents the end of the bacterial chromosome and the start of the cassette. The double forward slash indicates that the *yneE* gene sequence is not fully represented. **C)** DNA sequence from 5´ to 3´ representing the start of *lacI* gene in green, the *attB* site in white box and the end of *lsrG* gene in grey. The forward slash represents the end of the cassette and the start of the chromosome.